Westinghouse Electric Company
CE Nuclear Power LLC

2000 Day Hill Road
Windsor, CT 06095
USA

9 February, 2001
LD-2001-0009

U.S. Nuclear Regulatory Commission
Attn: Document Control Desk
Washington, DC 20555

SUBJECT: **SUBMITTAL OF NON-PROPRIETARY VERSION OF CENPD-404-P, REV. 0 REGARDING IMPLEMENTATION OF ZIRLO™ CLADDING MATERIAL IN CENP FUEL DESIGNS**

Reference: (1) Letter, P. W. Richardson (CENP) to USNRC Document Control Desk, "Submittal of CENPD-404-P, Rev. 0 Regarding Implementation of ZIRLO™ Cladding Material in CENP Fuel Assembly Designs", LD-2001-0005, January 22, 2001

The purpose of this letter is to submit to the Nuclear Regulatory Commission (NRC) CENPD-404-NP, Rev. 0, "Implementation of ZIRLO™ Cladding Material in CE Nuclear Power Fuel Assembly Designs" (Enclosure 1). This is the non-proprietary version of the topical report originally submitted by CE Nuclear Power LLC (CENP) in proprietary form only on January 22, 2001 (Reference 1). Enclosed are six (6) copies of CENPD-404-NP, Rev. 0, for your use.

If you have any questions regarding this matter, please do not hesitate to call Chuck Molnar of my staff at (860) 285-5205.

Very truly yours,
CE NUCLEAR POWER LLC

Philip W. Richardson
Licensing Project Manager
Windsor Nuclear Licensing

Enclosure: As stated

xc: J. S. Cushing (w/enclosures, NRC)

CE NUCLEAR POWER LLC

NON-PROPRIETARY VERSION OF CENPD-404-P, REV. 0, "IMPLEMENTATION OF ZIRLO™ CLADDING MATERIAL IN CE NUCLEAR POWER FUEL ASSEMBLY DESIGNS"

FEBRUARY 2001

Project Number:	2009656	Originator:	C. M. Molnar	Initials:	CMM

Project Name: ZIRLO™ Cladding Implementation

Document Number: LD-2001-0009 **Rev:** 000

Document Title:

Submittal of Non-Proprietary Version of CENPD-404-P, Rev. 0

Regarding Implementation of ZIRLO Cladding Material in

CENP Fuel Designs

Quality Record?

☐ No   ☑ Yes (See note below)

Quality Record Retention Period (see QP 17.1):

☑ Lifetime   ☐ 3 years   ☐ 10 years

Transmittal Reason: Provide the subject information to the NRC.

Reference: See attached document.

Name	Title	CEP Code	w / Encl.		Approval Required		Signature	Date
			Y	N	Y	N		
P. W. Richardson			☐	☑	☐	☑		
Z. E. Karoutas			☐	☑	☐	☑		
			☐	☐	☐	☐		
			☐	☐	☐	☐		
			☐	☐	☐	☐		
			☐	☐	☐	☐		
			☐	☐	☐	☐		
			☐	☐	☐	☐		
			☐	☐	☐	☐		
			☐	☐	☐	☐		
			☐	☐	☐	☐		
			☐	☐	☐	☐		
			☐	☐	☐	☐		
			☐	☐	☐	☐		
			☐	☐	☐	☐		
			☐	☐	☑	☐		
Licensing File			☐	☑	☐	☑		
DBPower	Prop. Rec. Controller		☑	☐	☐	☑		

Comments

Note: This form must include the attached document when designated a Quality Record.

◆◆◆◆◆◆◆◆◆◆◆◆◆◆◆◆◆◆◆◆

IMPLEMENTATION OF ZIRLO™ CLADDING MATERIAL IN CE NUCLEAR POWER FUEL ASSEMBLY DESIGNS

DATE: JANUARY 2001

CE NUCLEAR POWER LLC

◆◆◆◆◆◆◆◆◆◆◆◆◆◆◆◆◆◆◆

IMPLEMENTATION OF ZIRLO™ CLADDING MATERIAL IN CE NUCLEAR POWER FUEL ASSEMBLY DESIGNS

DATE: JANUARY 2001

CE NUCLEAR POWER LLC

ABSTRACT

This topical report describes the implementation of Nuclear Regulatory Commission (NRC) approved Westinghouse Electric Company developed ZIRLO™ fuel rod cladding material properties and correlations in NRC approved CE Nuclear Power LLC (CENP) design and licensing safety analysis procedures. These procedures include analyses, computer codes, and application methodologies. The ZIRLO™ cladding material is being introduced as an adjunction to the existing CENP OPTIN (optimized Zircaloy-4) cladding material currently in use, not as a replacement for it.

This topical report provides an integrated description of the incorporation of the Westinghouse developed ZIRLO™ cladding material into CENP fuel assembly designs. ZIRLO™ material properties are documented in NRC approved Westinghouse Electric Company topical reports. CENP has confirmed the range in the Westinghouse developed properties and data to also cover CENP's implementation. Similarly, Westinghouse performed data reduction and correlation development activities, including the definition of property uncertainties, in a specific manner which has also been confirmed to be compatible with CENP's intended application. Finally, CENP design and licensing safety analysis activities require the application of performance criteria or limits, which have been NRC approved for the CENP Zircaloy-4 cladding material, and have been confirmed to be consistent with, and applicable to, ZIRLO™ cladding as well. Following this extensive evaluation, CENP has concluded that application of ZIRLO™ in its existing fuel designs is straightforward and will not result in any surprises nor undesirable changes in predicted fuel performance or safety analysis results. To the contrary, use of ZIRLO™ results in significant improvements in waterside corrosion and provides a desirable and robust addition to CENP fuel designs. While modifications are required to include the ZIRLO™ option, no modifications are required to already NRC accepted ZIRLO™ properties or CENP application methodologies, design performance criteria, or regulatory acceptance criteria.

This topical report, with NRC approval, in combination with the applicable references discussed within each section constitutes justification for implementation of ZIRLO™ cladding material into CENP fuel designs and analysis methodologies.

TABLE OF CONTENTS

List of Tables

List of Figures

List of Acronyms

Acronym	Definition
AOO	Anticipated Operational Occurrence
CEA	Control Element Assembly
CEDM	Control Element Drive Mechanism
CENP	CE Nuclear Power LLC
DEG/PD	Double-Ended Guillotine/Pump Discharge
DNB	Departure from Nucleate Boiling
DPH	Diamond Pyramid Hardness
ECCS	Emergency Core Cooling System
EM	Evaluation Model
EOL	End Of Life
FDI	Fuel Duty Index
FSAR	Final Safety analysis Report
HFP	Hot Full Power
HZP	Hot Zero Power
LBLOCA	Large Break Loss-of-Coolant Accident
LHR	Linear Heat Rate
LOCA	Loss of Coolant Accident
LTA	Lead Test Assemblies
NCLO	No-Clad-Lift-Off
NRC	Nuclear Regulatory Commission
OFA	Optimized Fuel Assembly
OPTIN™	Optimized Process Low Tin Zircaloy-4
PCT	Peak Cladding Temperature
PLHGR	Peak Linear Heat Generation Rate
PTM	Power-to-Centerline Melt
PWR	Pressurized Water Reactor
RCP	Reactor Coolant Pump
RCS	Reactor Coolant System
S2M	Supplement 2 Evaluation Model
SAFDL	Specified Acceptable Fuel Design Limit
SBLOCA	Small Break Loss-of-Coolant Accident
SER	Safety Evaluation Report
SIT	Safety Injection Tank
SRP	Standard Review Plan
STD	Standard
UO_2	Uranium Dioxide
Westinghouse	Westinghouse Electric Company LLC

1.0 Purpose

This report describes the implementation of Nuclear Regulatory Commission (NRC) approved Westinghouse Electric Company developed ZIRLO™ fuel rod cladding material properties and correlations in the NRC approved CE Nuclear Power LLC (CENP) design and licensing analysis procedures. These procedures include analyses, computer codes, and application methodologies. ZIRLO™ cladding properties and correlations are implemented in addition to the existing CENP Zircaloy-4 properties and correlations currently in use.

Following extensive evaluation, CENP has concluded that the application of these ZIRLO™ properties is straightforward and does not result in any surprises nor undesirable changes in predicted fuel performance. While modifications are required to certain computer codes and analyses, no modifications are required for application methodologies or to performance criteria.

Use of ZIRLO™ fuel rod cladding results in significant improvements in waterside corrosion and provides a desirable and robust addition to CENP nuclear fuel designs.

2.0 Background

ZIRLO™ material properties are provided in NRC approved Westinghouse topical reports in several different formats consistent with Westinghouse requirements. Some correlations are presented with the measured property data, and some property data are in the form of tabular and/or graphical presentation. All measured properties cover a specific range of independent variables (i.e., temperature, stress, neutron flux and fluence, etc.). The range in the data has been confirmed to adequately cover CENP's implementation requirements as well. Measurements were made in a specific manner that has also been confirmed to be consistent and compatible with the intended implementation. Similarly, Westinghouse has performed data reduction and correlation development, including the definition of property uncertainties, in a specific manner that is also compatible with CENP's intended implementation. Finally, CENP design and licensing analysis activities require the application of performance criteria or limits, which have been NRC approved for CENP for Zircaloy-4, and have been demonstrated to be consistent with, and applicable to, ZIRLO™ behavior.

This report collects and summarizes the ZIRLO™ material properties as they pertain to fuel rod cladding material and provides an evaluation of those properties and correlations CENP intends to use in design and licensing analysis activities. Specific topical reports impacted by the implementation of ZIRLO™ cladding are identified and descriptions of required substitutions for implementing ZIRLO™ are provided. Furthermore, licensing analysis examples are provided which describe the specific changes anticipated in individual performance parameters and demonstrate that the impact is acceptable and does not result in any ZIRLO™ operational surprises in CENP fuel designs.

The evaluations include the Fuel Performance, Mechanical Design, Emergency Core Cooling System (ECCS) Performance Analysis (Loss of Coolant Accident (LOCA)), Non-LOCA Transient Analysis, and Nuclear Engineering (Physics) disciplines. The methodologies employed within this group of disciplines are themselves individually discussed and have been reviewed and accepted for use by the NRC via more than a dozen separate topical reports and their respective NRC Safety Evaluation Reports (SERs). One of the purposes of this report is to provide, in one place, the information needed for ZIRLO™ implementation, thereby precluding

the need for revision by CENP, and review by the NRC, of the dozen or more individual topical reports. The affected individual topical reports and associated NRC SERs are, and will, remain the licensing basis for their subject methodology. Detailed report cross-references are provided, for both users and NRC reviewers, delineating where the original comparable Zircaloy-4 cladding material discussions occur in these individual underlying base methodology topical reports. It is important to note that the methodology discussions provided herein do not supercede the original methodology discussion and justifications found in the referenced underlying base topical reports upon which the NRC's acceptance was originally formulated. Methodology discussions provided herein are only meant to provide a basic understanding of the methodology so that justification for implementation of ZIRLO™ cladding material properties into that methodology can be understood. That is, ZIRLO™ cladding material has already been accepted for use by the NRC for use in conjunction with Westinghouse design and safety analysis methodologies and nothing herein should be construed to change in any way the underlying ZIRLO™ topical reports or their NRC acceptance. Likewise, CENP design and safety analysis methodologies have already been accepted for use by the NRC, albeit for OPTIN™ cladding material, and nothing herein should be construed to change in any way the underlying methodology topical reports or NRC acceptance. This topical report simply brings together these previously NRC accepted topical reports and explains their linkage (i.e., ZIRLO™ into CENP fuel designs and safety analysis methodologies). Nothing in any of the previously NRC approved topical reports has been changed save the linking of the information in one to the other for the purpose of gaining NRC approval for the use of ZIRLO™ clad material in CENP designed fuel assemblies and the analysis of those fuel assemblies and the cores in which they reside.

Thus, this topical report, with NRC approval, in combination with the applicable references discussed within each subsequent section constitutes justification for CENP to implement ZIRLO™ cladding into the CENP fuel designs.

3.0 ZIRLO™ Fuel Design Features in CENP Plants

The purpose of this section is to provide an overview of ZIRLO™ fuel rod cladding material implementation in CENP designed nuclear fuel assemblies and to provide justification for full batch implementation. Full batch implementation is based on significant Westinghouse experience with the successful performance of fuel assemblies with ZIRLO™ cladding in either Zircaloy-4 or ZIRLO™ structural components. In addition to the Westinghouse experience, this section presents similar CENP experience with advanced cladding alloys and structural components which are similar to ZIRLO™. Finally, the recent industry trend toward more severe fuel rod duty cycles has been evaluated and compared to Westinghouse fuel duty experience with ZIRLO™ performance in Westinghouse designed fuel. It is shown that CENP implementation is bounded by the Westinghouse ZIRLO™ experience. Thus, the significant amount of in-reactor experience and available test data supports full batch implementation of CENP designed ZIRLO™ clad fuel.

3.1 ZIRLO™ Fuel Rod Cladding

ZIRLO™ is a Westinghouse proprietary modification of Zircaloy-4 material achieved by reducing the tin and iron content, eliminating the chromium content, and adding one percent niobium. OPTIN™ is the cladding material currently used in CENP fuel designs and is an Optimized Process Low Tin cladding that falls within the overall Zircaloy-4 material specification. The ZIRLO™ material composition and properties are described in Appendix A of Reference 3-1 and OPTIN cladding in Section 1-5 of Reference 3-3. The following table compares the two alloys:

Element	ZIRLO Alloy	CENP OPTIN
Sn, wt%	0.8-1.2	1.2-1.44
Fe, wt%	0.09-0.13	0.18-0.24
Cr, wt%	-	0.07-0.13
Nb, wt%	0.8-1.2	-
O, wt%	0.08-0.16	0.10-0.16
Zr, wt%	Balance	Balance

The changes in levels of tin, chromium, and niobium have an impact on the two-phase transformation temperatures. Tin is an alpha phase stabilizer, and chromium and niobium are beta stabilizers. However, niobium is a stronger beta stabilizer than chromium (a weak stabilizer). The net result is that compared to OPTIN, ZIRLO™ has lower two-phase transformation temperatures. Measurements performed at the Westinghouse Research Laboratories show that ZIRLO™ starts the transformation at 750° C and ends at 940° C. This compares to temperatures of 815°C and 970°C for Zircaloy-4. Since both the ZIRLO™ and OPTIN alloys are about 98 percent zirconium, the properties of the two alloys are not significantly different, except to the extent that they are affected by the differences in the phase change temperatures and tube manufacturing process.

The reports describing the ZIRLO™ properties and models and NRC approvals are given in References 3-1, 3-2 and 3-8. The implementation of the ZIRLO™ properties and models in CENP methods and the impact of ZIRLO™ on Fuel Performance, Mechanical Design, ECCS Performance, Non-LOCA Accidents and Nuclear Design are discussed in the remaining sections of this report.

3.2   Fuel Assembly Structural Materials

The ZIRLO™ cladding described in Section 3.1 will be implemented in CENP 14x14 and 16x16 fuel designs. Currently, CENP fuel designs utilize OPTIN cladding in Zircaloy-4 structural components. The Zircaloy-4 material used for mixing and non-mixing vane spacer grids, guide tubes, and end fittings are not being changed to ZIRLO™ in conjunction with the cladding material change. CENP has extensive successful experience with the current Zircaloy-4 structural component materials. No changes are being made to these materials at this time.

3.3   Applicable Westinghouse Experience Data Base

The ZIRLO™ cladding material described in Section 3-1 is in widespread use domestically in at least 38 Westinghouse designed nuclear power plants, as of the end of 1999. Table 3.3-1 summarizes the ZIRLO™ operating experience for cladding, guide tubes, and spacer grids.

Figure 3.3-1 provides a forecast of the number of plants expected to use ZIRLO™ in regions and full core applications in the future. Table 3.3-2 provides a summary of the high burnup experience of ZIRLO™ as of July 1999 and Table 3.3-3 summarizes the current LTA programs.

ZIRLO™ has improved corrosion resistance compared to Zircaloy-4 [

] Also, no oxide spalling has been observed in current ZIRLO™ fuel for either low or high duty operation. Westinghouse has also implemented over[

] Further discussion on grid-to-rod fretting is provided in Section 5.4.7.

3.4 ZIRLO™ Cladding and Fuel Duty Considerations

There has been an industry trend toward greater Pressurized Water Reactor (PWR) plant operating efficiencies over the last decade. The economic benefits derived from higher power ratings, extended burnups, and higher operating temperatures have led to aggressive fuel duty conditions, characterized by high fuel rod surface temperatures, with subcooled boiling, and high power densities at ever-greater residence times. Such harsher core environments have placed greater demands on fuel than ever before.

More demanding PWR fuel duties have necessitated closer evaluation of the corrosion resistance of fuel cladding materials. It has been common practice within the nuclear industry to present experimental fuel rod corrosion data as plots of the maximum oxide measured on a fuel rod versus the fuel rod average burnup. This type of plot is a convenient way to represent the data, since the measured oxide and burnup data are readily available. However, this representation of the data can be misleading. The plots show the range of burnups and thickness for which corrosion data are available. However, only limited conclusions about corrosion performance can, or should, be drawn from these plots.

3-3

Fuel rod corrosion is only a weak function of burnup, through the dependence on the fast flux. It is primarily a function of time at temperature. There are factors such as fast flux, coolant lithium concentration, boiling duty, cladding microstructural instability, and cladding hydrogen levels that may enhance the in-pile thermal corrosion rate compared to the out-of-pile thermal corrosion rate. However, these factors tend to increase the overall sensitivity of the in-pile corrosion rate to temperature variations, not to decrease it.

Fuel rod corrosion does increase with burnup, because burnup increases with time, a primary variable. However, for a given burnup and cladding type the corrosion can vary substantially due to other factors. These factors include the coolant inlet temperature, the coolant flow rate, the power peaking factors, adjacent rod powers, and the number of cycles, or time, taken to achieve the burnup. Corrosion values of the same cladding type obtained from two different reactors at equal burnups may vary substantially even though in both cases the cladding is behaving exactly as expected. This makes it very difficult to compare the relative merits of cladding types irradiated in different reactors, or even with different fuel management schemes within the same reactor.

Westinghouse has investigated alternatives to presenting corrosion data as a function of burnup. After some investigation, a term was identified which is called the Fuel Duty Index (FDI). FDI is defined as

$$FDI = \{(T_{avg} - 580)/100) \cdot (Hrs/1000)\}^2 \qquad (3-1)$$

where

T_{avg} = Time averaged oxide layer surface temperature, ^0F

Hrs = Total Irradiation time, hours

Comparisons of measured corrosion values illustrate that simple relationships exist between the measured corrosion values and the FDI. These relations exists for all grid spans of the fuel rod, not just the peak corrosion span, for reactors with different thermal duties, and for different fuel cycling schemes. Figure 3.4-1 is a plot of measured oxide thickness versus FDI for ZIRLO™ cladding. Further detail on the development of the FDI model can be found in Reference 3-4.

Corrosion data for ZIRLO™ cladding that was recently measured on lead test assemblies (LTA) have shown different behavior with respect to the FDI than was shown by earlier data. There are several groups of data that show significant deviations from a linear relation between measured oxide thickness and FDI. [

]

The deviations were associated with significant boiling during multiple irradiation cycles. [

]

When the cladding is in boiling, the surface temperature is essentially constant at a few degrees above the saturation temperature and the FDI becomes independent of the heat flux. It is known that the corrosion rate is dependent on the boiling rate. Thus, an additional term was added to the FDI to account for the increase in duty under boiling conditions. Since corrosion rate depends on the boiling rate, [

]

A modified FDI, [

]

A plot of the measured oxide thickness versus the modified FDI is shown in Figure 3.4-2. There is a much better overall trend of measured thickness with the modified FDI. Figure 3.4-2 represents the current corrosion performance versus fuel duty for the current ZIRLO™ cladding database.

3.5 Full Batch Implementation of ZIRLO™ Cladding in CENP 14x14 and 16x16 Fuel Designs

Full batch implementation of ZIRLO™ cladding may be implemented for the following CENP 14x14 and 16x16 fuel designs:

Array Size	Grid Design	Mixing Vanes	Spring Design	Pellet Design
16x16	STD	No	Cantilevered	Standard Pellet
16x16	STD	No	Cantilevered	Value Added Pellet
14x14	STD	No	Cantilevered	Value Added Pellet
14x14	Turbo	Yes	"I" Spring	Value Added Pellet

The Zircaloy-4 Standard (STD) grid is the current spacer design used in CENP 14x14 and 16x16 fuel designs. The STD grid does not use mixing vanes and utilizes a cantilevered type grid spring. The Zircaloy-4 Turbo grid is a next generation type spacer design for the 14x14 geometry. A next generation type spacer grid may also be considered for use in the 16x16 geometry in the future. The 14x14 Turbo grid is scheduled for initial full batch implementation in Calvert Cliffs Unit 1 in the Spring of 2002. The Turbo grid uses mixing vanes to improve Departure from Nucleate Boiling (DNB) performance and an "I" spring (vertical type) to improve grid-to-rod fretting resistance. The "I" spring contains increased contact length and is cold-worked so the spring grows outward toward the fuel rod (due to irradiation), thus maintaining contact with the fuel rod. Further details on Turbo grid fuel is described in Reference 3-5. Both grid types have demonstrated good wear performance in-reactor. The STD grid has been used at least 30 years in-reactor with some fuel failures (with low safety significance) due to loose cells [

] For Turbo grid fuel, recent LTA examinations have shown a significant improvement in fuel rod wear performance compared to STD grids for symmetric assemblies adjacent to the core shroud. The implementation of ZIRLO™ cladding in both STD and Turbo grid designs may produce a reduction in wear margin relative to OPTIN cladding due to the reduced axial growth and oxide thickness of the ZIRLO™ cladding. However, it is expected that this reduction in wear margin can be accommodated in the initially planned fuel designs, similar to what was observed

when ZIRLO™ was implemented in the Westinghouse OFA grid design. Further discussion on grid-to-rod fretting is provided in Section 5.4.7.

CENP has implemented different advanced cladding materials in LTAs utilizing the STD and Turbo grid designs. Table 3.5-1 summarizes these LTA test programs. In these test programs fuel rod wear measurements have been made which demonstrate negligible wear differences due to the use of the advanced cladding materials. [

] Table 3.5-2 summarizes the differences in chemical compositions of the different advanced cladding materials evaluated. Even though the composition of the advanced cladding materials used in these LTAs are not exactly the same as ZIRLO™ cladding, the wear performance for ZIRLO™ is expected to be similar [

]

CENP uses two different type of fuel pellet designs, standard and value added. The value added fuel pellet contains smaller end dishes, an increased diameter, and a slight increase in density to increase uranium loading compared to the standard fuel pellet design. The FATES3B fuel performance code will be used to evaluate both pellet designs in the reload analysis with the ZIRLO™ cladding.

ZIRLO™ cladding is more robust than OPTIN cladding due to its improved corrosion resistance and lack of oxide spallation. [

] Typical maximum FDI values for CENP plant designs were evaluated using the methodology described in Section 3.4. [

] Therefore, the application of ZIRLO™ in CENP plants is well within the ZIRLO™ database shown in Figure 3.4-2.

3.6 ZIRLO™ Application to High Burnup

ZIRLO™ has been approved by the NRC as an acceptable cladding material and is licensable to a peak rod average burnup of 62 MWd/kgU (References 3-1, 3-2, and 3-8). Furthermore, ZIRLO™ cladding has been shown to be capable of significantly higher burnups than 62 MWd/kgU because of its resistance to waterside corrosion and improved dimensional stability

under irradiation. CENP burnup application will remain consistent with approved burnups for the CENP fleet of plants as described below.

3.6.1 Application to NRC Approved 60 MWd/kgU Peak Pin Burnup

The current NRC approved 1-pin peak burnup limit for the CENP 14x14 fuel design is 60 MWd/kgU, Reference 3-6. Similarly, the approved 1-pin peak burnup limit for the CENP 16x16 fuel design is also 60 MWd/kgU, Reference 3-7. Consequently, CENP will limit ZIRLO™ cladding to a 1-pin peak burnup of 60 MWd/kgU, even though it has demonstrated acceptable performance in excess of this value.

3.6.2 Application to 62 MWd/kgU in Conjunction with CENP High Burnup OPTIN Topical

Reference 3-3 provided the justification for extending the operation of CENP PWR fuel designs to peak pin burnups in excess of 60 MWd/kgU. Although Reference 3-3 requested a peak burnup of 65 MWd/kgU, it is now understood by CENP that burnup will be limited for the foreseeable future by the NRC to 62 MWd/kgU. As documented in Reference 3-3, it was intended that OPTIN cladding only be irradiated to burnups in excess of 60 MWd/kgU under operating conditions characterized as low duty. It is recognized that if the duty cycle is too severe, one or more of the design and safety analysis criteria could be threatened. Consequently, it became necessary to define the low duty application of Reference 3-3 in order to continue forward. Efforts to successfully define low duty and obtain approval of Reference 3-3 are in progress.

Design and licensing issues for extending peak burnups above 60 MWd/kgU have been addressed in Reference 3-3 for the other fuel assembly components. The models related to the fuel stack, for example, were shown to be valid and acceptable to [   ] The response of the fuel assembly and structural components to extended burnup were also shown to be acceptable. Therefore, the substitution of a more robust cladding material such as ZIRLO™ supports the successful operation to 62 MWd/kgU without duty limitations. Existing duty cycles are within the successful experience database for ZIRLO™ cladding.

3-8

Consequently, it is expected that NRC approval of Reference 3-3 will be consistent with the restriction that the 1-pin burnup limit of CENP plants utilizing ZIRLO™ cladding will be 62 MWd/kgU and that the low duty cycle defined for OPTIN will not be applied to CENP fuel assemblies that utilize ZIRLO™ cladding.

3.7 References

3-1   WCAP-12610-P-A, "Vantage+ Fuel Assembly Reference Core Report," April 1995.

3-2   WCAP-15063-P-A, Rev. 1 w/errata, "Westinghouse Improved Performance Analysis and Design Model (PAD 4.0)," July 2000.

3-3   CENPD-388-P, "Extension of the 1-Pin Burnup Limit to 65 MWd/kgU for ABB PWR Fuel with OPTIN cladding," February 1998.

3-4   R. S. Kaiser, W. J. Leech, A. L. Casadei, "The Fuel Duty Index (FDI) – A New Measure of Fuel Rod Cladding Performance," Light Water Reactor Fuel Performance Conference Proceedings, Park City Utah, April 10-13, 2000.

3-5   Z. E. Karoutas, "Supporting Test Data and Analysis for ABB CE's TURBO™ PWR Fuel Design" presented at 12th Annual KAIF/KNS Conference, April 3-4, 1997, in Seoul Korea.

3-6   CEN-382(B)-P-A, "Verification of the Acceptability of a 1-Pin Burnup Limit of 60 MWD/kgU for Combustion Engineering 14x14 PWR Fuel," August 1993.

3-7   CEN-386-P-A, "Verification of the Acceptability of a 1-Pin Burnup Limit of 60 MWD/kgU for Combustion Engineering 16x16 PWR Fuel," August 1992.

3-8   WCAP-12488-A, "Westinghouse Fuel Criteria Evaluation Process," October 1994.

Table 3.3-1

ZIRLO™ Operating Experience

Table 3.3-2

ZIRLO™ High Burnup Experience

Table 3.3-3

Summary of Westinghouse LTA Programs

Table 3.5-1
CENP PWR Lead Fuel Programs

[

]
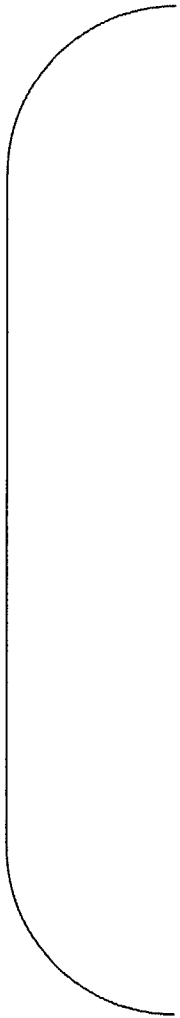
Table 3.5-2

Chemical Compositions of Cladding Alloys

Figure 3.3-1

Figure 3.3-1

ZIRLO Cladding in Westinghouse-Fueled PWRs

Figure 3.4-1 ZIRLO Measured Oxide Thickness vs. Fuel Duty Index
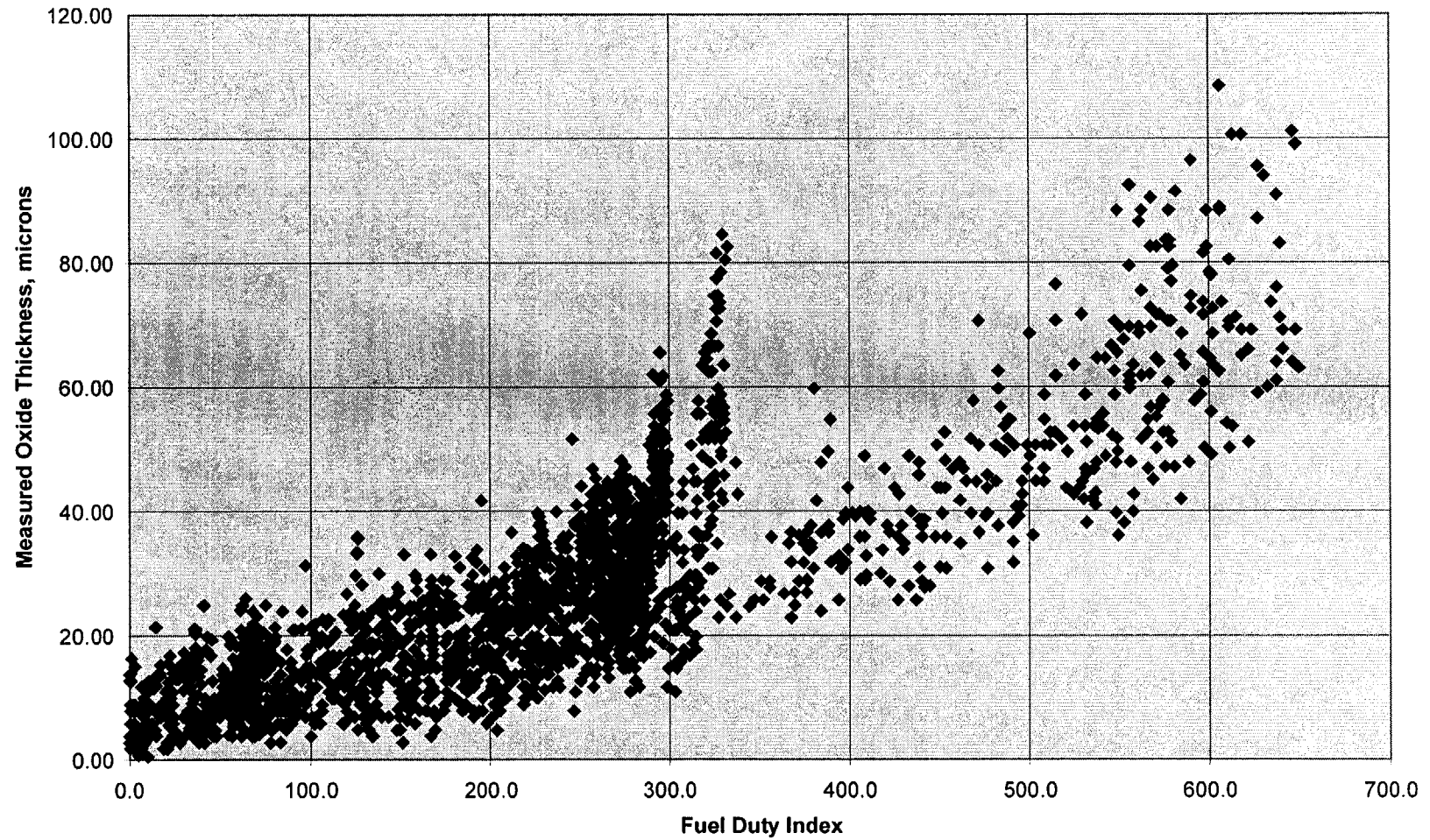
Figure 3.4-2 ZIRLO Measured Oxide Thickness vs. Modified Fuel Duty Index

4.0 Fuel Performance

4.1 Introduction

Reload fuel performance design and safety analyses are performed with the FATES3B computer code. FATES3B is applied to uranium dioxide (UO_2) fuel pellets, erbia bearing UO_2 fuel pellets, and gadolinia bearing UO_2 fuel pellets. Historically, the cladding material was Zircaloy-4. Following acceptance of the Westinghouse developed ZIRLO™ cladding material for use the NRC incorporated ZIRLO™, along with Zircaloy, into the pertinent sections of Title 10 of the Code of Federal Regulations. Westinghouse developed ZIRLO™ cladding material properties and correlations have been added to the FATES3B code. FATES3B is used for thermal performance evaluations under normal operation considering steady-state and anticipated transient conditions. The power-to-centerline melt Specified Acceptable Fuel Design Limit (SAFDL) and maximum pressure SAFDL are shown to be met using FATES3B. Additionally, FATES3B is used to generate initial fuel/clad conditions for other design analyses, transient analyses, and accident analyses. A separate procedure for the prediction of fuel rod deformation and burst behavior under conditions of DNB for the purpose of evaluating DNB propagation has been developed. This procedure, which handles accumulation of large deformations, is a standalone computer code called INTEG (INTEGration). INTEG has also been modified to handle high temperature ZIRLO™ creep and burst behavior.

A summary of the CENP Zircaloy-4 cladding material model and property descriptions, pointing to associated topical reports, is provided in Section 4.2. ZIRLO™ properties and correlations for FATES3B are described in Section 4.3. Section 4.3 also provides a justification and description for the applications in FATES3B. High temperature correlations used in INTEG and justification for the ZIRLO™ correlations are described in Section 4.4. Waterside corrosion is described in Section 4.5. Finally, Section 4.6 provides a discussion of the expected influence of ZIRLO™ on the performance parameters for typical CENP 14x14 and 16x16 fuel designs.

4.2 Summary of Cladding-Related Models in the Fuel Performance Evaluation Models

This section provides an overview of the fuel performance models pertaining to the fuel rod cladding which are used in design and licensing analyses. Fuel performance analyses are performed with the fuel performance code FATES3B, References 4-1, 4-2, and 4-3. The no-clad-lift-off (NCLO) maximum pressure criterion with justification for fuel rod operation with maximum internal hot gas pressure in excess of the reactor coolant system (RCS) pressure is described in Reference 4-4. The evaluation of maximum internal hot gas pressure during normal operation and the calculation for the maximum allowable internal pressure to meet a NCLO criterion is performed with FATES3B. A consequence of operation with higher than RCS pressure is the possibility of fuel rod ballooning under DNB and propagating DNB conditions to adjacent fuel rods. DNB propagation evaluations for transients and DNB accidents are performed with the INTEG code. High temperature cladding properties used in INTEG are described in Reference 4-4. DNB propagation evaluations are performed when the internal pressure exceeds nominal RCS pressure during normal operation. Other fuel models related to the additions of the burnable absorber materials erbia and gadolinia are described in References 4-5, 4-6, and 4-7. Design and licensing applications of the FATES3B and INTEG computer codes described in References 4-8 and 4-9 include:

- maximum internal hot gas pressure
- critical pressure for NCLO
- fission gas release (mechanical design evaluations)
- minimum internal gas pressure (mechanical design evaluations)
- power-to-centerline melt
- initial hot and average fuel rod conditions in hot assembly (LOCA and non-LOCA evaluations)
- engineering factor on LHR and stored energy
- core average densification factor
- fuel stored energy for containment analysis
- maximum fuel-clad gap conductance
- minimum fuel-clad gap conductance
- maximum internal gas pressure in spent fuel pool
- temperature-power correlations for physics

- high temperature creep and rupture for DNB propagation

A summary of the NRC accepted CENP topical report references which contain cladding properties and correlations used for fuel performance analyses is given in Table 4.2-1. Sections of these reports where the cladding properties and correlations are described and/or description of clad behavioral models where they are used are identified within the table. The cladding properties and correlations as described herein will be applied for reload fuel batches in CENP designed nuclear power plants where ZIRLO™ is used. This ZIRLO™ report is consistent with the historically established process of submitting individual reports on new materials when introduced into CENP fuel designs.

4.3   ZIRLO™ Properties for FATES3B Fuel Performance

An important behavior of fuel rod cladding is the creep deformation. Cladding creep is important during fuel-clad gap closure (compressive creepdown and gap thermal response) and is important during postulated pressure induced outward creep (tensile creep) during the later life of the fuel rod. Typically, tensile creep might occur after sufficient fission gas has been generated and released to the fuel rod plenum to result in the potential for pressure induced fuel-clad separation during normal operation. Such fuel-clad separation is considered to be a potential damage condition (possibly leading to failure) and is prevented by imposing the maximum pressure NCLO criterion. Also, high temperature tensile creep and potential bursting is important during DNB transients. Ballooning of the fuel rod is evaluated to determine the extent of DNB propagation to adjacent fuel rods from fuel rods initially in DNB due to degraded thermal-hydraulic conditions that exist during the transient.

A second important characteristic of the cladding is waterside corrosion behavior. ZIRLO™ cladding material is more resistant to corrosion than standard Zircaloy-4 or OPTIN™ and results in an improved and, therefore, acceptable performance in CENP nuclear fuel designs.

The third important property of the cladding which affects fuel performance is axial growth of the fuel rod because growth has an impact on the plenum volume available for fission gases released from the fuel pellets. Consequently, axial growth directly impacts internal gas pressure.

Additional cladding properties and correlations considered in CENP fuel performance are thermal conductivity, thermal expansion, elastic modulus, surface hardness (DPH), hemispherical emittance, and the Poisson's ratio. These properties play a minor role in the resulting thermal performance of ZIRLO™ compared to OPTIN.

ZIRLO™ cladding properties and correlations are individually discussed in the sections that follow.

It should be noted that certain dimensional characteristics of ZIRLO™ cladding affecting fuel performance are handled via analysis input parameters and are based on manufacturing tolerances, or are based on as-built measurements on a case-by-case basis if needed or desirable. Examples of these characteristics include surface roughness and fuel rod diametral or length tolerances. These dimensional characteristics are expected to be similar or identical to OPTIN cladding and are not discussed further herein. Section 4.6 evaluations performed to assess the effect of ZIRLO™ on CENP fuel performance presume identical values for these characteristics. Implementation of ZIRLO™ cladding in a reload batch will necessarily utilize the specific ZIRLO™ dimensional characteristics if they differ from those of OPTIN used in the evaluations.

4.3.1 ZIRLO™ Cladding Creep Correlations

The creep correlation for ZIRLO™ cladding (Reference 4-10) is empirical and is based on clad diametral creepdown deformation measurements which generally follow the first cycle of irradiation. First cycle creepdown measurements are used in order to eliminate or minimize pellet-clad interaction effects. Data for ZIRLO™ has been obtained from fuel rodsIrradiated [

] The form of the correlation is based on a large combined Westinghouse database for ZIRLO™ and Zircaloy-4 cladding types as described in Reference 4-10. [

] The ZIRLO™ creep correlations are incorporated into FATES3B as a user specified cladding option.

The relationships between loads and stresses are straightforward during the creepdown phase because there is no pellet-clad interaction, and loads are simply the internal gas pressure and

external system pressure. Similarly, the relationships under NCLO conditions are simple internal gas pressure versus external pressure. However, during pellet-clad interaction, the relationship is complicated. The pellet-clad interface conditions are not unique, well established conditions and, to a large extent, require somewhat arbitrary modeling assumptions on the interaction mechanisms. These assumptions include interface friction, possible pellet-clad lock-up (either locally or elsewhere along the fuel column), fuel-clad bonding, and even pellet mechanical response to an interference load (e.g., several pellet inelastic deformation mechanisms exist). There is a wide range of potentially reasonable models and, consequently, stress results. Several observations concerning potential fuel-clad interface conditions are applicable here:

(1)   The ZIRLO™ creep correlation is based on a fit to diameter measurements without pellet-clad interaction. Thus, the presence of a contact load is not relevant to the correlation's coefficients.

(2)   Application in FATES3B for creepdown does not involve pellet-clad interaction.

(3)   Application for outward creep for NCLO in FATES3B does not involve pellet-clad mechanical interference.

(4)   The creep correlation has no impact on axial deformations in FATES3B. Axial deformation of the fuel rod is based on the empirical rod growth correlation.

(5)   No pellet inelastic deformation models are used in FATES3B. Thus, the pellet forces the cladding outward at the restrained pellet swelling rate. Stress in the cladding automatically reaches an equilibrium condition with the required deformation regardless of the pellet-clad interface model used.

(6)   Cladding deformation during pellet clad contact has an insignificant impact on thermal performance or internal gas pressure.

Consequently, although the stress and strain formulations for ZIRLO™ creep correlations must be consistent with the development of the creep correlation, the mechanical interface model between pellet and cladding can and is independent. The stresses for ZIRLO™ cladding are obtained from the conventional thick-wall cylinder equations, consistent with model development.

The ZIRLO™ creep correlation, Reference 4-10, consists of two conventional components, irradiation creep and thermal creep. [

]

[   ]   (4-1)

The accumulated thermal creep strain is given by

[   ]   (4-2)

where

[   ]   (4-2a)

[   ]   (4-2b)

The thermal creep rate is obtained by differentiating Equation 4-2

[·]   (4-3)

where

[   ]   (4-3a)

[   ]   (4-3b)

[   ]   (4-4)

The definitions of variables in the above equations are

[

                                                                    ]

                          [.   ]   (4-5)

                              [   ]   (4-6)

[

                          [   ]   (4-7)

                              [   ]   (4-8)

The combined irradiation and thermal creep rate is

                              [   ]   (4-9)

[

]

[

]

[

(4-10)

] (4-10a)

and

[   ]

[   ]

A comparison of measured ZIRLO™ creepdown with predicted creepdown from FATES3B is provided in Section 4.3.6 to verify that the application is acceptable.

4.3.1.1   Thick-Wall Cylinder Stress Equations

Cladding stress used in the ZIRLO™ creep correlation development is determined from the classical elastic solution for a pressurized thick-wall cylinder. Although the stresses within the wall of a pressurized thick-wall cylinder are 3-dimensional, [

] Thus, the same thick-wall relationships must be applied in FATES3B to properly simulate creep behavior.

The classical thick-wall stress components in the circumferential, radial, and axial directions are given by

$$\sigma_\theta = \frac{P_g + P_c - k^2 P_s}{k^2 - 1} + \frac{P_g + P_c - P_s}{k^2 - 1} \frac{R_o^2}{r^2} \tag{4-11}$$

$$\sigma_r = \frac{P_g + P_c - k^2 P_s}{k^2 - 1} - \frac{P_g + P_c - P_s}{k^2 - 1} \frac{R_o^2}{r^2} \tag{4-12}$$

$$\sigma_z = \frac{P_g + P_c - k^2 P_s}{k^2 - 1} \qquad (4\text{-}13)$$

$$k = \frac{R_o}{R_i} \qquad (4\text{-}14)$$

P_g = fuel rod internal gas pressure, psia

P_c = pellet-clad mechanical interference pressure, psia

P_s = reactor coolant system pressure, psia

R_o = cladding outer radius, inches

R_i = cladding inner radius, inches

r = radial position within cladding, inches

Stress components [   ] are obtained by substitution of

[   ] $\qquad (4\text{-}15)$

4.3.1.2 Equivalent Stress-Strain Relationships

The cladding circumferential stress used in the creep equations is given by

[   ] $\qquad (4\text{-}16)$

where

[   ]

4-10

[

]

[ ] (4-17)

[

]

[ ] (4-18)

[

]

[

.]

4.3.1.3 Isotropy and Prandtl-Reuss Equations

[

]

[ ] (4-19)

[.]

Substituting stress component equations from Section 4.3.1.1 into Equation 4-19 results in

4-11

[   ]   (4-20)

Use of Equation 4-20 in FATES3B is consistent with the creepdown data where creep correlation fitting coefficients are determined using measured hoop strains.

4.3.1.4   NCLO Application and Creep Rate Uncertainty

A creep rate [   ] is applied for Zircaloy-4 cladding in the CENP fuel performance analysis for NCLO critical pressure in FATES3B as described in Reference 4-4. The ZIRLO™ cladding creep rate [

] have been established in Reference 4-10 as [

] is used in the ZIRLO™ NCLO application in FATES3B.

[

]

It has been concluded that the CENP internal pressure and the NCLO analysis is quite conservative (discussed in considerable detail in Reference 4-4). Thus, any small potential differences [   ] in the stress range of interest are insignificant.

4.3.2   Fuel Rod Axial Growth

Fuel rod axial growth occurs in-reactor as a result of fast neutron irradiation. Fuel rod axial growth is applied in FATES3B to obtain clad length relative to the length of the fuel column to

determine the fuel rod end plenum length. FATES3B utilizes a best-estimate fuel rod growth model. The ZIRLO™ fuel rod growth model developed by Westinghouse was observed to be

[

] of the Westinghouse Zircaloy-4 rod growth. Since Westinghouse Zircaloy-4 fuel rod growth is given by Reference 4-19 as

$$[\qquad \qquad] \qquad\qquad (4\text{-}21)$$

[.

]

then the growth for ZIRLO™ is given by [   ] or

[   ]

Reference 4-10 further modified the axial growth of ZIRLO™ to include [

]

$$[\qquad\qquad\qquad\qquad] \qquad (4\text{-}21a)$$

$$[\qquad\qquad\qquad\qquad] \qquad (4\text{-}21b)$$

and the fuel rod axial growth is

$$[\qquad] \qquad\qquad (4\text{-}22)$$

[

]

4.3.3 Cladding Thermal Conductivity

The correlation for measured thermal conductivity of ZIRLO™ cladding material is provided in Reference 4-10. Thermal conductivity is given by

$$[\qquad\qquad\qquad\qquad] \qquad (4\text{-}23)$$

where

k = thermal conductivity, BTU/(hr-ft-°F)

T_F = temperature, °F

Thermal conductivity used in FATES3B for Zircaloy-4 (OPTIN) cladding material, Reference 4-1, is given by

$$[\qquad\qquad] \qquad (4\text{-}24)$$

This correlation for CENP OPTIN conductivity is nearly identical to ZIRLO™ conductivity over the range of interest for FATES3B and fuel mechanical design. Consequently, Equation 4-24 will be used for both ZIRLO™ and OPTIN. Thus, no modification to thermal conductivity is made in the CENP analyses.

4.3.4 Cladding Thermal Expansion

Reported thermal expansion coefficients for ZIRLO™ are anisotropic. Reference 4-12 provides the circumferential and axial thermal expansion for ZIRLO™ and Westinghouse Zircaloy-4 as

used in PAD 3.4.   Thermal expansion was not modified for ZIRLO™ as documented by References 4-10 and 4-11. The thermal expansions in the circumferential and axial directions are given by

$$[\hspace{8cm}] \hspace{2cm} (4\text{-}25)$$

$$[\hspace{8cm}] \hspace{2cm} (4\text{-}26)$$

where

ε_θ = circumferential thermal expansion, in/in

ε_z = axial thermal expansion, in/in

T_F = temperature, °F

Axial thermal expansion for FATES3B is identical to Equation 4-26 and will continue to be used. The FATES3B radial thermal expansion, Reference 4-1, is given by

$$[\hspace{8cm}] \hspace{2cm} (4\text{-}27)$$

While the form of Equation 4-27 differs from Equation 4-25, a comparison of value as a function of temperature demonstrates that the thermal expansion in the temperature range of interest (i.e., at operating conditions) is nearly identical.   Thus, Equation 4-27 will also be used for ZIRLO™ in FATES3B.

4.3.5 Other ZIRLO™ Fuel Performance Properties and Correlations

4.3.5.1   Modulus of Elasticity

The ZIRLO™ modulus of elasticity is inferred in Reference 4-12 to be the same as the PAD3.4 Zircaloy-4 and was not modified by References 4-10 and 4-11. Static moduli of elasticity are anisotropic and given by

$$[\qquad\qquad] \qquad\qquad (4\text{-}28)$$

$$[\qquad\qquad] \qquad\qquad (4\text{-}29)$$

where

E_r = radial modulus of elasticity, psi

E_z = axial modulus of elasticity, psi

T_F = temperature, °F

The modulus of elasticity used in FATES3B for OPTIN is given by

$$[\qquad\qquad] \qquad\qquad (4\text{-}30)$$

Since the value for the moduli of elasticity given by Equations 4-28, 4-29, and 4-30 do not differ significantly at cladding temperatures of interest, i.e., at operating temperatures used in design and licensing analyses, Equation 4-30 is also applied to ZIRLO™ in the CENP analyses.

4.3.5.2   Poisson's Ratio

Poisson's ratio for ZIRLO™ is anisotropic. Poisson's ratio for ZIRLO™ is inferred to be the same as the PAD 3.4 Zircaloy-4 (Reference 4-12) and has not been modified in later topical reports on ZIRLO™ (References 4-10 and 4-11). Poisson's ratio is given by

$$[\qquad \qquad] \qquad\qquad (4\text{-}31)$$

$$[\cdot \qquad \qquad] \qquad\qquad (4\text{-}32)$$

where

μ_r = radial Poisson's Ratio

μ_z = axial Poisson's Ratio

T_F = temperature, °F

FATES3B applies Equation 4-32 for OPTIN and will apply the same equation to ZIRLO™.

4.3.5.3 Hemispherical Emittance

Hemispherical emittance is a clad property applicable to the radiation heat transfer component of fuel-clad gap conductance. It is not used in Westinghouse fuel performance evaluations and has not been reported on by Westinghouse. Radiation heat transfer is not a significant contributor and, furthermore, differences in hemispherical emittance between Zircaloy-4 and ZIRLO™ would be expected to be very minor. Therefore, ZIRLO™ hemisphericalemittance will be assumed to be the same as that which CENP employs for OPTIN. The effect of this assumption is insignificant.

4.3.5.4 Diamond Pyramid Hardness (DPH)

The claddding surface hardness obtained from the diamond pyramid hardness (DPH) test is applied in the CENP fuel-clad contact conductance model. DPH is not used in the Westinghouse gap conductance model. However, contact conductance is a relatively small contributor to the overall gap conductance. Since DPH differences between ZIRLO™ and Zircaloy-4 are also expected to be small, DPH for ZIRLO™ is assumed to be the same as that which CENP employs for OPTIN. The effect of this assumption is insignificant.

4.3.6 Verification of FATES3B (Creepdown)

The review of ZIRLO™ cladding material properties and correlations described above has resulted in the conclusion that only the ZIRLO™ creep (creepdown and NCLO applications) and ZIRLO™ axial growth correlations need to be modeled in the FATES3B fuel performance computer code to adequately simulate ZIRLO™ clad fuel rod performance in CENP nuclear fuel designs. Other thermal and mechanical properties used in FATES3B are sufficiently similar to, or identical to, Zircaloy-4 (OPTIN), and do not need to be modified.

The purpose of this section is to provide verification results of comparisons between the FATES3B predictions for creepdown of the [   ] fuel rods clad with ZIRLO™ with the measured creepdown data. For this benchmarking exercise, the [   ] fuel rods which were simulated with the PAD 4.0 code, Reference 4-10, were simulated with FATES3B modified for ZIRLO™ applications. The fuel stack was also modeled in FATES3B to simulate the expected behavior of the fuel based on the PAD 4.0 simulation. The data used for benchmarking FATES3B consists of [

            ] was irradiated for one cycle to minimize or eliminate pellet-clad interaction effects. These fuel rods attained an average burnup of about [

        .] These [   ] fuel rods each experienced similar axial power shapes and peak power histories. Minor corrections were made to the diameter predictions to account for expected oxide thicknesses which were included in the Westinghouse measured diameters. Diameter measurements were made at up to [   ] of each fuel rod. However, the measurements were made at the [   ] for each rod.

A scatter plot of predicted versus measured diameter is shown in Figure 4.3.6-1 for individual measurements. These predictions are concluded to be very good. The diametral creepdown was also averaged for all [   ] fuel rods and plotted in Figure 4.3.6-2. Again, the predictions are concluded to be good. In general, the FATES3B predicted cladding creepdown for all [

                ] because the design characteristics and the power histories were nearly identical. The measured creepdown differed between individual fuel rods to a greater

degree than did the predictions. This observed behavior is not surprising and is typical of creepdown data. The maximum and the minimum creepdown distributions amongst [

] are shown in Figure 4.3.6-3 along with the FATES3B predictions for those rods. It can be seen that the predictions, which are nearly identical, are well bounded within the range of the measured data.

Thus, it is concluded that the FATES3B predictions of ZIRLO™ cladding creepdown are very good.

4.3.7   Design Criteria and Methodology Validation

Fuel rod thermal design criteria, the no-clad-lift-off (NCLO) criterion and the no centerline melt criterion, are verified as being met using the FATES3B fuel performance computer code. These criteria themselves are not impacted by the use of ZIRLO™ cladding material.

The design and licensing applications of FATES3B were summarized in Section 4.2. The introduction of ZIRLO™ cladding has no impact on the applications, application methodology, or on the conservatisms, other than the NCLO creep uncertainty of Section 4.3.1.4, defined for each application. The applications and conservatisms of the FATES3B code and analyses remain the same as described in References 4-8 and 4-9. References 4-8 and 4-9 were submitted in support of the FATES3B improvement topical reports, References 4-2 and 4-3.

A statistical analysis is employed in the determination of the engineering factor (Reference 4-1). In addition, a statistical evaluation of the uncertainty in fuel temperature predictions is employed to verify that fuel temperatures for the stored energy used for initializing Loss-of-Coolant Accidents (LOCA) evaluations bound the hot rod at a 95% probability or better. Substitution of ZIRLO™ does not alter the conservatism required to achieve a 95% probability on the stored energy.

The application of FATES3B in design and licensing analyses is [.]
Conservative [   ] is introduced through certain input parameters depending on the particular application, including [   ].

4-19

Substitution of ZIRLO™ cladding does not alter this methodology.

4.4 Application of ZIRLO™ and DNB Analysis

ZIRLO™ cladding will not impact the models and methodology for the determination of DNB. However, cladding behavior during DNB is dependent on the properties of the ZIRLO™ cladding material. A discussion of DNB analyses of CENP nuclear fuel designs using ZIRLO™ clad fuel is provided below.

4.4.1 Impact on CHF and DNBR

There is no impact on Critical Heat Flux (CHF) due to use of ZIRLO™ cladding versus OPTIN cladding. The evaluation of CHF is determined by use of a Critical Heat Flux correlation which is dependent on spacer grid design and fuel geometry. The CE-1 CHF correlation defined in References 4-20 to 4-22 and the ABB-NV CHF correlation defined in Reference 4-23 are used for evaluating CHF for CENP 14x14 and 16x16 non-mixing vane grid fuel. The ABB-TV CHF correlation defined in Reference 4-23 is used for 14x14 Turbo mixing vane grid fuel. These CHF correlations were developed based on performing 5x5 or 6x6 array CHF tests with electrically heated rods fabricated with Inconel tubing. The measurement of CHF is dependent on local coolant conditions (i.e., pressure, mass velocity, quality) and geometry parameters (i.e., channel wetted hydraulic diameter, heated perimeter, grid design, grid spacing, cold wall, etc). Cladding material has not been found to have a meaningful influence on CHF.

The Departure from Nucleate Boiling Ratio (DNBR) safety limit can be affected for any different cladding material if fabrication tolerances on fuel rod outer diameter change. Any variation in fuel rod outer diameter would have a direct impact on fuel rod heat flux and DNBR. This variation is accounted for in the heat flux engineering factor which is addressed in the evaluation of the DNBR safety limit. If there is a change in the fuel rod outer diameter tolerances for the ZIRLO™ cladding, the variation will be accounted for in CENP's methodology.

4.4.2   Impact on DNB Propagation (NCLO)

The impact of ZIRLO™ on DNB propagation is a consideration for DNB transients.   High temperature creep and rupture of ZIRLO™ cladding during DNB is modeled and accounted for in the evaluations of fuel failure and the calculations of dose consequences.

4.4.2.1   High Temperature Creep and Rupture

High temperature creep behavior of ZIRLO™, required for mechanistic DNB propagation evaluations (Reference 4-4), is obtained from Reference 4-11. High temperature creep strains were measured as a function of time on ZIRLO™ tubing under conditions of [

                                                                      ] Different deformation mechanisms were observed which depend on the stress level and phase of the material.

Strain rate is given by

                                    [   ]   (4-33)

where

[

                        .   .   ]

and

                                                [   ]

                                                            [

                                                                        ]
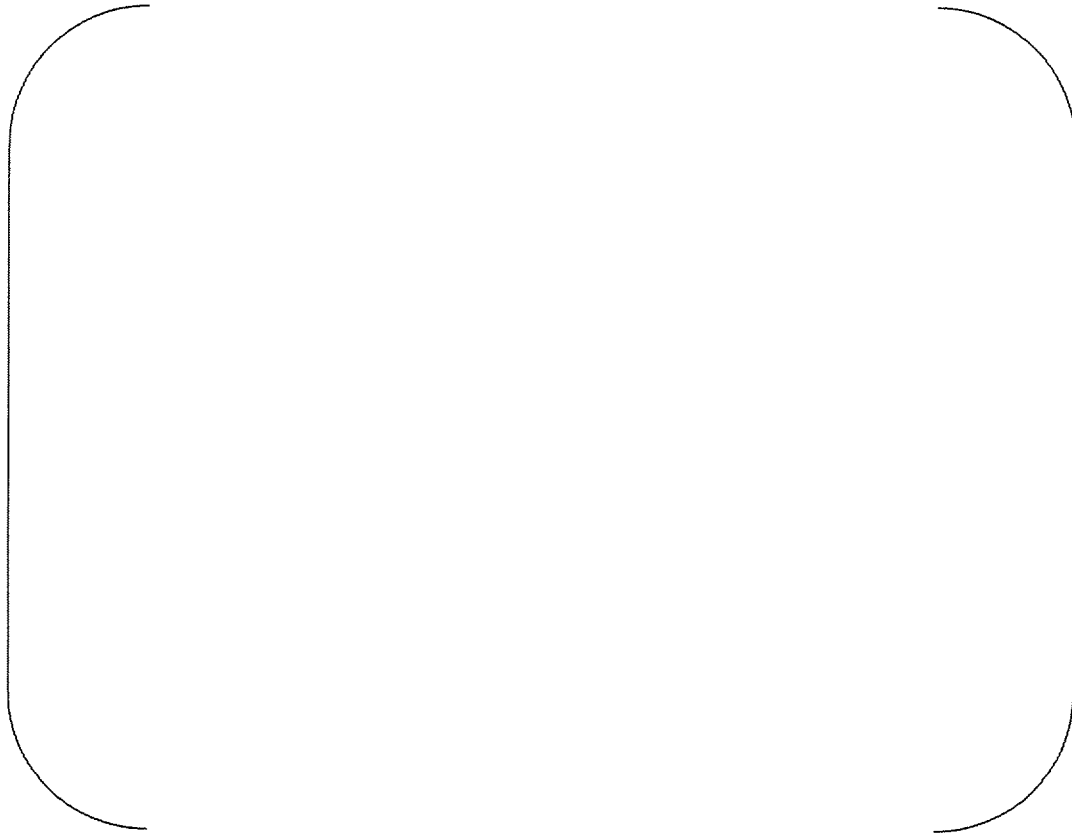
The coefficients are obtained directly from Reference 4-11. These coefficients [   ] are given in the following table for ZIRLO™:

[

] and should be calculated with the following coefficients:

[   ] creep

rates (Reference 4-11) as given by the following equations.

$$[\cdot \qquad \qquad]$$

$$[\qquad \qquad] \qquad \qquad (4\text{-}34)$$

$$[\qquad \qquad] \qquad \qquad (4\text{-}35)$$

The accumulated true strain e can be obtained from the numerical integration of Equation 4-33 and can be converted into engineering strain by the relationship

$$e = \ln(1 + \varepsilon)$$

or

$$\varepsilon = \exp(e) - 1$$

where

$\varepsilon = $ engineering strain, in/in

Since large deformations occur, the effect of an increasing diameter and a decreasing wall thickness must be included. Dimensional changes for large deformations are given by

$$D = D_o(1 + \varepsilon) \qquad \qquad (4\text{-}36)$$

$$w = \frac{w_o}{(1 + \varepsilon)} \qquad \qquad (4\text{-}37)$$

and the stress is given by

4-23

$$[\qquad] \qquad\qquad (4\text{-}38)$$

where

ΔP = pressure difference across wall, MPa

D_o = initial tube diameter, inches

w_o = initial wall thickness, inches

D = deformed diameter, inches

w = deformed wall thickness, inches

[

]

[

]

$$[\qquad\qquad] \qquad\qquad (4\text{-}39)$$

where

[

]

Creep of the cladding during a DNB transient stops if the cladding is perforated and the internal pressure is relieved. Reference 4-11 provides data on engineering burst stress (based on initial dimensions) versus temperature for ZIRLO™ cladding and is provided in the table below. If the engineering hoop stress exceeds the value in the table at the temperature shown, credit is taken for cladding rupture, and the creep strain process is terminated.

4.4.2.2   Strain Criterion for Channel Blockage

The amount of channel blockage is limited to prevent degradation of the cooling of adjacent fuel rods as described in Reference 4-4. The strain criterion for channel blockage is based on geometric effects and coolant redistribution. Although the high temperature creep behavior and rupture of ZIRLO™ may impact the kinetics of the DNB propagation evaluation, ZIRLO™ will not impact the channel blockage criterion. Reference 4-4 provides an NRC approved blockage criterion of [   ] If blockage [   ] propagation to the adjacent fuel rods is assumed. This criterion on strain, which is engineering strain, is applied to ZIRLO™ cladding.

4.4.2.3   DNB Propagation Methodology

Although not necessarily true, DNB is considered to be a fuel failure mechanism. Consequently, if DNB is predicted to occur, fuel failure is assumed and the consequences of the radiological dose are considered. DNB is not allowed during normal operation, including anticipated operational occurrences (AOOs). Core power, flow rates, etc., are monitored to ensure that DNB does not occur. However, DNB may occur during less frequent events, in which case the extent of DNB and fuel failures are ascertained. The implementation of the NCLO maximum pressure criterion results in the potential for some portion of the fuel rods to achieve internal gas pressures that are in excess of the external RCS pressure. During a DNB transient the surface temperature increases significantly, resulting in a potentially significant increase in creep rate. If the fuel rod experiences both DNB and high internal pressure conditions, the potential exists for clad ballooning to occur, thereby degrading heat transfer from adjacent fuel rods. Under such conditions, the adjacent fuel rods may experience DNB as well and the DNB phenomenon may propagate through several rows of additional fuel rods. The mechanistic high temperature creep and rupture correlations described in Section 4.4.2.1 are used to determine total accumulated strain during a DNB transient. If the strain exceeds the strain criterion defined in Section 4.4.2.2, DNB propagation to the adjacent fuel rods is assumed to occur. Strains in the adjacent rods are then evaluated to determine if the propagation continues to yet further rows of fuel rods.

Evaluations of DNB for Zircaloy-4 cladding in CENP cores have demonstrated that strains are generally not sufficient to result in any propagation. A comparison of high temperature creep and rupture of ZIRLO™ with Zircaloy-4 indicate that ZIRLO™ is less likely than Zircaloy-4 to attain the strain necessary to propagate DNB. Thus, implementation of ZIRLO™ is expected to increase the margin to potential DNB propagation. However, high temperature creep and rupture properties have been incorporated into the INTEG computer code and evaluations are performed as needed.

4.4.2.4   Discussion of Conservatism for DNB Propagation

The CENP analysis of DNB propagation is extremely conservative. Reference 4-4 provides a detailed discussion of the propagation model conservatisms. The fuel rod maximum internal gas pressure is also [   ] and the methodology for determining the allowable maximum pressure limit (i.e., the NCLO limit) is conservative.

In addition to these documented conservatisms, it has been concluded that DNB propagation is not a likely event because of the local thermal effects and deformation mechanisms associated with DNB and clad ballooning. Rod-to-rod gap closure from a ballooning fuel rod experiencing DNB clearly degrades the surface heat transfer of an adjacent rod only at a local area on the circumference. Thus, occurrence of DNB on an adjacent rod will be highly circumferentially oriented and high temperature deformation would likely occur only on the surface of the adjacent fuel rod facing the original fuel rod experiencing DNB. Consequently, DNB propagation and fuel rod failure are construed to involve at most only one additional row of adjacent fuel rods. However, if a worst case scenario is envisioned (i.e., where the ballooning occurs symmetrically), the resulting fuel-clad internal void volume within the ballooning region of the fuel rod acts to rapidly reduce the internal pressure and, thereby, halt DNB propagation. This is the case even if the bulk of the fission gases present in the fuel matrix is released due to local temperature increases. A clad strain less than the strain level required for DNB propagation equalizes internal pressure with external pressure, and terminates the clad ballooning. Therefore, while DNB propagation is conservatively assumed, the physical mechanisms involved do not actually support the occurrence of DNB propagation.

4.4.2.5   Hydrides and Hydride Reorientation in ZIRLO™

The presence of hydrides and the potential for hydride reorientation due to operation with internal pressure in excess of external pressure (i.e., NCLO) was evaluated in Reference 4-4. Tensile stresses and temperatures are the controlling parameters for adverse hydride orientation. The tensile stresses and peak temperatures for operation at NCLO conditions were concluded to be [   ] that might result in adverse hydride reorientation. Similar observations were made by Westinghouse in Reference 4-24 for operation at higher than RCS pressure. Therefore, operation with ZIRLO™ will be similar to operation with Zircaloy-

4 (see Section 4.6). In addition, as indicated in References 4-4 and 4-24, texture of the cladding is appropriately controlled to resist the formation of adverse hydride orientation. Consequently, the potential for stress induced hydride reorientation is not affected by operation at fuel rod internal pressures limited by NCLO for ZIRLO™.

4.5   Waterside Corrosion Limits

Acceptable operation for CENP PWR designed fuel to high burnups requires that waterside corrosion not result in thermal or mechanical conditions which compromise cladding integrity. High burnup exposure of fuel rod cladding is of interest because the combination of neutron flux exposure with waterside corrosion can result in a loss of cladding wall material, a possible loss of cladding ductility, and, because of the oxide layer, a temperature increase in the fuel rod.

4.5.1   OPTIN Waterside Corrosion Analysis

It was demonstrated in References 4-13 through 4-18 that CENP Zircaloy-4 cladding integrity is not compromised due to neutron irradiation and corrosion to a burnup of 60 MWd/kgU. This was accomplished through an assessment of the oxide thermal effects and mechanical performance effects of wall thinning.

The maximum measured oxide thickness presented in NRC-approved References 4-13 through 4-16 was generally typical of high burnup, non-optimized Zircaloy-4 fuel employed in the 1980s. The maximum oxide thickness was [   ] at 60 MWd/kgU. Both thermal and mechanical effects were evaluated, and it was concluded in Reference 4-14 that a maximum oxide thickness of [   ] was acceptable. Changes in thermal and mechanical performance were acceptable and the clad wall integrity was not compromised. Similar conclusions were reached in Reference 4-15 and 4-16.

Oxide thickness measured for more modern CENP PWR fuel cladding (i.e., OPTIN), was presented in Reference 4-17 to support continued applicability of CENP high burnup methodology to rod average burnups of 60 MWd/kgU. All CENP PWR fuel rods have been fabricated using OPTIN cladding since the early 1990's. Improved corrosion performance relative to the earlier non-optimized cladding is clearly evident in the data presented. As

concluded in Reference 4-17, the OPTIN data is clearly bounded by Reference 4-14 (and 4-15 and 4-16) and additional margin to limits provided by References 4-14, 4-15, and 4-16 exists. CENP therefore currently supports use of OPTIN cladding through NRC approval of References 4-13 through 4-16.

CENP submitted Reference 4-18 to the NRC for the purposes of extending the fuel rod average burnup limit above 60 MWd/kgU for OPTIN cladding. Measured oxide thickness data on OPTIN cladding was provided in Reference 4-18 to fuel rod average burnups [

] These data followed the well-behaved trends for improved corrosion performance of OPTIN cladding identified in Reference 4-17. In Reference 4-18, CENP also proposed an oxide thickness limit and presented a waterside corrosion model benchmarked to the OPTIN data that would be used to calculate the uniform oxide thickness for comparison to the proposed oxide thickness limit for high burnup fuel. CENP further proposed to use the corrosion model to predict maximum oxide thickness to be used in design verification according to Standard Review Plan (SRP) 4.2 for 1-pin peak burnups of up to the extended burnup limit. As applicable, CENP will apply approved corrosion models to verify acceptable behavior of OPTIN cladding per requirements to approved oxide thickness limits for extended burnups.

4.5.2 ZIRLO™ Waterside Corrosion Analysis

Waterside corrosion of ZIRLO™ cladding material is well understood. A significant amount of ZIRLO™ experience (large numbers of fuel rods operating with a variety of power histories to high burnup levels) has been accumulated to-date in cores operating with Westinghouse designed fuel. ZIRLO™ corrosion performance is significantly improved over that of Zircaloy-4. Maximum oxide thicknesses for ZIRLO™ clad fuel rods are shown as a function of rod average burnup in Figure 4.5.2-1. The robustness of ZIRLO™ can be seen by comparing Figure 4.5.2-1 with Figure 3.4-2, which shows the ZIRLO™ oxide thicknesses plotted as a function of fuel duty index. Oxide thicknesses [   ] which do not exhibit any evidence of spallation, have been attained at high burnup. Of most importance is the observation that such thicknesses are concomitant only with a high fuel duty index. The lower the fuel duty index, the lower the oxide thickness at high burnup. Consequently, it can be concluded that the maximum oxide thickness that will be experienced by ZIRLO™ clad fuel rods in CENP fuel designs will be

4-29

bounded by the data in Figure 4.5.2-1. The approach licensed by CENP for OPTIN for a peak rod average burnup of up to 60 MWd/kgU will be applied to ZIRLO™.

When extended burnup is approved for rod average burnups in excess of 60 MWd/kgU (up to 62 MWd/kgU) ZIRLO™ corrosion will be evaluated to determine the maximum oxide thickness that will be used in design verification according to Standard Review Plan (SRP) 4.2. The corrosion model for ZIRLO™ cladding will be used to ensure that maximum expected oxide thickness will not exceed the required disign limit for CENP nuclear fuel designs for fuel rod average burnups of up to 62 MWd/kgU. It is expected that high power and high burnup fuel rods will be surveyed and analyzed as part of the reload analysis process to assure that the maximum oxide thickness will not be exceeded for a given reactor cycle.

4.6   Impact of ZIRLO™ on Fuel Performance

The purpose of this section is to provide fuel performance comparisons of ZIRLO™ clad fuel rods with OPTIN clad fuel rods for CENP supplied reloads. A CENP typical 14x14 fuel design (represented by the Calvert Cliffs fuel design) and a typical 16x16 fuel design (represented by the Palo Verde fuel design) are presented. This comparison is based on recent reload evaluations for these fuel designs as reference cases. The core operating limits and fuel designs are identical to that of recent reloads with the exception that ZIRLO™ cladding material is substituted for OPTIN cladding material. Design and licensing application methods are, of course, identical. It is shown that the resulting fuel performance parameters do not change significantly because of the use of the ZIRLO™ cladding. The only significant difference in reload performance using ZIRLO™ cladding is the beneficial reduction in the amount of cladding oxidation.

4.6.1   ZIRLO™ Impact on Thermal Performance

This section describes the impact of ZIRLO™ cladding on fuel rod thermal performance. The parameters that are most significant and meaningful to characterize the relative fuel thermal performance behavior are fuel centerline temperatures, power-to-centerline melt, and hot internal gas pressure. Fuel rod mechanical performance is discussed in Section 5.0.

A description of the CENP typical reload analysis methodology is given in Reference 4-8 and is summarized here. An erbia bearing fuel rod is used as the reference design basis for the analysis of each fuel type (14x14 and 16x16). [

]

[

] The burnup dependent radial peaking factor used herein, normalized to 1.0, for the 14x14 design and the 16x16 design are shown in Figures 4.6.1-1 and 4.6.1-2, respectively. Axial power distributions in terms ofLHR's are shown in Figures 4.6.1-3 and 4.6.1-4. The LHR history of the fuel rod is, therefore, the axial LHR distribution multiplied by the radial peaking factor as a function ofburnup. In this case, the radial peaking factor has been determined to be that which results in a [

] Consequently, this type of radial fall-off curve may typically be used to guide fuel management.

4.6.1.1 Fuel Temperatures

The only cladding properties or correlations which required modification to enable FATES3B to model ZIRLO™ cladding were circumferential creep and irradiation induced axial growth. Creep and growth are time dependent deformation. Consequently, conditions in the OPTIN clad fuel rod and the ZIRLO™ clad fuel rod will be identical near beginning of life. Fuel temperatures remain quite similar and differ a small amount during gap closure due to feedback effects of the deformations of the cladding. The fuel centerline temperatures differ between the OPTIN design and the ZIRLO™ design by [

] when gap closure has occurred. The differences in temperatures are considered to be insignificant.

4.6.1.2   Power-to-Centerline Melt (PTM)

The power-to-centerline melt for the 14x14 fuel rod design and the 16x16 fuel rod design are shown in Figures 4.6.1.2-1 and 4.6.1.2-2, respectively. It can be seen that centerline melt is predicted to occur at [   ] LHRs for OPTIN clad fuel rods and ZIRLO™ clad fuel rods. [

                    ] Reactivity decreases precludes higher burnup fuel rods from attaining LHR's that would cause melting.

4.6.1.3   Internal Hot Gas Pressure

Internal hot gas pressure for the 14x14 fuel rod design and the 16x16 fuel rod design are shown in Figures 4.6.1.3-1 and 4.6.1.3-2, respectively. Internal pressure initially decreases from beginning of life due to fuel densification and then gradually increases as fission gas builds up in the fuel matrix and is released. The decrease in radial peaking factor (and, therefore, LHR) at burnups above about 40 MWd/kgU is sufficient to keep the internal pressure [

                    ] Identical power histories have been applied to the OPTIN clad fuel rod and the ZIRLO™ clad fuel rod as described in Section 4.6.1. It can be seen that the pressure in the ZIRLO™ clad fuel rod gradually [   ] than the OPTIN clad fuel rod. This [

        ] experienced by the ZIRLO™ clad fuel rod. [

                    ] in the ZIRLO™ clad fuel rod relative to the OPTIN clad fuel rod. The difference, however, is considered to be insignificant. Note that although the ZIRLO™ clad fuel rod internal pressure would [   ] of the OPTIN clad fuel rod, it is [   ] of the ZIRLO™ clad fuel rod. Critical pressure limits are discussed in the next section.

4.6.1.4   Critical Pressure Limit for NCLO

Critical pressure limits are determined by the FATES3B fuel performance code based on the NCLO pressure criterion. That is, the critical pressure limit is the internal hot gas pressure where outward tensile creep of the cladding due to the differential pressure loads would just

equal the fuel pellet swelling. Thus, fuel-clad gap separation due to pressure induced creep does not occur at or below this critical pressure limit. It can be seen that the critical pressure for ZIRLO™ cladding is [   ] than for OPTIN cladding. This result is because the ZIRLO™ creep rate at the NCLO pressure conditions is [   ] than the creep rate of OPTIN. [   ] are applied as previously described for both ZIRLO™ and OPTIN.

4.6.1.5   Other Design and Licensing Applications

Minimum internal gas pressure follows the same trend as maximum internal pressure. Minimum internal pressure is [

] behavior evaluated in Section 5.0). The impact of ZIRLO™ cladding on other design and licensing applications (of the FATES3B fuel performance code) has been reviewed and found to be insignificant.

4.6.2 ZIRLO™ Impact on DNB Propagation

An evaluation of the ZIRLO™ cladding impact on the potential for DNB propagation was performed using the INTEG code described in Section 4.4.2. The most limiting DNB transient of Reference 4-4, the Calvert Cliffs Steam Line Rupture, was repeated for ZIRLO™ cladding. The predicted strains for this transient are shown in Figure 4.6.2-1. It can be seen that the ZIRLO™ cladding reaches a strain of [   ] than the OPTIN cladding which reached a strain [   ] It is expected that this result will be typical of ZIRLO™ versus Zircaloy-4 for most, if not all, DNB transients.

Strain predictions for a small selection of high temperature creep tests reported in Reference 4-11 were made to demonstrate satisfactory performance of the INTEG code. [

] Although the measured strain is plotted versus time as a continuous curve in Reference 4-11, only a single representative point of strain and time was extracted from the graphs and shown here. This representative point is at the time to attain a strain of [   ] selected as a value reasonably near the DNB propagation limit. The results are shown in Figures 4.6.2-2 through 4.6.2-5. INTEG predictions are shown as

4-33

solid lines and the measured data is shown as single points in these figures. It is concluded that the INTEG code predictions are excellent.

4.7   Conclusions

NRC approved ZIRLO™ cladding properties and correlations have been evaluated and, as appropriate, successfully incorporated into the NRC approved CENP fuel performance analysis methodology.   Application of ZIRLO™ properties and correlations have been found to be consistent with NRC approved CENP design and licensing models and methodology. Evaluations have been performed to demonstrate the effect of ZIRLO™ cladding on fuel performance for CENP nuclear fuel designs.   It is concluded that the effect of ZIRLO™ cladding on the thermal performance of the fuel is insignificant.   Thus, the beneficial effects of improved waterside corrosion makes the implementation of ZIRLO™ clad fuel in the CENP fuel designs a significant contributor to improved operational safety.

4.8   References

4-1   CENPD-139-P-A, "Fuel Evaluation Model," July 1974.

4-2   CEN-161(B)-P-A, "Improvements to Fuel Evaluation Model," August 1989.

4-3   CEN-161(B)-P, Supplement 1-P-A, "Improvements to Fuel Evaluation Model," January 1992.

4-4   CEN-372-P-A, "Fuel Rod Maximum Allowable Gas Pressure," May 1990.

4-5   CENPD-382-P-A, "Methodology for Core Designs Containing Erbium Burnable Absorbers," August 1993.

4-6   CENPD-275-P, Revision 1-P-A, "C-E Methodology for Core Designs Containing Gadolinia-Urania Burnable Absorbers," May 1988.

4-7   CENPD-275-P, Revision 1-P, Supplement 1-P-A, "C-E Methodology for PWR Core Designs Containing Gadolinia-Urania Burnable Absorbers," April 1999.

4-8   CEN-193(B)-P, Supplement 2-P, "Partial Response to NRC Questions on CEN-161(B)-P, Improvements to Fuel Evaluation Model," March 21, 1982.

4-9   CEN-345(B)-P, "Responses to NRC Questions on FATES3B," October 17, 1986.

4-10   WCAP-15063-P-A Revision 1, with Errata, "Westinghouse Improved Performance Analysis and Design Model (PAD 4.0)," July 2000.

4-11   WCAP-12610-P-A, "VANTAGE+ Fuel Assembly Reference Core Report," April 1995.

4-12   WCAP-9179, "Properties of Fuel and Core Component Materials," July 1978. (Proprietary)

4-13   CENPD-269-P Revision 1-P, "Extended Burnup Operation of Combustion Engineering PWR Fuel," July 1984.

4-14   CEN-382(B)-P-A, "Verification of the Acceptability of a 1-Pin Burnup Limit of 60 MWD/kgU for Combustion Engineering 14x14 PWR Fuel," August 1993.

4-15   CEN-386-P-A, "Verification of the Acceptability of a 1-Pin Burnup Limit of 60 MWD/kgU for Combustion Engineering 16x16 PWR Fuel," August 1992.

4-16   CEN-396(L)-P, "Verification of the Acceptability of a 1-Pin Burnup Limit of 60 MWD/KG for St. Lucie Unit 2," November 1989.

—

4-17 CENPD-384-P, "Report on the Continued Applicability of 60 MWD/kgU for ABB Combustion Engineering PWR Fuel," September 1995.

4-18 CENPD-388-P, "Extension of the 1-Pin Burnup Limit to 65 MWd/kgU for ABB PWR Fuel with OPTIN Cladding," February 1998.

4-19 WCAP-10851-P-A, "Improved Fuel Performance Models for Westinghouse Fuel Rod Design and Safety Evaluations," August 1988.

4-20 CENPD-162-P-A, "C-E Critical Heat Flux, Critical Heat Flux Correlation for C-E Fuel Assemblies with Standard Spacer Grids, Part 1 Uniform Axial Power Distribution," September 1976.

4-21 CENPD-207-P-A, "C-E Critical Heat Flux, Critical Heat Flux Correlation for C-E Fuel Assemblies with Standard Spacer Grids, Part 2 Nonuniform Axial Power Distribution," December 1984.

4-22 CENPD-162-A Supplement 1-A, "C-E Critical Heat Flux, Critical Heat Flux Correlation for C-E Fuel Assemblies with Standard Spacer Grids, Part 1 Uniform Axial Power Distribution," February 1977.

4-23 CENPD-387-P-A Rev. 000, "ABB Critical Heat Flux Correlations for PWR Fuel", May 2000.

4-24 WCAP-8963-P-A, "Safety Analysis for the Revised Fuel Rod Internal Pressure Design Basis," August 1978.

Table 4.2-1

CENP Zircaloy-4 Clad Property Correlations Used in Fuel Performance

Property	Source Reference	Section
Creep (Normal Operation)	4-1	2.1.5
Creep (NCLO)	4-4	3.1.1
Axial Growth	4-2	7.0
Thermal Conductivity	4-1	2.1.2
Thermal Expansion (Radial)	4-1	2.1.3
Thermal Expansion (Axial)	4-1	-
Modulus of Elasticity	4-1	2.1.4
Poisson's Ratio	4-1	2.1.4
Hemispherical Emittance	4-1	2.5.4
Hardness (DPH)	4-1	2.5.4
Creep (High Temperature)	4-4	Appendix A
Rupture Stress	4-4	Appendix A

Figure 4.3.6-1
FATES3B ZIRLO™ Diametral Creepdown - North Anna 1
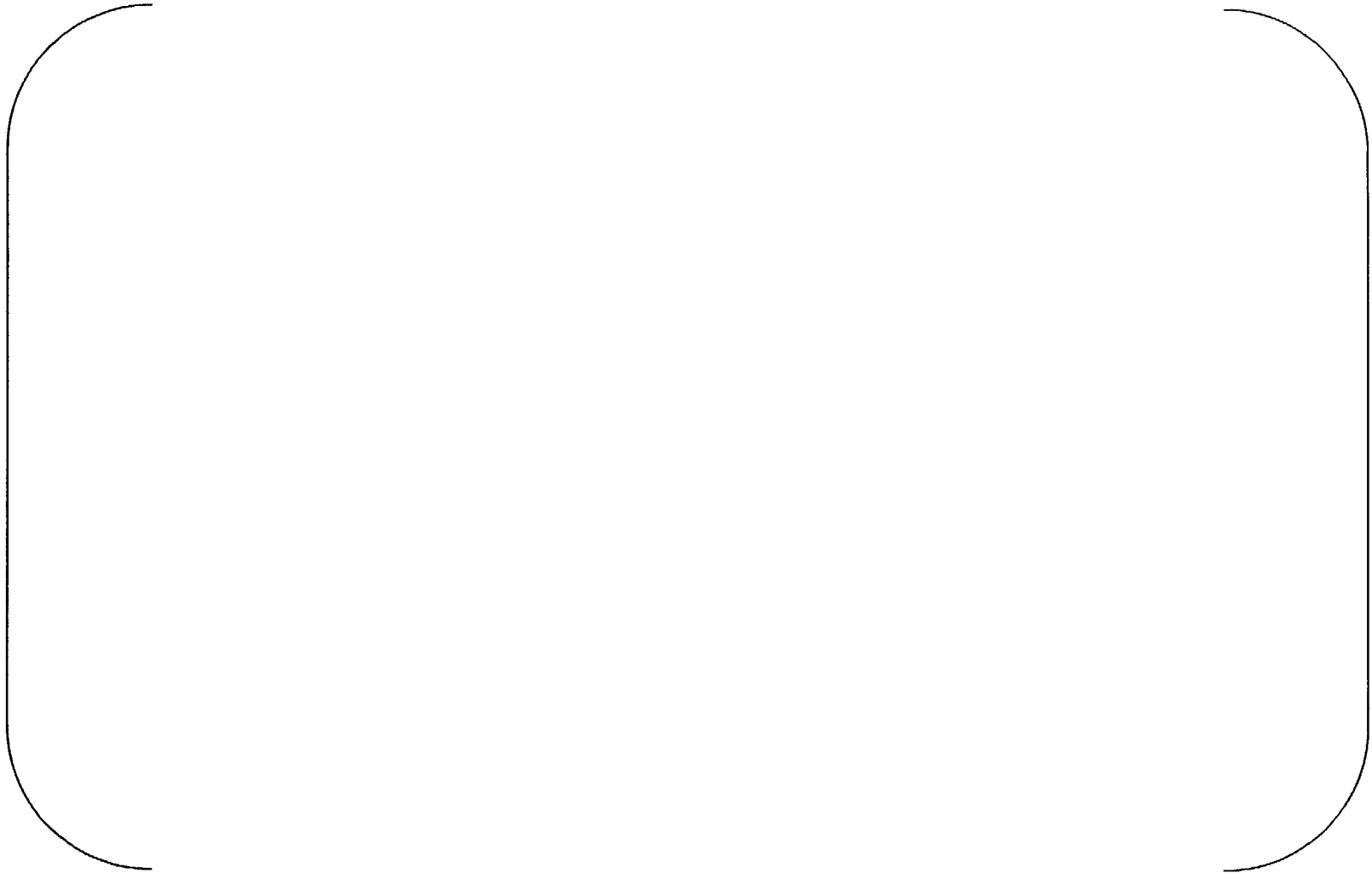
Figure 4.3.6-2
FATES3B ZIRLO™ Diametral Creepdown – North Anna 1 Assembly Rod Average

Figure 4.3.6-3
FATES3B ZIRLO™ Diametral Creepdown

Figure 4.5.2-1
Maximum ZIRLO™ Cladding Oxide Thickness versus Rod Average Burnup

Figure 4.6.1-1
Radial Peaking Factor versus Burnup – 14x14 Design
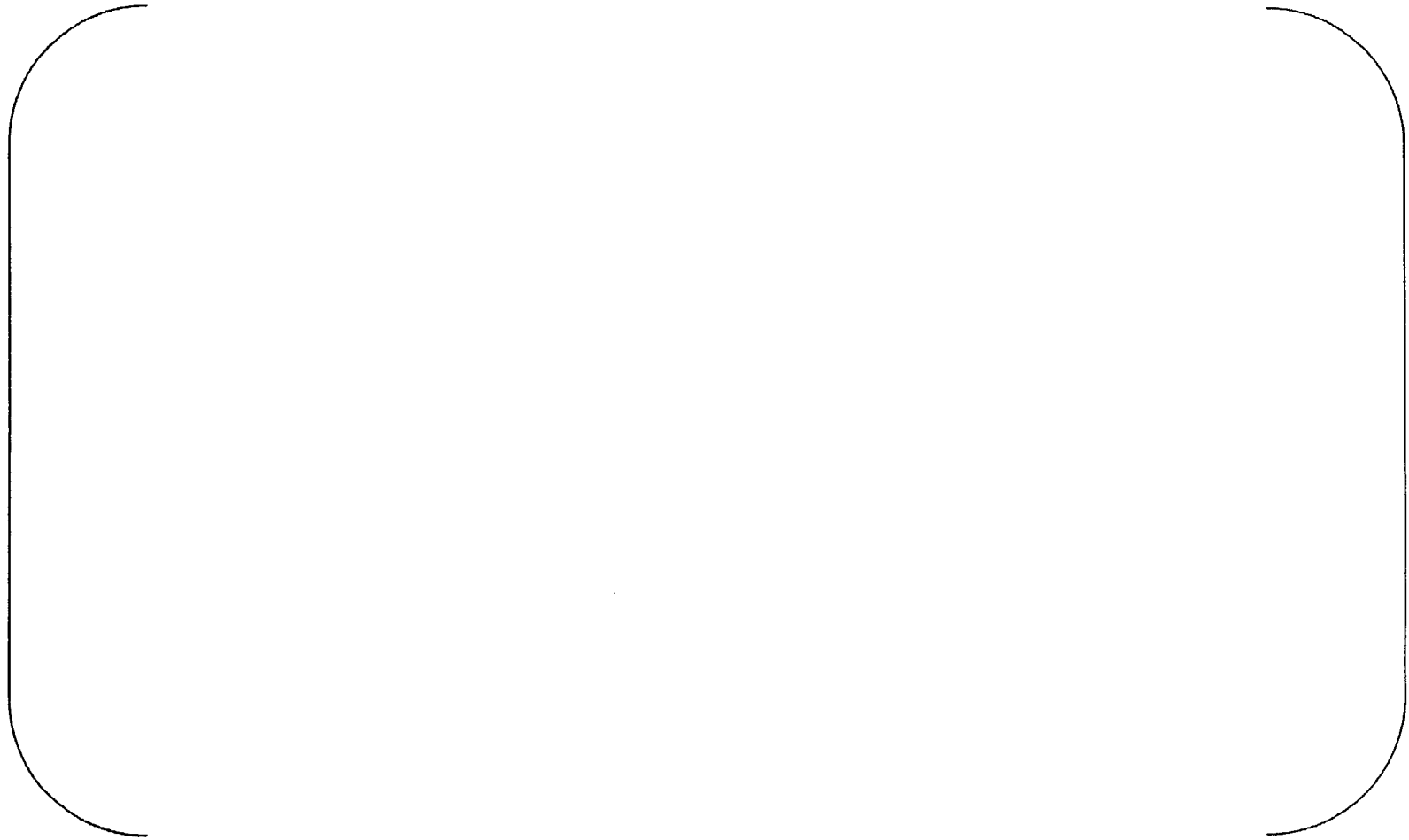
Figure 4.6.1-2
Radial Peaking Factor versus Burnup – 16x16 Design

Figure 4.6.1-3
Axial Power Distributions – 14x14 Design

Figure 4.6.1-4
Axial Power Distributions – 16x16 Design

Figure 4.6.1.2-1
Power-to-Centerline Melt – 14x14 Design

Figure 4.6.1.2-2
Power-to-Centerline Melt – 16x16 Design

Figure 4.6.1.3-1
Maximum Internal Hot Gas Pressure – 14x14 Design

Figure 4.6.1.3-2
Maximum Internal Hot Gas Pressure – 16x16 Design

Figure 4.6.2-1
DNB Propagation Strain for Calvert Cliffs Steam Line Break

Figure 4.6.2-2
Strain Prediction for ZIRLO™ [   ]
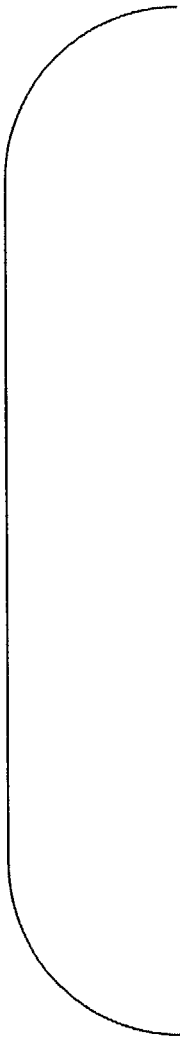
Figure 4.6.2-3
Strain Prediction for ZIRLO™ [   ]

Figure 4.6.2-4
Strain Prediction for ZIRLO™ [   ]
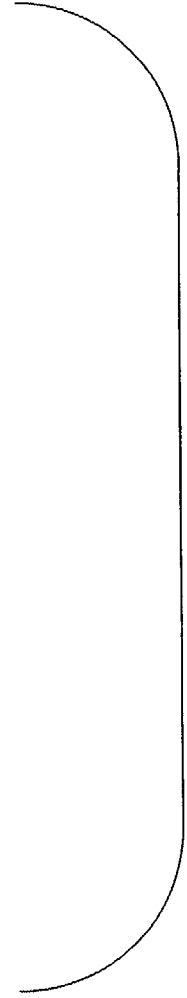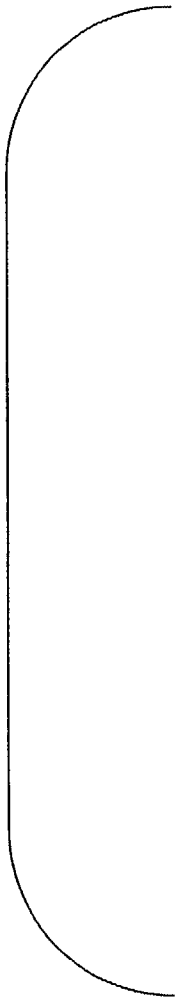
Figure 4.6.2-5
Strain Prediction for ZIRLO™ [   ]
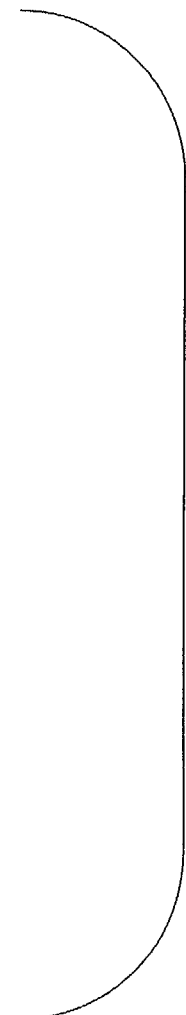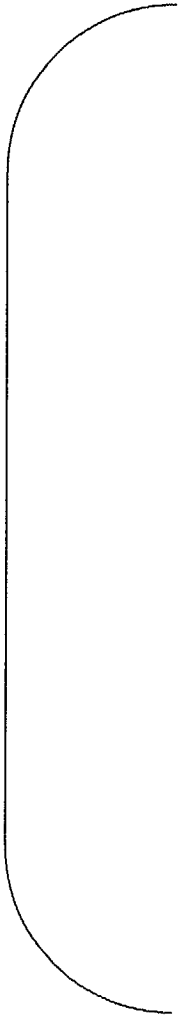
5.0 Fuel Mechanical Design

5.1 Introduction

The change to ZIRLO™ cladding material has been evaluated from a mechanical design perspective to insure that the introduction of this material in the CENP fuel reload designs is acceptable. The CENP mechanical design methodology has been outlined previously in Reference 5-1, including the relevant properties of the current OPTIN™ cladding material, and the information in that reference served as a starting point for the evaluation of the change to ZIRLO™ cladding.

The discussions below detail the mechanical design evaluation of the change for burnup levels up to 62 MWd/kgU, and demonstrate its acceptability for use in all CENP design applications.

5.2 Cladding Parameters Used in Fuel Mechanical Design Methodology

Several mechanical design analyses are potentially affected by changes in cladding properties. The current versions of the CENP fuel mechanical design methods are described in Reference 5-1 and its various references.

Listed below are the cladding-related parameters that are utilized in the mechanical design models. For reload fuel batches in CENP plants where ZIRLO™ is used, the properties described in Section 5.3 of this report will be used for these parameters.

- Creep Rate
- Irradiation-Induced Axial Growth
- Thermal Conductivity
- Thermal Expansion
- Strain and Fatigue Capability
- Mechanical Strength
- Modulus of Elasticity
- Poisson's ratio

- Density

Table 5.2-1 lists the topical reports and NRC's Safety Evaluation Reports (SERs) associated with these models.

Each of the following subsections describes the overall fuel mechanical design models, and specifically addresses the particular OPTIN cladding models used by each computer code or computerized model. Table 5.2-2 summarizes the cladding models (equations, correlations, properties, etc.) that are affected due to the introduction of ZIRLO™.

5.2.1 CEPAN Model

References 5-8, 5-9, 5-10, and 5-11 describe a method which utilizes the CEPAN computer code to predict creep deformation and collapse time of OPTIN cladding containing an initial ovality. [

]

The method of selecting input to CEPAN resulted in a deterministic combination of the worst case cladding as-built dimensions and worst case operating conditions during the fuel lifetime. The NRC concluded that CEPAN provided an acceptable analytical procedure for determining the minimum time to collapse for CENP clad fuel. [

]

A modification of the above method is described in Reference 5-11. This modification is applied to the normal CEPAN results to account for the support provided to the cladding by the pellets at the edges of the gap. The adjustment varies as a function of the length of the gap or unsupported cladding. As the gap considered becomes longer, the results approach the normal CEPAN results. In addition, CEPAN is applied in the plenum region where no support is assumed for the plenum spring. This method modification was utilized in NRC approved References 5-3 (for 16x16 designs) and 5-4 (for 14x14 designs).

The CEPAN model (References 5-8 and 5-9) employs OPTIN cladding parameters for initial ovality and yield strength as input conditions. Young's modulus (Modulus of Elasticity) and Poisson's ratio for OPTIN are modeled in the CEPAN computer code in data arrays corresponding to temperature values. Values for Young's modulus and Poisson's ratio values at a given temperature are ascertained by linear interpolation. Corresponding modifications have been incorporated for the ZIRLO™ cladding material properties.

Cladding collapse is a creep related phenomenon and a creep model is present in CEPAN. The CEPAN creep model is described in Reference 5-8 and is further discussed in Section 5.3.1.

5.2.2 SIGREEP Model

The SIGREEP computer code (Reference 5-12) is used to predict the axial length change of the fuel assembly and the change in the gap between the fuel rods and upper end fitting (shoulder gap). Basically, SIGREEP [

]. The input constants and input variables define the fuel assembly geometry, its operating conditions and material properties of the fuel rod and guide tube. The input parameters that are [

].

A fuel rod axial growth model is included in SIGREEP evaluations that ensure adequate clearance (shoulder gap). [

]. The OPTIN fuel rod growth model of SIGREEP is discussed in further detail in Section 2.3.1.2 of Reference 5-1.

In addition to evaluations of fuel rod axial growth accomodation, the SIGREEP code is employed in performing the fuel assembly dimensional evaluations. These include axial assembly growth accomodation, holddown spring clearance to solid height, holddown force and margin, and fuel assembly engagement with reactor internals structures. These evaluations are controlled by the

axial length variation of the guide tubes, which are made of Zircaloy-4. The use of ZIRLO™ for the cladding will, therefore, not affect these quantities.

5.2.3 Rod Bow Model

Rod bow models are based on empirical data which is particularly sensitive to geometric fuel assembly parameters such as spacer grid configuration, spacer grid axial spacing and fuel assembly and rod stiffness. Changes due to the implementation of ZIRLO™ are not directly related to the above geometric considerations and, as such, do not have any significant impact on existing rod bow models, as defined in Reference 5-13. The fuel rod creep characteristics associated with ZIRLO™ differs slightly from OPTIN but are not expected to have any significant effect on rod bow, as discussed in Section 5.4.6.

5.2.4 Seismic / LOCA Model

The seismic and LOCA structural analysis models are not affected by the transition to ZIRLO™ and, therefore, do not affect the existing topical report (Reference 5-16). However, the increase in ZIRLO™ tensile strength allowables, as compared to OPTIN, will result in greater margins in meeting stress criteria defined in Reference 5-16. Implementation of ZIRLO™ into the new LOCA evaluation model is described in Section 6.

5.3 ZIRLO™ Mechanical Design Properties

ZIRLO™ is a modification of Zircaloy-4 composition that has been achieved by reducing the tin and iron content, eliminating the chromium content, and adding 1% niobium. The following sections document the ZIRLO™ properties for those parameters that impact the fuel mechanical design evaluations.

5.3.1 ZIRLO™ Creep Considerations

The methodology used to calculate stress, strain, and cumulative fatigue damage fraction for fuel rods utilize diametral creep rate models for the cladding, as discussed in Reference 5-1.

The creep correlations described in Section 4.3.1 of this report will be used in each of these evaluations for reloads that include ZIRLO™ cladding material.

Modifications to account for ZIRLO™ cladding properties have been implemented in the cladding collapse methodology as described below.

5.3.1.1 Creep Correlations for Cladding Collapse Method

The OPTIN stress-strain relationships for the CENP cladding collapse evaluation method (CEPAN) are described in References 5-8 , 5-9, 5-10, and 5-11. Also discussed in these references is the effective stress-effective strain rate creep law that is applicable to OPTIN cladding in a state of biaxial stress. A consistent set of equations is implemented which governs the radial, tangential, and axial creep deformation of the cladding.

The analysis presented in the above references yields a set of partial differential equations in terms of displacement components with creep effects included through the presence of force and moment arising from creep strains. Application of the generalized plane strain hypothesis eliminates the axial dependency in the governing system and enables the biaxial response of the shell to be determined.

The CENP OPTIN creep model is described in Section 5.6 of Reference 5-7. The model is intended to give a best estimate of in-reactor tangential creep rate for biaxially pressurized tubing for specific ranges of hoop stress, temperature, and neutron flux (E>1MeV). The specific form of the model equation is obtained by expressing the uniaxial hoop stress - hoop strain relation given in Reference 5-7 in terms of effective stress and strain.

The creep model in the CEPAN method (References 5-8, 5-9, 5-10, and 5-11) has been modified to include the ZIRLO™ creep correlation (Reference 5-6). The application of the model to ZIRLO™ is relatively straightforward. The fluence forms of the creep correlations will be used in CEPAN to be consistent with FATES3B (Reference 5-7).

In the existing CEPAN creep correlations, the relationship between the stress and strain components and effective stress and strain are based on the isotropic von Mises yield and Prandtl-Reuss equations. Reference 5-8 demonstrates this basis. Since the ZIRLO™ creep correlation provides the effective strain rate as a function of the effective stress and is already based on isotropic von Mises yield and Prandtl-Reuss equations, the ZIRLO™ creep correlation can be substituted directly for the CENP Zircaloy creep correlation.

5.3.2   Fuel Rod Axial Growth

Fuel rod axial growth is one of the parameters included in the mechanical design methodology to assess irradiation-induced dimensional changes of the fuel. It is well established that Zircaloy-clad fuel rods exhibit axial elongation when irradiated in a neutron flux. The overall elongation of fuel rods is due to several contributing mechanisms. These mechanisms include:

- [,]
- [   ]
- [.]

Due to the complex interactions among these mechanisms, empirical correlations have been utilized in the CENP methodology.

Fuel rod growth with ZIRLO™ cladding has been observed to be less than that of the Westinghouse Zircaloy-4 fuel rod growth. However, Reference 5-5 requires that the ZIRLO™ rod growth model be the same as the Westinghouse Zircaloy-4 growth model for evaluations of shoulder gap.

The functional form of the Westinghouse Zircaloy-4 rod growth model is the same as that currently used for CENP OPTIN fuel rods. Therefore, the application of the model in the CENP methodology to represent ZIRLO™ behavior is relatively straightforward.

The functional form of the fuel rod growth model is:

[   ]

where:

$$\left[\right]$$

The constants for the ZIRLO™ fuel rod growth equation are:

$$\left[\right]$$

5.3.3 Cladding Thermal Conductivity

Thermal conductivity for ZIRLO™ is provided in Reference 5-5 and is discussed in detail in Section 4.3.3. Conductivity used for FATES3B for OPTIN, Reference 5-7, is nearly identical to the ZIRLO™ conductivity over the range of interest for FATES3B and fuel mechanical design. Consequently, thermal conductivity for OPTIN is to be used for both ZIRLO™ and OPTIN.

5.3.4 Thermal Expansion

A discussion of thermal expansion coefficients for ZIRLO™ is provided in Section 4.3.4. For the reasons provided in Section 4.3.4 the FATES3B thermal expansion, Equation 4-7, will be used in modeling thermal expansion in all applicable mechanical design methods.

5.3.5 Strain Capability

Ductility is a function of irradiation and hydride formation in the cladding wall. The ductility of ZIRLO™ [   ] Waterside corrosion for ZIRLO™ is [   ] and will result in [   ] Total strain capability of ZIRLO™ is projected to be in excess of 1% at burnups of [   ]

Thus, a 1% strain limit will continue to be applied by CENP as a strain criterion in fuel mechanical design analysis.

5.3.6 Fatigue Capability

The cyclic strain fatigue damage model applied to ZIRLO™ is identical to a conservative cyclic strain fatigue damage model applied to Westinghouse Zircaloy-4, and is based on a modified Langer-O'Donnell fatigue model (Reference 5-5). In both cases, the accumulated fatigue damage is limited to 1.0. The CENP fatigue damage evaluation for OPTIN cladding is also based on a conservative interpretation of the Langer-O'Donnell fatigue model. However, the CENP criterion limits the accumulated fatigue damage to [   ] (Reference 5-1).

Fatigue data obtained by Westinghouse for ZIRLO™ (number of cycles versus strain increment), although high cycle fatigue data, in the 30,000 to 100,000 cycle range, fall well above the CENP design curve. Furthermore, the data fall above the design curve at the more realistic range of 10,000 cycles, indicating significant margin. [

]

Consequently, no change is required for calculation of fatigue for ZIRLO™ cladding in CENP fuel designs. The fatigue damage curve and accumulated damage fraction [   ] for OPTIN is also applied to ZIRLO™.

5.3.7 Mechanical Strength

ZIRLO™ yield strength and ultimate strength are discussed in Reference 5-5. The following sections provide the correlations that are applicable for mechanical design evaluations.

5.3.7.1   Yield Strength

Best-estimate unirradiated yield strength of ZIRLO™, in psi, is given by

[   ]

[']

5.3.7.2   Ultimate Strength

Best-estimate unirradiated ultimate strength of ZIRLO™, in psi, is given by

[   ]

[   ]

5.3.8 Modulus of Elasticity

A discussion of ZIRLO™ modulus of elasticity is provided in Section 4.3.5.1. For the reasons provided in Section 4.3.5.1 the modulus of elasticity for OPTIN (Equation 4-30) is used in applicable mechanical design analysis.

5.3.9 Poisson's Ratio

A discussion of Poisson's ratio for ZIRLO™ is provided in Section 4.3.5.2. For the reasons provided in Section 4.3.5.2 the Poisson's ratio for OPTIN (Equation 4-32) is used in applicable mechanical design analysis.

5.3.10 Oxide Buildup

From a mechanical design standpoint, it is conservatively assumed that the maximum reduction in base-metal wall thickness due to oxidation is the same for the ZIRLO™ and OPTIN cladding materials. A corrosion allowance of [   ] is assumed for the maximum rod average burnup addressed in this report.

5.3.11 Density

Density of ZIRLO™ is [   ] g/cc compared to [   ] g/cc for Zircaloy-4. CENP uses a density of [   ] g/cc for OPTIN extracted from similar zirconium alloys. The difference in Zircaloy-4 values is not significant but, where appropriate, the reported density for ZIRLO™ (Reference 5-5). is used. Recent data has shown that the difference in density conditions discussed above is reduced further, as such, the effects on the design evaluations should be negligible.

5.4   Fuel Mechanical Design Impact

This section discusses the effect on fuel mechanical performance when ZIRLO™ cladding is substituted for OPTIN material in current CENP fuel rods. Areas of investigation include both individual fuel rods and the entire fuel assembly. The fuel rods are evaluated for differences in creep collapse, fuel rod stress, strain, fatigue damage, shoulder gap margin, rod bow and cladding wear/fretting. The fuel assembly is evaluated for differences in assembly bow, spacer grid growth and spring tab relaxation, hold down margin, spent fuel handling accident and seismic and LOCA loads.

5.4.1   Creep Collapse

Since cladding collapse is a creep-related phenomenon, different creep properties of the cladding will result in different predicted collapse times for unsupported cladding. Also, cladding corrosion reduces the thickness of the cladding as a function of burnup, and this reduction in cladding thickness is accounted for in the analysis of cladding collapse.

CENP performs cladding collapse calculations in the fuel and plenum regions with the method described in Reference 5-8 and Reference 5-11. The assumed length of the axial gap in the fuel region bounds the largest hot axial gap in CENP fuel designs, and a limiting amount of oxide thickness is assumed. Also, no credit is taken for any additional support from the plenum spring in the plenum region. These calculations have historically shown that the predicted collapse

times exceed the longest residence time expected for CENP fuel that is operated to a maximum 1-pin burnup of 62 MWd/kgU.

5.4.1.1   Conclusion Related to Creep Collapse

Comparative runs were made using the 14x14 and 16x16 current CENP fuel rod designs with both OPTIN and ZIRLO™ materials. The ZIRLO™ properties discussed in Section 5.3 were included, as appropriate. The results of these comparative evaluations show that usingZIRLO™ cladding produces [   ] than the current OPTIN material. The use ofZIRLO™ cladding in the current CENP fuel bundle designs will therefore meet the required creep collapse criteria.

5.4.2   Fuel Rod Stress

The following design criteria are considered with regard to the cladding stresses:

- Under normal operating and upset conditions, the primary tensile and compressive stresses in the cladding shall not exceed 66 2/3% and 100% respectively of the minimum unirradiated yield strength at the applicable temperature. Under emergency and accident conditions, the stress allowables are as described in Reference 5-16.

The method used to perform the stress analysis of CENP fuel rod designs accounts for power dependent and time dependent changes (e.g., fuel rod void volume, fission gas release and gas temperature, differential cladding pressure, cladding creep and thermal expansion) that can affect stresses in the fuel rod cladding. As noted above, the allowable stress is based upon the material strength properties.

5.4.2.1   Conclusion Related to Fuel Rod Stress

Comparative analyses were performed using the current 14x14 and 16x16 CENP fuel rod designs with both OPTIN and ZIRLO™ materials. The ZIRLO™ properties discussed in Section

5.3 were included, as appropriate. The results of these comparative evaluations show that using ZIRLO™ cladding produces [   ] than the current OPTIN material. The introduction of ZIRLO™ cladding in the current CENP fuel bundle designs will therefore meet the required stress criteria.

5.4.3 Fuel Rod Strain

The following design criterion is considered with regard to the cladding strain:

- At any time during the fuel rod lifetime, the net unrecoverable circumferential tensile clad strain shall not exceed 1%, based on the BOL clad dimensions. This condition is applicable to normal operating conditions, and following a single Condition 2 or 3 event.
- For fuel rod axial average burnups greater than 52 MWd/kgU, the total (elastic plus plastic) circumferential clad strain increment produced as a result of a single Condition 2 or 3 event, shall not exceed 1%.

The method used to evaluate the strain in CENP fuel rod designs accounts for power dependent and time dependent changes (e.g., fuel rod void volume, fission gas release and gas temperature, differential cladding pressure, cladding creep and thermal expansion) that can produce strain in the fuel rod cladding. As noted in Section 5.3.5, the strain capability of ZIRLO™ cladding remains at 1%.

5.4.3.1   Conclusion Related to Fuel Rod Strain

Comparative strain analyses were performed using the 14x14 and 16x16 current CENP fuel rod designs with both OPTIN and ZIRLO™ materials. The ZIRLO™ properties discussed in Section 5.3 were included, as appropriate. The results of these comparative evaluations show that using ZIRLO™ cladding [   ] than the current OPTIN material. The use of ZIRLO™ cladding in the current CENP fuel bundle designs therefore meets the required strain criteria.

5.4.4 Fuel Rod Fatigue Damage

The method used for fatigue analysis of CENP fuel rod designs accounts for power dependent and time dependent changes (e.g., rod void volume, fission gas release and gas temperature, cladding creep and thermal expansion, and pellet swelling and thermal expansion) that can produce cyclic straining of the fuel rod cladding. In this method, the cladding is assumed to conform to the predicted diameter of the pellet during periods of contact (i.e., elastic compression and hot pressing of the pellet are conservatively ignored).

In each specific design analysis, conservative assumptions are used to select the starting dimensions of the fuel rod. [

.]

The method for fatigue analysis results in a series of cladding strain ranges covering the fuel lifetime. The cumulative fatigue damage fraction is determined by summing the ratios of the number of cycles in a given strain range to the permitted number in that range. The permitted number of cycles in any strain range is the same for the two cladding materials, as discussed in Section 5.3.6.

5.4.4.1   Conclusion Related to Fuel Rod Fatigue Damage

Comparative fatigue damage calculations were performed for the 14x14 and 16x16 current CENP fuel rod designs using both OPTIN and ZIRLO™ materials. The ZIRLO™ properties discussed in Section 5.3 were included, as appropriate. The results of those comparative evaluations show that using ZIRLO™ cladding produces [

] than the current OPTIN material. The use of ZIRLO™ cladding in the current CENP fuel bundle designs will therefore meet the required fatigue damage criterion.

5.4.5 Shoulder Gap Margin

The SIGREEP computer code is used to predict the shoulder gap as described in Reference 5-1 and Section 5.2.2 of the current report. The design criterion on shoulder gap change is that the gap must not close for the upper 95% probability prediction at the maximum rod discharge exposure in the assembly (an appropriate lower value is used in the shoulder gap analysis for the corresponding guide tube fluence).

The CENP guide tube material has not been changed from standard Zircaloy-4 requirements; therefore all fuel assembly length change SIGREEP predictions [   ] are relevant to designs containing ZIRLO™ fuel rods.

5.4.5.1   Conclusion Related to Shoulder Gap Margin

Section 5.3.2 documents the irradiation growth model for the ZIRLO™-clad fuel rods. Applying these growth characteristics to the shoulder gap calculation results in end-of-life gaps that are [   ] for CENP fuel bundles with OPTIN fuel rods. Specific reload batch evaluations will verify that adequate shoulder gap margins are maintained.

5.4.6 Rod Bow

The bowing of fuel rods results in [   ] of the rods. The primary mechanism causing this bowing is [   ]. The fuel rod behaves like a column with multiple supports at each grid location. The degree of bowing is a function of basic design features, the initial rod bow resulting during fabrication, and burnup. Bowing of fuel and poison rods affects local nuclear power peaking and the local heat transfer to the coolant. Rather than placing design limits on the amount of bowing that is permitted, the effects of bowing are included in the safety analysis. This is consistent with the NRC Standard Review Plan.

The CENP analysis methods used to account for the effect of fuel and poison rod bow in 14x14 and 16x16 fuel assemblies are presented in References 5-2 and 5-13, and the supplements to

Reference 5-13. These methods were initially approved by the NRC in References 5-2 and 5-14 for fuel rods and Type 3 poison rods. The further application of these methods to[   ] MWd/kgU was approved in References 5-3 and 5-4.

In summary, the primary design characteristics that affect rod bow are rod stiffness and spacer grid axial spacing. These characteristics do not change due to the introduction of ZIRLO™. Secondary effects due to the long term differences between ZIRLO™ and OPTIN creep and axial growth may result in slight differences of behavior in rod bow. Nevertheless, this potential difference in bow characteristics is not judged to significantly alter the rod bow as a function of burnup. To date, there have been no observations of increased bow as a result of Westinghouse adoption of ZIRLO™ cladding.

5.4.6.1   Conclusions Related to Rod Bow

No design changes have been introduced or will be introduced with the implementation of ZIRLO™ cladding that are projected to significanly increase either as-fabricated rod bow or rod bow with burnup relative to the measured rod bow reported in Reference 5-2.

5.4.7 Grid-to-Rod Fretting Wear

Grid-to-rod fretting wear is a concern because excessive wear between the fuel rod cladding tube and the spacer grid support features can result in a breach of the cladding wall. Reference 5-1 provided information on operating CENP fuel designs and fretting failure experience as of its date of publication. Tables 5.4.7-1 and 5.4.7-2 of this report are an update of that information.

[   ] of the fretting failures in Table 5.4.7-2 occurred at the bottom spacer grid, which is made from Inconel material. In all cases, the bottom grid designs for these fuel batches preceded the CENP GUARDIAN design. All future fuel deliveries will include the GUARDIAN bottom grid. There will be no effect of the change to ZIRLO™ cladding material on rod performance at the GUARDIAN spacer grid. [

].

The remaining fretting failures in Table 5.4.7-2 [

]. Evaluations of the experience at Zircaloy-4 spacer grid locations have identified a combination of factors [

]. As discussed below, the use of ZIRLO™ cladding is not expected to significantly affect the contributing factors [   ].

An assessment of the significance of grid-to-rod fretting wear failures was provided to the NRC for information in References 5-17 and 5-18. Reference 5-18 was issued following the[

],

and concluded that the grid-to-rod fretting wear is not a reactor safety or fuel operability concern. The [   ] do not alter this conclusion.

5.4.7.1   Grid-to-Rod Fretting Wear at Zircaloy Spacer Grids

The grid-to-fuel rod fretting wear failures listed at the bottom of Table 5.4.7-2 [

]. Eddy current testing and/or visual examination of [

].

Evaluations of grid-to-rod fretting have concluded that [

]

[   ].

5.4.7.2   Evaluation of the Change to ZIRLO™ Cladding on Grid-to-Rod Fretting Wear

The factors that contribute to the grid-to-rod fretting wear were outlined in Section 5.4.7.1. The effect of using ZIRLO™ cladding material in the CENP fuel designs was first evaluated by assessing the difference, if any, that would be produced for each contributing factor. [

].

Table 5.4.7-3 summarizes the results. Based on the evaluation of the effects of ZIRLO™ cladding on the factors associated with grid-to-rod fretting, it is expected that there[

]. Since most or all of the

failures [   ], the

potential for a significant increase in failure rate [

] is small.

Likewise, the use of ZIRLO™ cladding is not expected to result in a significant increase in

failures [   ]. However, Table 5.4.7-3 shows that the

situation at these [

].

These interrelated effects, when combined with the range of operating conditions in a typical core, can produce [

]. In addition, the difference in oxide thickness between the two materials will increase as burnup increases, and the rate of axial growth of the rods will differ.

Because of these [   ], the best basis for comparisons of fretting behavior is the actual performance in reactors where the transition has already been made between cladding materials. The cases that are considered most relevant [

].

Table 5.4.7-4 lists the applicable experience [

].

The experience with [   ] is also relevant, since the fuel assembly designs were deployed in a [

]. Inspection results are shown in Table 5.4.7-5. Note that [   ] was made at the same time as the transition from low-tin Zircaloy-4 to ZIRLO™ cladding.

5.4.7.3   Conclusions Related to Grid-to-Rod Fretting Wear

The effect of the change from OPTIN to ZIRLO™ cladding on grid-to-rod fretting will involve complex interactions among the various factors contributing to the fretting mechanism. Based on a review of the individual contributing factors, and on the available data from relevant reactor experience, the incidence of fretting failures in the CENP fuel designs is expected to remain small.

The initial applications of ZIRLO™ cladding in CENP fuel are expected to be in plants and designs with margin to fretting failures. This fuel will be carefully monitored to confirm the expected performance.

5.4.8 Fuel Assembly Considerations

The design effect of introducing ZIRLO™ cladding into CENP designed fuel rods associated with overall behavior of a fuel assembly and/or its structural components are discussed in this section. The topics include assembly bow, spacer grid irradiation growth and spring tab relaxation, assembly hold down margin, and assembly structural performance, including consideration of the spent fuel handling accident and seismic and LOCA loads.

5.4.8.1 Fuel Assembly Bow

Section 2.3.4 of Reference 5-1 evaluated the topic of fuel assembly bow for reactor cores with CENP OPTIN clad fuel. It was stated that assembly bow for CENP designed reactor cores in CENP designed NSSSs has been acceptable and that the effects of extending the 1-pin burnup limit from [   ] will be negligible relative to assembly bow.

Reference 5-1 and Reference 5-22 indicate that a major contributor to assembly bow is believed to be lateral flow forces on fuel rods and guide tubes associated with radial crossflows that result from center-peaked coolant mass flow distributions at the core inlet. Other mechanisms that may influence assembly bow are axial loads on the fuel assembly due to the difference between assembly hold down force and coolant uplift forces and differential guide tube creep and/or growth that occurs in the presence of a fast neutron flux. Secondary contributing mechanisms include moments exerted on the fuel assembly and differential thermal expansion of the guide tubes within the assembly. The moments may be exerted on the upper and lower end fittings by deflections of the core support and/or alignment plates.

The existence of fuel assembly bowing for 17x17 Westinghouse designs was attributed to the thimble tube design, and this has resulted in the incomplete control rod insertion issue. In

Reference 22-22 it was concluded that the robust interface between the CENP 14x14 and 16x16 guide tubes and control element assemblies (CEAs) is sufficient to preclude any similar issue for CENP reactors. Specifically, [   ] on the critical buckling force that exists with CENP type guide tubes due to the larger geometric shape, as compared to Westinghouse 17x17 thimble tubes, to resist tube buckling induced distortions that may result from differential behavior of the guide tubes during irradiation or from variations in material properties.

The above discussion does not indicate a strong dependence on fuel rod behavior for the fuel assembly bow phenomena. However, the introduction of ZIRLO™ will alter the dynamics of the Zircaloy-4 creep rate early in life and these differences may produce small differences in the rod bow which may have a feed back effect on overall lateral fuel assembly stiffness and possible bow effects. These effects are judged to be relatively insignificant based on the Westinghouse observations that assembly bow has not increased with the introduction of ZIRLO™.

5.4.8.2　　Spacer Grid Irradiation Growth and Spring Tab Relaxation

The spacer grids will continue to be fabricated from Zircaloy-4 for CENP fuel assemblies with ZIRLO™ clad fuel rods. Therefore, growth and relaxation properties of the grids will not be affected.

5.4.8.3　　Fuel Assembly Hold Down Margin

The only parameter in the hold down evaluation that would be influenced by the use of ZIRLO™ cladding in a CENP fuel assembly would be that related to the weight of the fuel bundle. Section 5.3.11 shows the density of ZIRLO™ to be [   ] than that of OPTIN. When this [   ] fuel rod density is considered with all other key parameters in the analyses of record for 14x14 and 16x16 CENP current fuel bundle designs, the hold down margins calculated by the SIGREEP code continue to meet the required criterion. Thus, the use of ZIRLO™ cladding in current CENP fuel bundle designs is acceptable from a hold down margin standpoint.

5.4.8.4   Assembly Structural Performance

This section assesses the structural performance of the fuel assemblies with the addition of ZIRLO™ fuel rods during a spent fuel handling accident or under seismic and LOCA loads. The evaluations show that there will be either no effect caused by the addition of ZIRLO™ cladding or that the structural performance of the fuel assembly actually improves.

5.4.8.4.1   Spent Fuel Handling

The response of the Zircaloy-4 structural components and ZIRLO™ fuel rods to the loads produced by fuel handling is determined by conventional static stress analysis methods. No changes to the stress analysis methods are required as a result of the change in cladding material.

5.4.8.4.2   Fuel Assembly Damage Under Seismic and LOCA Loads

The methods and criteria used to evaluate fuel assembly structural performance under the deflections and loads induced by seismic and LOCA conditions are described in Reference 5-16. These methods are unaffected by the change to ZIRLO™ cladding material. However, certain properties and input to the method, and the allowable stress values resulting from the criteria, may be affected, as discussed below.

<u>Full Core Analysis</u>

The dynamic core analysis model covers one complete row of fuel assemblies across the core. In the actual case of an operating reactor with CENP designed fuel assemblies, there will be a mix of assemblies containing OPTIN or ZIRLO™ cladding due to the fuel management. Of the specific parameters that are modeled in the core analysis, the only ones that would be affected by the use of ZIRLO™ cladding [

]

5-21

The weight difference between OPTIN and ZIRLO™ cladding amounts to a [   ] for the ZIRLO™ cladding. But the cladding weight is a very small fraction (about 6%) of the total weight of the fuel rods. The resulting [   ] of the fuel assembly is thus small enough to be considered negligible for dynamic core analysis considerations. In addition, as highlighted in Section 5.3.11, recent data has shown the difference in density conditions has been reduced and thus will further support the conclusion of negligible impact.

There is a contribution from the fuel rod properties (mass and stiffness) to the fuel assembly natural frequency. The weight of the fuel rods will be reduced by the [   ] density of the ZIRLO™ cladding, but the stiffness will [   ] because both the rod dimensions and cladding elastic modulus [   ]. As mentioned above, the weight change is a

[   ]

in the natural frequency of the fuel rods as well.

Detailed Fuel Assembly Analysis and Design Criteria

Based on the discussions above, it is concluded that the effects of using ZIRLO™ cladding in place of OPTIN material, for burnup levels of up to 60,000 MWd/MTU and above, are covered by the conservative input values that have been used historically in the two phases of the seismic/LOCA analysis, and in the determination of limiting values from the existing design criteria.

5.5 Overall Conclusion for Fuel Mechanical Design

The impact of using ZIRLO™ in place of OPTIN for the fuel rods in current CENP fuel bundle designs has been assessed. Evaluation of the change examined the mechanical performance areas of creep collapse, stress, strain, fatigue damage, shoulder gap margin, rod bow, cladding wear/fretting, assembly bow, spacer grid growth and spring tab relaxation, and hold down margin.

The overall conclusion is that the use of ZIRLO™ in place of OPTIN cladding would result in CENP fuel assembly designs that are fully capable of meeting their current design criteria.

5.6   References

5-1   CENP-388-P, "Extension of the 1-Pin Burnup Limit to 65 MWd/kgU for ABB PWR Fuel with OPTIN™ Cladding," February 1998.

5-2   CENPD-269-P Revision 1-P, "Extended Burnup Operation of Combustion Engineering PWR Fuel," July 1984.

5-3   CEN-386-P-A, "Verification of the Acceptability of a 1-Pin Burnup Limit of 60 MWD/kgU for Combustion Engineering 16x16 PWR Fuel," August 1992.

5-4   CEN-382(B)-P-A, "Verification of the Acceptability of a 1-Pin Burnup Limit of 60 MWD/kgU for Combustion Engineering 14x14 PWR Fuel," August 1993.

5-5   WCAP-12610-P-A, "VANTAGE+ Fuel Assembly Reference Core Report," Westinghouse Electric Company LLC, April 1995.

5-6   WCAP-15063-P-A Revision 1, with Errata, "Westinghouse Improved Performance Analysis and Design Model (PAD 4.0)," Westinghouse Electric Company LLC Nuclear Fuel, July 2000.

5-7   CENPD-139-P-A, "Fuel Evaluation Model", July 1974.

5-8   CENPD-187-P-A, "CEPAN Method of Analyzing Creep Collapse of Oval Cladding," April 1976; Supplement 1-P-A, June 1977.

5-9   EPRI NP-3966 "CEPAN Method of Analyzing Creep Collapse of Oval Cladding – Volume 1: General Description," April 1985.

5-10   EPRI NP-3966-CCMP, "CEPAN Method of Analyzing Creep Collapse of Oval Cladding – Volume 4: Finite Axial-Length Version," April 1985.

5-11   EPRI NP-3966-CCM, "CEPAN Method of Analyzing Creep Collapse of Oval Cladding - Volume 5: Evaluation of Interpellet Gap Formation and Cladding Collapse in Modern PWR Fuel Rods," April 1985.

5-12   CEN-183(B)-P, "Application of CENPD-198 to Zircaloy Component Dimensional Changes," September 1981.

5-13   CENPD-225-P-A and Supplements 1, 2 and 3, "Fuel and Poison Rod Bowing," June 1983.

5-14   Letter from E. J. Butcher (USNRC) to A. E. Lundvall, Jr. (BGE) regarding Safety Evaluation Report for CENPD-269-P. October 10, 1985.

5-15   CEN-289(A)-P, "Revised Rod Bow Penalties for Arkansas Nuclear One Unit 2," December 1984.

5-16   CENPD-178-P, Rev. 1-P, "Structural Analysis of Fuel Assemblies for Seismic and Loss of Coolant Accident Loading," August 1981.

5-17   Letter S. A. Toelle (CENP) to T. E. Collins (NRC), LD-94-021, dated April 1, 1994, transmitting Combustion Engineering *TechNote* No. 94-03, "Grid-to-Fuel Rod Fretting Wear," April 1, 1994.

5-18   Letter I. C. Rickard (CENP) to T. E. Collins (NRC), LD-96-044, dated October 11, 1996, transmitting Combustion Engineering *TechNote* No. 94-03, Supplement 1, "Grid-to-Rod Fretting Wear," October 7, 1996.

5-19   O. D. Parr (NRC) to A. E. Scherer (CE), Untitled, February 10, 1976.

5-20   C. O. Thomas (NRC) to A. E. Scherer (CE), " Acceptance for Referencing of Topical Report CENPD-225-P," February 15, 1983.

5-21   H. Bernard (NRC) to A. E. Scherer (CE), " Acceptance for Referencing of Licensing Topical Report CENPD-178," August 6, 1982.

5-22   CE NPSD-1049-P, "Potential for Delayed CEA Insertion Times at C-E Designed Plants," Prepared for the C-E Owners Group, June 1986.

Table 5.2-1

Topical Reports and Safety Evaluations for the Mechanical Design Models

Subject	Topical Report Reference	Safety Evaluation Report Reference

CEPAN Model
    CENPD-187-P-A
    Supplement 1
Downgraded to Non-Proprietary
	5-8
	5-8
		5-19
		none[1]

SIGREEP Model CEN-183(B)-P	5-12	none[2]

Rod Bow Model
    CENPD-225-P-A
    Supplement 1
    Supplement 2
    Supplement 3
	5-13	5-20
		5-20
		5-20
		5-20

Seismic / LOCA Model CENPD-178-P	5-16	5-21

Note 1: Supplement 1 is only an abstract with two tables from which some proprietary information was removed. As such, no SER was required.

Note 2: No explicit SER has been identified for this application but acceptance of the SIGREEP model is inferred from the acceptance of References 5-2, 5-3, and 5-4.

Table 5.2-2

Cladding Models Used in Mechanical Design Models

Cladding Related Parameters	Fuel Mechanical Design Model	
	CEPAN	SIGREEP
Creep		
Thermal	Yes	Yes
Irradiation	Yes	Yes
Thermal Expansion	No	Yes
Yield Strength	Yes	No
Modulus of Elasticity	Yes	No
Poisson's Ratio	Yes	No
Initial Ovality	Yes	No
Rod Axial Growth	No	Yes
Uncertainties	No	Yes

Note: Analytical models for rod bow and seismic/LOCA evaluations, References 5-13 and 5-16, are not included in the above table since the introduction of ZIRLO™ will have no effect on these models. Sections 5.2.3 and 5.2.4 discuss the rationale associated with this no model impact conclusion.

Table 5.4.7-1
Implementation of Advanced Laser Welded Grids
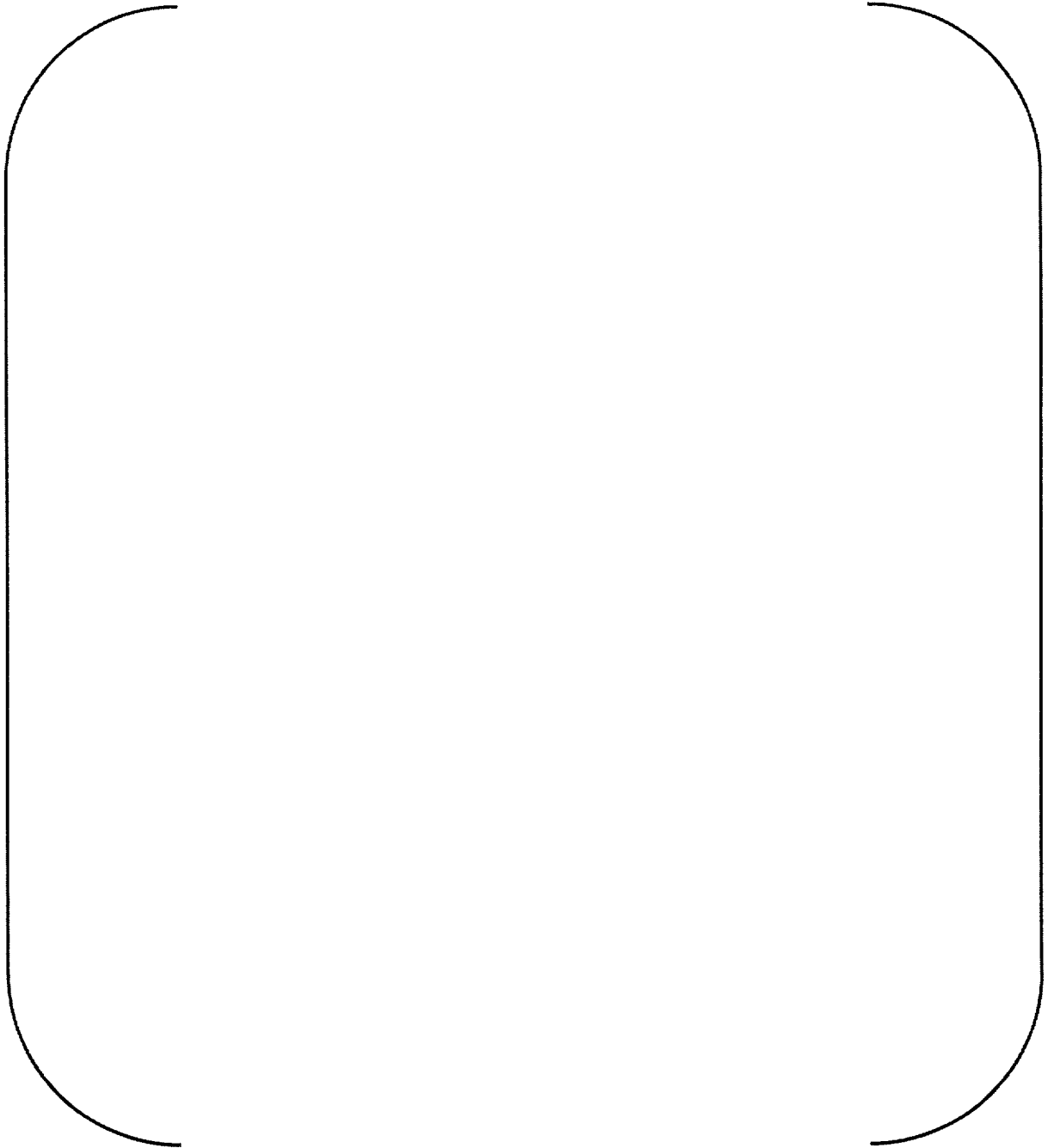
Table 5.4.7-2
Grid-to-Rod Fretting Wear Induced Failures in
CENP US PWR Fuel Supplied Since 1984

Table 5.4.7-3
Effect of Cladding Material Change on Factors Contributing to Fretting Failures
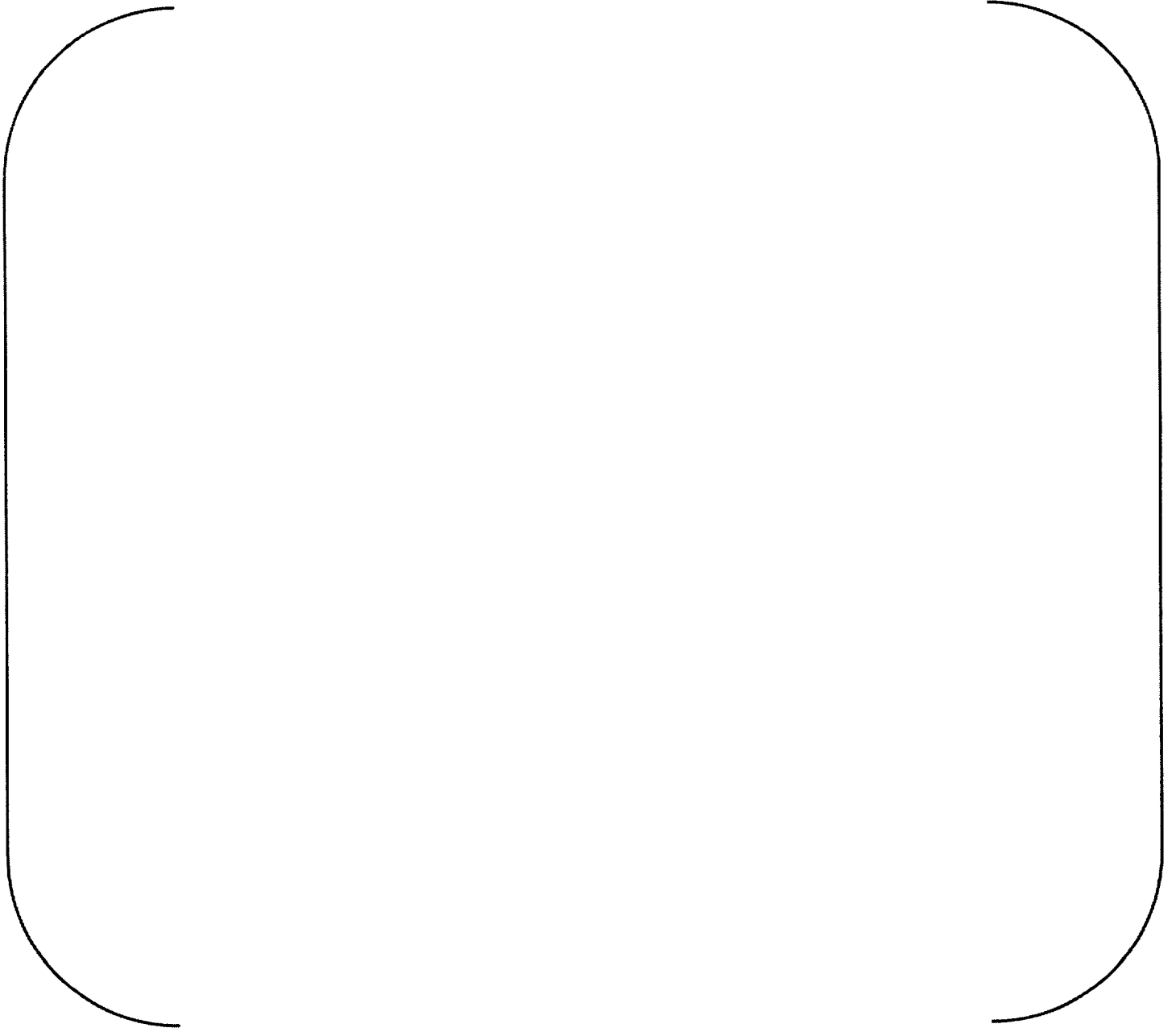
Table 5.4.7-4
Relevant Experience*

Table 5.4.7-5
Additional Experience

6.0 ECCS Performance Analysis

6.1 Introduction

This section describes the implementation of ZIRLO™ cladding in the CE Nuclear Power (CENP) Large Break Loss-of-Coolant Accident (LBLOCA) and Small Break Loss-of-Coolant Accident (SBLOCA) Emergency Core Cooling System (ECCS) performance evaluation models. Section 6.2 describes the cladding related models for Zircaloy-4 used in the CENP LBLOCA and SBLOCA evaluation models. Section 6.3 describes the modifications that have been made to those models to represent ZIRLO™ cladding. It includes a description of the cladding model for ZIRLO™ for each parameter that requires a model different than that used for Zircaloy-4. It also identifies those parameters for which the Zircaloy-4 model is applicable to ZIRLO™ and provides a basis for the applicability of the Zircaloy-4 model to ZIRLO™. Section 6.4 discusses the maintenance of the interface between the fuel performance model, FATES3B, and the ECCS performance evaluation model for ZIRLO™ cladding. Section 6.5 presents the results of both a LBLOCA and SBLOCA ECCS performance analysis of ZIRLO™ cladding. The results are compared to the results of equivalent analyses of Zircaloy-4 cladding. The conclusions of the implementation of ZIRLO™ cladding in the CENP LBLOCA and SBLOCA ECCS performance evaluation models are presented in Section 6.6.

The implementation of ZIRLO™ cladding in the CENP evaluation models is based on the NRC-accepted implementation of ZIRLO™ cladding in the Westinghouse Appendix K evaluation models (Reference 6-45). As described in Reference 6-45, Westinghouse determined that many of the physical and mechanical properties of ZIRLO™ are similar to those of Zircaloy-4 when the two alloys are in the same metallurgical phase. Consequently, many of the material property models for Zircaloy-4 are applicable to ZIRLO™. However, the change from the alpha phase to the beta phase for ZIRLO™ occurs over a different temperature range than it does for Zircaloy-4. This requires that several material property models applicable to Zircaloy-4 be modified to represent ZIRLO™. In particular, the models for [

] were modified to represent ZIRLO™ in the Westinghouse Appendix K evaluation models. The

6-1

Westinghouse ZIRLO™ models are implemented in the CENP evaluation models as described herein.

Westinghouse also demonstrated that the use of the Baker-Just model for the calculation of the metal-water reaction rate, which is a required feature of Appendix K evaluation models, is suitably conservative for ZIRLO™ cladding. The CENP evaluation models retain the use of the Baker-Just model as described herein.

Lastly, it is noted that 10 CFR 50.46, which identifies the ECCS acceptance criteria for light-water nuclear power reactors, has been revised to extend the applicability of the criteria to fuel that is clad with ZIRLO™ cladding. Consequently, no exemptions to 10 CFR 50.46 or Appendix K to 10 CFR 50 are needed to apply the criteria to CENP designed fuel clad with ZIRLO™.

6.2   Summary of Cladding-Related Models in the CENP ECCS Performance Evaluation Models

The current versions of the CENP ECCS performance evaluation models are the 1999 Evaluation Model (1999 EM) for LBLOCA and the S2M (Supplement 2 Evaluation Model) for SBLOCA. Table 6.2-1 lists the topical reports and the NRC's Safety Evaluation Reports (SERs) associated with the 1999 EM and the S2M.

The 1999 EM includes the following computer codes. CEFLASH-4A and COMPERC-II perform the blowdown and refill/reflood hydraulic analyses, respectively. In addition, COMPERC-II calculates the minimum containment pressure and FLECHT-based reflood heat transfer coefficients. PARCH and HCROSS calculate steam cooling heat transfer coefficients. STRIKIN-II performs the hot rod heatup analysis. COMZIRC, which is a derivative of the COMPERC-II code, calculates the core-wide cladding oxidation percentage.

The S2M uses the following computer codes. CEFLASH-4AS performs the hydraulic analysis prior to the time that the Safety Injection Tanks (SITs) begin to inject. After injection from the SITs begins, COMPERC-II is used to perform the hydraulic analysis. The hot rod heatup

analysis is performed by STRIKIN-II during the initial period of forced convection heat transfer and by PARCH during the subsequent period of pool boiling heat transfer.

The 1999 EM and S2M are NRC-accepted for ECCS performance analyses of CENP designed Pressurized Water Reactors (PWRs) fueled with Zircaloy-4 clad fuel assemblies. Table 6.2-2 lists the cladding related models that are used in the evaluation models and identifies the source document for each model. The following three references are the primary source documents for the models. Reference 6-38 is the source for the majority of the thermophysical and mechanical properties. It is also the source for the cladding rupture and swelling models used in the S2M. NUREG-0630 (Reference 6-39) is the source for the cladding rupture, swelling and blockage models used in the 1999 EM. As required by Appendix K to 10 CFR 50, the Baker-Just model (Reference 6-41) is the source document for the metal-water reaction rate model.

The following sections identify the topical report documentation associated with the specific Zircaloy-4 models used by each computer code. For ease of presentation of the information, the models are combined into four groups:

1. Thermophysical properties of specific heat, density and thermal conductivity
2. Thermal and mechanical properties used in the calculation of the fuel-to-cladding gap conductance and the inside diameter of the cladding. The properties in this group include thermal expansion, modulus of elasticity, Poisson's ratio, and diamond pyramid hardness. Also included in the group is thermal emissivity, which is used in the STRIKIN-II rod-to-rod thermal radiation model and the PARCH radiation heat transfer to steam model, as well as the gap conductance model.
3. Cladding rupture, swelling, and blockage models, including pre-rupture plastic strain
4. Metal-water reaction rate model

6.2.1 CEFLASH-4A

The Zircaloy-4 models for specific heat and thermal conductivity used in CEFLASH-4A are described in Section III.B.11 of Reference 6-9. The specific heat is used in conjunction with a constant value for density equal to 409 lbm/ft^3.

Prior to the 1999 EM version of the CENP LBLOCA evaluation model (i.e., the 1985 EM (Reference 6-4) and earlier versions), the CEFLASH-4A fuel rod model represented the fuel-to-cladding gap with a constant gap conductance and internal pressure. Consequently, the code did not include cladding models for thermal emissivity, thermal expansion, modulus of elasticity, Poisson's ratio, and diamond pyramid hardness. The 1999 EM introduced a dynamic fuel rod internal pressure model. The model is described in Section 2.3 of Reference 6-5. The model represents cladding dimensional changes due to thermal and mechanical expansion and contraction using the model described in the PARCH topical report. In particular, it uses the Zircaloy-4 models for Poisson's ratio and modulus of elasticity described in Reference 6-22, Section 3.4.1 and the thermal expansion model described in Reference 6-24, Appendix B.

CEFLASH-4A uses the NUREG-0630 (Reference 6-39) models for cladding rupture temperature, cladding rupture strain, and assembly blockage. The models are described in Sections 3.2.1 and 3.2.2 and Appendix C.3 of Reference 6-25 and in Section 2.1.2 of Reference 6-5. With the introduction of the dynamic fuel rod internal pressure model in the 1999 EM, the NRC plastic strain model, which is the plastic strain model used in STRIKIN-II, was added to CEFLASH-4A (Reference 6-5, Section 2.3). The model is described in Reference 6-19, Section II.B.

CEFLASH-4A uses the Baker-Just metal-water reaction rate model. It is described in Section III.B.10 of Reference 6-9.

6.2.2 CEFLASH-4AS

CEFLASH-4AS uses the same models for specific heat and density for Zircaloy-4 as are used in CEFLASH-4A. The Zircaloy-4 model for thermal conductivity used in CEFLASH-4AS is described in Section I (page 3) of Reference 6-13.

Similar to the pre-1999 EM versions of CEFLASH-4A, CEFLASH-4AS represents the fuel-to-cladding gap with a constant gap conductance. Consequently, it does not contain cladding models for thermal emissivity, thermal expansion, modulus of elasticity, Poisson's ratio, and diamond pyramid hardness.

Because the CEFLASH-4AS core model represents the average rod in the core, it does not model cladding rupture and assembly blockage. Likewise, it does not model pre-rupture plastic strain.

CEFLASH-4AS uses the Baker-Just metal-water reaction rate model. It is described in Section III.B.10 of Reference 6-9.

6.2.3 COMPERC-II

The Zircaloy-4 models for specific heat and thermal conductivity used in COMPERC-II are described in Appendix C of Reference 6-15. They are the same models that are used by CEFLASH-4A, STRIKIN-II, and PARCH. The specific heat is used in conjunction with a constant input value for cladding mass per foot of fuel rod (i.e., the product of the cladding density and cross-sectional area). A value of 409 lbm/ft^3 is typically used for the density of Zircaloy-4 in the calculation of the cladding mass per foot.

COMPERC-II uses a constant value for the gap conductance. The value, which isa code input, is obtained from CEFLASH-4A. Therefore, COMPERC-II does not model cladding thermal emissivity, thermal expansion, modulus of elasticity, Poisson's ratio, or diamond pyramid hardness.

COMPERC-II does not model cladding rupture, assembly blockage, or pre-rupture plastic strain.

COMPERC-II uses the Baker-Just metal-water reaction rate model. The model is described in Appendix D of Reference 6-15.

6.2.4 STRIKIN-II

The Zircaloy-4 models for specific heat and thermal conductivity used in STRIKIN-II are described in Appendix I of Reference 6-18. They are the same models that are used by CEFLASH-4A, COMPERC-II, and PARCH. Also like those codes, it uses a constant value of 409 lbm/ft^3 for the density of Zircaloy-4.

Appendix I of Reference 6-18 also documents the Zircaloy-4 models for thermal emissivity, thermal expansion, modulus of elasticity, Poisson's ratio, and diamond pyramid hardness that STRIKIN-II uses.

STRIKIN-II uses the NUREG-0630 (Reference 6-39) models for cladding rupture temperature, rupture strain, and assembly blockage. The models are described in Sections 3.2.1 and 3.2.2 and Appendix C.2 of Reference 6-25 and in Section 2.1.2 of Reference 6-5. The pre-rupture plastic strain model used by STRIKIN-II is the NRC model described in Section II.B and Appendix A of Reference 6-19.

STRIKIN-II uses the Baker-Just metal-water reaction rate model. The model is described in Section II.9 of Reference 6-18.

6.2.5 PARCH

The Zircaloy-4 models for specific heat and thermal conductivity used in PARCH are described in Section 3.4.4 of Reference 6-22. They are the same models that are used by CEFLASH-4A, COMPERC-II, and STRIKIN-II. Also like those codes, it uses a constant value of 409 lbm/ft^3 for the density of Zircaloy-4.

Section 3.4.1 of Reference 6-22 documents the Zircaloy-4 models for thermal emissivity, modulus of elasticity, Poisson's ratio, and diamond pyramid hardness that are used by PARCH. The model for the modulus of elasticity described in Section 3.4.1 is an equation for the linear portion of the curve for the modulus of elasticity plotted in Figure 2 of Reference 6-38. The model was modified as described in Reference 6-42 to better represent the non-linear portion of the curve. The model for thermal expansion is documented in Section II.b and Appendix B of Reference 6-24. It consists of a functional fit of the graphical representation of thermal expansion in Reference 6-38.

The Zircaloy-4 models for cladding rupture temperature and rupture strain used in PARCH for SBLOCA analyses are described in Section 3.4.2 of Reference 6-22. PARCH uses the [

] curve for rupture temperature versus differential pressure and the [   ] curve for

6-6

rupture strain versus differential pressure described in Reference 6-38. (Note: the SBLOCA evaluation model does not use the NUREG-0630 cladding rupture and swelling models as described in Section 1.2.2 of Reference 6-25.) Applicability of the models described in Reference 6-38 to CENP's 16x16 fuel assemblies is documented in Reference 6-43. Reference 6-44 is the SER for Reference 6-43. PARCH does not model assembly blockage or pre-rupture plastic strain.

The preceding discussion of the PARCH cladding rupture and strain models is applicable to the SBLOCA evaluation model. In the LBLOCA evaluation model, PARCH is used to calculate steam cooling heat transfer coefficients that are applied at and above the elevation of cladding rupture, i.e., it is used after STRIKIN-II has calculated the time of cladding rupture and the amount of rupture strain and assembly blockage. Consequently, the PARCH cladding rupture temperature and rupture strain models are not used in LBLOCA applications.

PARCH uses the Baker-Just metal-water reaction rate model. The model is described in Section 3.4.3 of Reference 6-22.

6.2.6 COMZIRC

The cladding models used by COMZIRC are the same as those described in Section 6.2.3 for COMPERC-II.

6.2.7 HCROSS

HCROSS does not use any of the cladding models listed in Table 6.2-2. HCROSS calculates normalized blocked channel steam flow fractions, which are used by PARCH to calculate the steam cooling heat transfer coefficients used by STRIKIN-II. The amount of assembly blockage, which is determined by STRIKIN-II, is an input to HCROSS.

6.3 ZIRLO™ Properties and Correlations in the CENP ECCS Performance Evaluation Models

6.3.1 Specific Heat

The specific heat of ZIRLO™ used in the Westinghouse Appendix K and Best Estimate evaluation models is given by the values listed in Tables 6.3.1-1 and 6.3.1-2, respectively. The values include the heat of transformation associated with the alpha-to-beta phase change that occurs between 1382°F and 1724°F. The specific heat of ZIRLO™ is different from that of Zircaloy-4 primarily because of the difference in the temperature range over which the alpha-to-beta phase change occurs for the two alloys.

In the CENP evaluation models, the specific heat of Zircaloy-4, which is obtained from Reference 6-37, is represented by the values listed in Table 6.3.1-3. It is compared to the two ZIRLO™ models for specific heat in Figure 6.3.1-1. The comparison shows that both the Westinghouse Best Estimate model for ZIRLO™ and the CENP model for Zircaloy-4 represent the alpha-to-beta phase change heat of transformation with more detail than is used in the Westinghouse Appendix K model for ZIRLO™. Therefore, in order to maintain the same level of detail as is currently used in the CENP evaluation models to represent the specific heat of Zircaloy-4, the CENP evaluation models use the Westinghouse Best Estimate model for the specific heat of ZIRLO™.

6.3.2 Density

The Westinghouse Appendix K evaluation models represent the density (ρ, lbm/ft^3) of ZIRLO™ with the same equation used for Zircaloy-4. The equation is as follows:

$$\rho = 410 / (1 + 9.66 \times 10^{-6}T)$$

where T is the cladding temperature (°F). The CENP evaluation models use a constant value of 409 lbm/ft^3 for the density of Zircaloy-4.

In comparison, for cladding temperatures ≤2200°F, the Westinghouse equation that is used for both Zircaloy-4 and ZIRLO™ gives a density that is less than 2% different than the constant value that is used for Zircaloy-4 in the CENP evaluation models. On the basis that this is an insignificant difference, the CENP evaluation models use the same constant value of density (i.e., 409 lbm/ft³) for ZIRLO™ as used for Zircaloy-4.

6.3.3 Thermal Conductivity

The thermal conductivity of Zircaloy-4 is used for ZIRLO™ in the Westinghouse Appendix K evaluation models. In the Westinghouse Appendix K evaluation models, the thermal conductivity (k, BTU/hr-ft-°F) is the maximum of the two values obtained from the following equations:

$$k = 7.404 + 2.9 \times 10^{-3} T$$
$$k = 5.621 + 5.3 \times 10^{-3} T$$

where T is cladding temperature (°F).

The equation for thermal conductivity for Zircaloy-4 used in the CENP evaluation models, with the exception of CEFLASH-4AS, is the following equation, which is taken from Reference 6-38:

[   ]

CEFLASH-4AS uses the following equation given on page 3 of Reference 6-13:

[   ]

The three models are compared in Figure 6.3.3-1. The thermal conductivity calculated using the Westinghouse model ranges from [   ] different from that calculated using the CENP model over the temperature range of interest. The CENP model also compares favorably with the data for ZIRLO™ and Zircaloy-4 presented in Reference 6-45 (page 62 of Section G). Therefore, consistent with the approach used in the Westinghouse Appendix K evaluation

models, the CENP evaluation models use the same equations for thermal conductivity for ZIRLO™ as used for Zircaloy-4.

6.3.4 Thermal Emissivity

The thermal emissivity of Zircaloy-4 is used for ZIRLO™ in the Westinghouse Appendix K evaluation models. Consistent with the Westinghouse approach, the CENP evaluation models also use the thermal emissivity of Zircaloy-4 for ZIRLO™.

In the CENP evaluation models, the following equation from Reference 6-38 is used to represent the hemispherical emissivity (ε) of oxidized Zircaloy-4 and ZIRLO™ :

$$\varepsilon = -6.006 \times 10^{-2} + 1.367 \times 10^{-3}T - 5.579 \times 10^{-7}T^2$$

where T is the cladding temperature (°C). Figure 6.3.4-1 presents the equation in graphical form. Note that in STRIKIN-II, the value for the emissivity is set to a minimum value of 0.25 below 253°C (487°F).

Application of the CENP model for the thermal emissivity of oxidized Zircaloy-4 to ZIRLO™ is acceptable on the following basis. As stated in Appendix A of Reference 6-45, since ZIRLO™ and Zircaloy-4 are both approximately 98% zirconium, their properties are expected to be insignificantly different except to the extent that they are affected by the differences in the temperature range over which the alpha-to-beta phase change occurs. As shown in Figure 6.3.4-1, the emissivity of Zircaloy-4 is not dependent on its alpha-to-beta transition temperature range (i.e., there are no inflections, discontinuities, etc., in the behavior of the emissivity over the transition temperature range). Consequently, it is expected that the emissivity of ZIRLO™ is also not dependent on its alpha-to-beta transition temperature range and, therefore, its emissivity would be similar to that of Zircaloy-4. Furthermore, the model is for oxidized cladding and, as noted above, Zircaloy-4 and ZIRLO™ are both approximately 98% zirconium. Therefore, it is concluded that the Zircaloy-4 model is applicable to ZIRLO™.

6.3.5 Thermal Expansion

The thermal expansion for Zircaloy-4 is used for ZIRLO™ in the Westinghouse Appendix K evaluation models for both radial and axial expansion. The model for thermal expansion in the radial direction ($\Delta r/r$) is given by the following equation:

$$[\qquad\qquad]$$

where T is cladding temperature (°F).

The CENP evaluation models use the thermal expansion model described in Reference 6-38. Note that in the CENP evaluation models, only the radial thermal expansion model is used. In Reference 6-38, the model is presented as a graph of thermal expansion versus temperature. As coded in STRIKIN-II, the model consists of a table of values for thermal expansion versus temperature (Reference 6-18, Appendix I). In PARCH, the model consists of a functional fit of the graphical information (Reference 6-24, Section II.b and Appendix B). As stated in Section 6.2.1, CEFLASH-4A uses the same model as used in PARCH.

The Westinghouse and CENP models are compared in Figure 6.3.5-1. As seen in the comparison, the change in thermal expansion that occurs as a result of the transformation from the alpha to the beta phase is reflected in the CENP model for Zircaloy-4. [

] Based on this lack of sensitivity of the PCT to changes in the

cladding thermal expansion model, the CENP evaluation models use the CENP Zircaloy-4 thermal expansion model for ZIRLO™.

6.3.6 Modulus of Elasticity

The modulus of elasticity for Zircaloy-4 is used for ZIRLO™ in the Westinghouse Appendix K evaluation models. Consistent with the Westinghouse approach, the CENP evaluation models also use the modulus of elasticity of Zircaloy-4 for ZIRLO™.

The model for the modulus of elasticity (E, kpsi) for Zircaloy-4 used in the CENP evaluation models is described in Reference 6-38. As coded in STRIKIN-II and PARCH, the model uses an equation for temperatures less than or equal to [   ] and linear interpolation from a table of values for temperatures above [   ] The equation used in PARCH is as follows:

[   ]

where T is cladding temperature (°F). The same equation, but with more significant figures for the constants, is used in STRIKIN-II. The following table of values is used for temperatures above [.]

[

                                                                                      ]

The model is depicted in Figure 6.3.6-1.

Any actual difference between the modulus of elasticity of Zircaloy-4 and ZIRLO™ will have an insignificant impact on PCT for the following reasons. The modulus of elasticity, in conjunction with Poisson's ratio, is used in the calculation of the change in the cladding inside diameter due to mechanical expansion/contraction of the cladding. This change, together with the change

due to thermal expansion and plastic strain, is used to calculate the cladding inside diameter that is used in the calculation of the gap conductance in STRIKIN-II and PARCH. The mechanical component of the change in cladding diameter is small in comparison to the change due to thermal expansion and, when it occurs, plastic strain. Also, after the cladding ruptures, there is no differential pressure across the cladding and, consequently, there is no longer a mechanical component to the change in cladding diameter.

The cladding inside diameter is also used in the calculation of the gap pressure. In particular, it is used to calculate the volume of the gap between the fuel and the cladding. This volume is combined with the plenum volume at the top of the fuel rod and the fuel dish and porosity volumes to give the total gas volume used in the calculation of the gap pressure. For the same reason as described above, variations in the modulus of elasticity will have an insignificant impact on the gas volume and gap pressure.

Lastly, the modulus of elasticity is used in the calculation of the mechanical interface pressure between the fuel and the cladding, which is used in the calculation of the gap conductance when the fuel and cladding are in contact with each other. As described in Section 6.3.8, for a given transient, the fuel and cladding are either never in contact or are in contact for a short length of time. Consequently, variations in the modulus of elasticity will not have a significant impact on the transient gap conductance.

6.3.7 Poisson's Ratio

Poisson's ratio for Zircaloy-4 is used for ZIRLO™ in the Westinghouse Appendix K evaluation models. Consistent with the Westinghouse approach, the CENP evaluation models also use Poisson's ratio for Zircaloy-4 for ZIRLO™.

The equation for Poisson's ratio (μ) for Zircaloy-4 used in the CENP evaluation models is the following equation from Reference 6-38:

$$\mu = 0.301 - 7.03 \times 10^{-5} T \quad [\qquad]$$

where T is cladding temperature (°F). [   ] is used for
Poisson's ratio. The model is depicted in Figure 6.3.7-1.

As described in Section 6.3.6, Poisson's ratio, in conjunction with the modulus of elasticity, is used in the calculation of the inside diameter of the cladding, which is used in the calculation of the gap conductance and the gap pressure. For the same reasons described in Section 6.3.6, variations in Poisson's ratio will have an insignificant impact on the transient gap conductance and gap pressure and, hence, on the cladding temperature.

6.3.8   Diamond Pyramid Hardness

Cladding hardness is not used in the Westinghouse Appendix K evaluation models. However, it is used in the CENP evaluation models. In particular, the diamond pyramid hardness is used in the calculation of the fuel-to-cladding gap conductance in the STRIKIN-II and PARCH computer codes when the fuel and cladding are in contact with each other.

Figure 6.3.8-1 depicts the model for the diamond pyramid hardness used in the CENP evaluation models for Zircaloy-4. The model is described in Reference 6-38. It is based on data obtained for temperatures ranging from room temperature to 1600°F. Above 1600°F Zircaloy-4 becomes soft and hardness measurements are difficult. Consequently, above 1600°F the model consists of [

]

Since the Westinghouse Appendix K evaluation models do not use a cladding hardness model, Reference 6-45 does not provide any specific information regarding the hardness of ZIRLO™. However, as described in Reference 6-45, the material properties of ZIRLO™ are similar to those of Zircaloy-4, except as they may be impacted by the difference in the temperature range over which the alpha-to-beta phase change occurs. As shown in Figure 6.3.8-1, there is no significant change in the behavior of the hardness of Zircaloy-4 as a result of the alpha-to-beta phase change. Therefore, it is expected that the hardness of ZIRLO™ is not significantly different from that of Zircaloy-4 even given the different temperature range over which the alpha-to-beta phase change occurs for the two alloys.

In addition, the cladding hardness is used in the calculation of the gap conductance only when the fuel and cladding are in contact. They are not initially in contact at low burnup, including the burnup (typically ~1000 MWD/MTU) that produces the minimum initial gap conductance and maximum initial fuel average temperature. Also, at higher burnup, when the fuel and cladding may initially be in contact, they will remain in contact for only a short period of time during the LOCA transient as a result of the thermal and mechanical expansion of the cladding. Therefore, any differences in the diamond pyramid hardness between Zircaloy-4 and ZIRLO™ will have an insignificant impact on the transient gap conductance and, hence, on the cladding temperature.

For these reasons, the CENP evaluation models use the Zircaloy-4 model for diamond pyramid hardness for ZIRLO™.

6.3.9   Cladding Rupture Temperature

6.3.9.1   CENP Large Break LOCA Evaluation Model

NUREG-0630 (Reference 6-39) describes the cladding rupture temperature, rupture strain, and assembly blockage models that were developed by the NRC for use in Appendix K evaluation models. The NUREG-0630 models for cladding rupture temperature, rupture strain, and assembly blockage are used in the Westinghouse Appendix K LBLOCA evaluation model and in the CENP LBLOCA evaluation model. However, because of the change in the temperature range over which the alpha-to-beta phase change occurs for ZIRLO™ versus Zircaloy-4, the models are not applicable to ZIRLO™ cladding. Consequently, Westinghouse conducted a rod burst test program for ZIRLO™ cladding and, following the methodology of NUREG-0630, developed rupture and blockage models for ZIRLO™ cladding that are used in the Westinghouse Appendix K evaluation models.

The ZIRLO™ cladding rupture temperature model is described in Reference 6-45 (pages 31-32 and Appendix D). The model is compared to the NUREG-0630 model in Figure 6.3.9.1-1. As described in Reference 6-45, [   ]

[

]

In implementing the rupture temperature versus engineering hoop stress model depicted in Figure 6.3.9.1-1, the Westinghouse LBLOCA Appendix K evaluation model includes a second criterion for predicting the occurrence of cladding rupture, namely, that [

]

The CENP LBLOCA evaluation model uses the Westinghouse model for the rupture temperature of ZIRLO™ cladding depicted in Figure 6.3.9.1-1. The model is presented in tabular form in Table 6.3.9.1-1 for the cladding dimensions of the CENP 14x14 and 16x16 fuel assemblies. The CENP LBLOCA evaluation model does not employ the second criterion [

] This results in earlier cladding rupture for any case in which the rupture temperature is reached before [   ] Calculating early cladding rupture is consistent with Appendix K, which requires that the incidence of cladding rupture shall not be underestimated.

6.3.9.2   CENP Small Break LOCA Evaluation Model

The CENP SBLOCA evaluation model uses the Westinghouse model for the rupture temperature of ZIRLO™ cladding [   ] The model is presented in tabular form in Table 6.3.9.1-1 for the cladding dimensions of the CENP 14x14 and 16x16 fuel assemblies.

As described in Section 6.2.5, the CENP SBLOCA evaluation model does not use the NUREG-0630 cladding rupture temperature model for Zircaloy-4 cladding. Rather, it uses the [

] curve for rupture temperature versus differential pressure described in Reference 6-38. The curve is compared to the Westinghouse ZIRLO™ model in Figure 6.3.9.2-1 for the cladding dimensions of the CENP 14x14 and 16x16 fuel assemblies that are identified in Table 6.3.9.1-1.

6.3.10   Cladding Rupture Strain

6.3.10.1   CENP Large Break LOCA Evaluation Model

The ZIRLO™ model for circumferential strain at the burst elevation developed by Westinghouse is described in Reference 6-45 (page 32 and Appendix D). The model is a correlation of rupture strain as a function of rupture temperature that conservatively bounds the ZIRLO™ test data. The model is compared to the NUREG-0630 model in Figure 6.3.10.1-1. Similar to the ZIRLO™ cladding rupture temperature model, [

]

The CENP LBLOCA evaluation model uses the Westinghouse ZIRLO™ model for circumferential rupture strain described above. The model is presented in tabular form in Table 6.3.10.1-1.

Note that the Westinghouse rupture strain model, for both Zircaloy-4 and ZIRLO™ , [

]

This revision to the rupture strain model, which is applicable to both the LBLOCA and SBLOCA evaluation models, is described in Reference 6-46. It was reviewed and accepted by the NRC in Reference 6-47.

The CENP evaluation model for Zircaloy-4 does not include [

] Consequently, the ZIRLO™ rupture strain model described above is applied [

] in the CENP LBLOCA evaluation model.

6.3.10.2 CENP Small Break LOCA Evaluation Model

The CENP SBLOCA evaluation model uses the Westinghouse ZIRLO™ model for circumferential rupture strain as a function of rupture temperature. The model is presented in tabular form in Table 6.3.10.1-1. The model does not include the [   ] described in Section 6.3.10.1.

As described in Section 6.2.5, the CENP SBLOCA evaluation model does not use the NUREG-0630 cladding rupture strain model for Zircaloy-4 cladding. Rather, it uses the [   ] curve for rupture strain versus differential pressure described in Reference 6-38. The [   ] curves for both the CENP 14x14 and 16x16 fuel assembly dimensions are compared to the Westinghouse ZIRLO™ model in Figure 6.3.10.2-1.

6.3.11 Assembly Blockage versus Rupture Temperature

The ZIRLO™ model for assembly blockage is described in Reference 6-45 (pages 32-33). It was developed from [

                                    ] The model is compared to the NUREG-0630 model in Figure 6.3.11-1.

The CENP LBLOCA evaluation model uses the Westinghouse ZIRLO™ model for assembly blockage. The model is presented in tabular form in Table 6.3.11-1. The CENP SBLOCA evaluation model does not use an assembly blockage model.

6.3.12 Pre-Rupture Plastic Strain

The pre-rupture plastic strain model used in the CENP LBLOCA evaluation model calculates plastic strain as a function of the cladding temperature and the cladding rupture temperature and rupture strain. The model is used in STRIKIN-II to determine the inside diameter of the cladding that is used in the calculation of the fuel-to-cladding gap conductance and in the calculation of the fuel rod internal pressure. The model is also used in the CEFLASH-4A dynamic fuel rod internal pressure model. Because the results of SBLOCA analyses are less sensitive to the

fuel-to-cladding gap conductance, the CENP SBLOCA evaluation model does not use the plastic strain model.

The plastic strain model used in the LBLOCA evaluation model is the NRC model described in Reference 6-19 (Section II.B and Appendix A). It uses the following equation to calculate the amount of plastic strain:

$$\varepsilon_P = 0.2 * \varepsilon_R * EXP(0.0153 * (T - T_R))$$

where:

ε_P = cladding plastic strain, %

ε_R = cladding rupture strain, %

T = cladding temperature, °F

T_R = cladding rupture temperature, °F

As described in Section C.2 of Reference 6-25, the amount of plastic strain prior to cladding rupture is limited to a maximum of 10% in STRIKIN-II.

In applying the plastic strain model to ZIRLO™ cladding, the ZIRLO™ models for cladding rupture temperature and rupture strain, which are described in Sections 6.3.9.1 and 6.3.10.1, are used to specify the cladding rupture temperature and rupture strain. No other changes to the plastic strain model are required in order for it to be applicable to ZIRLO™.

In summary, the LBLOCA evaluation model uses the pre-rupture plastic strain model, described above, for ZIRLO™ with the rupture temperature and rupture strain calculated as described in Sections 6.3.9.1 and 6.3.10.1.

6.3.13   Metal-Water Reaction Rate

Appendix E (Section H) to Reference 6-45 describes the ZIRLO™ metal-water reaction rate model. The model is based on data obtained from high temperature oxidation tests that were performed for twenty-four ZIRLO™ tubing samples. The parabolic rate constant, K, was

determined for each sample. An equation for K was then obtained by linear regression analysis of the logarithmic transform of the Arrhenius equation:

$$K = A * EXP(-Q/RT)$$

where:

K = parabolic rate constant, $(gm/cm^2)^2/sec$

A = constant, $(gm/cm^2)^2/sec$

Q = activation energy, cal/mole

R = gas constant, 1.987 cal/mole-°K

T = cladding temperature, °K

This yielded the following equation for the parabolic rate constant for ZIRLO™, at the upper 90% confidence level:

[   ]

where:

K = parabolic rate constant, $(gm\ O/cm^2)^2/sec$

T = cladding temperature, °K

Figure 6.3.13-1 compares the equation for the ZIRLO™ parabolic rate constant with the Baker-Just model equation (Reference 6-41). The comparison shows that the Baker-Just model predicts higher reaction rate constants than the ZIRLO™ model for temperatures above approximately 1800°F.

In compliance with Appendix K to 10 CFR 50, the CENP evaluation models use the Baker-Just metal-water reaction rate model for ZIRLO™ cladding. Since the Baker-Just model predicts higher reaction rates than the upper 90% confidence level fit to the ZIRLO™ oxidation test data, it provides a conservative prediction of the metal-water reaction rate for ZIRLO™ cladding.

6.4 Interface with Fuel Performance Model, FATES3B

Section 6.3 describes the implementation of cladding models for ZIRLO™ in the CENP LBLOCA and SBLOCA ECCS performance evaluation models. Section 4 describes the implementation of cladding models for ZIRLO™ in the CENP fuel performance model, FATES3B. FATES3B provides the initial fuel centerline temperatures used by CEFLASH-4A and CEFLASH-4AS and the initial cladding dimensions, as well as other inputs, used by STRIKIN-II. This section compares the implementation of ZIRLO™ in the ECCS performance evaluation models and the fuel performance model. The purpose of the comparison is to demonstrate that the interface between the models is maintained and that, consequently, the STRIKIN-II initial fuel average temperatures continue to equal or exceed those calculated by FATES3B.

As described in Section 6.3, most of the Zircaloy-4 cladding models used in the CENP LBLOCA and SBLOCA ECCS performance evaluation models are applicable to ZIRLO™. However, ZIRLO™-specific models were implemented for specific heat and the cladding rupture temperature, rupture strain, and assembly blockage models. The models for these parameters were modified primarily because these parameters are dependent on the temperature range of the alpha-to-beta phase change, which is different for ZIRLO™ as compared to Zircaloy-4. Cladding specific heat is not used in FATES3B. Likewise, cladding rupture models are not used in FATES3B since FATES3B analyzes steady state fuel performance whereas cladding rupture models are required for transient analyses. Thus, none of the cladding models that were changed in the CENP ECCS performance evaluation models for ZIRLO™ are used in the fuel evaluation model.

As described in Section 4, ZIRLO™-specific models were implemented for thermal and irradiation induced creep and fuel rod axial growth in the fuel performance model. Neither the creep nor the axial growth models are used in the CENP ECCS performance evaluation models.

As further described in Section 6.3 and Section 4, none of the Zircaloy-4 cladding models used in the calculation of gap conductance (i.e., thermal emissivity, thermal expansion, modulus of elasticity, Poisson's ratio, and diamond pyramid hardness) were changed for ZIRLO™ in either STRIKIN-II or FATES3B.

Based on the above, it is seen that FATES3B continues to provide cold, creeped-down cladding dimensions to STRIKIN-II and STRIKIN-II continues to calculate initial hot cladding dimensions from those dimensions using the same thermal expansion models as previously used. Likewise, both codes continue to use the same models for the cladding parameters that are used in the calculation of gap conductance that were previously used for Zircaloy-4. Therefore, no changes have been made to either STRIKIN-II or FATES3B that impact the interface between the two codes. Consequently, the STRIKIN-II initial fuel average temperatures will continue to equal or exceed those calculated by FATES3B for ZIRLO™ as they do for Zircaloy-4.

6.5   Impact of ZIRLO™ on ECCS Performance

This section presents the results of an ECCS performance analysis for a typical CENP designed PWR fueled with ZIRLO™ clad CENP fuel assemblies. Results are provided for both a typical limiting LBLOCA (Section 6.5.1) and SBLOCA (Section 6.5.2). The results are compared to the results of equivalent analyses of Zircaloy-4 clad CENP fuel assemblies.

The analyses are presented as samples that are indicative of the transient behavior of ZIRLO™ cladding versus Zircaloy-4 cladding as calculated by the CENP LBLOCA and SBLOCA evaluation models. They are not intended to be referenced by licensees whose ECCS performance analyses use the CENP evaluation models when implementing ZIRLO™ cladding. The effect of implementing ZIRLO™ on PCT will be reported to the NRC in accordance with 10 CFR 50.46(a)(3)(ii) for each plant-specific implementation of ZIRLO™ cladding in CENP designed PWRs licensed with CENP ECCS performance evaluation models.

6.5.1   LBLOCA ECCS Performance

6.5.1.1   Method of Analysis

The LBLOCA ECCS performance analysis described in this section uses the 1999 EM version of the CENP LBLOCA evaluation model (Reference 6-5) in conjunction with the ZIRLO™ cladding models described in Section 6.3 of this topical report. The computer codes that

comprise the 1999 EM are briefly described in Section 6.2. Table 6.2-1 provides a complete listing of the topical reports (excluding this topical report) that comprise the 1999 EM.

The analysis was performed for a 0.6 Double-Ended Guillotine break in the Reactor Coolant Pump Discharge Leg (0.6 DEG/PD), which is a typical limiting break size in the LBLOCA analyses of CENP designed PWRs using the CENP LBLOCA evaluation model. In the context of this analysis, analyzing a typical limiting break size is sufficient since the purpose of the analysis is to demonstrate the behavior of ZIRLO™ cladding under typical licensing analysis conditions and to compare the behavior to that of Zircaloy-4 cladding.

Hot rod heatup calculations were performed at the burnup with the maximum initial fuel stored energy and at the burnup with the highest initial rod internal pressure at the Peak Linear Heat Generation Rate (PLHGR) for both ZIRLO™ and Zircaloy-4 cladding. These two times-in-life were selected to provide examples of the impact of ZIRLO™ at two extremes in the burnup range of a reload cycle.

6.5.1.2   Plant Design Data

The sample LBLOCA analysis described in this section was performed for a typical CENP designed PWR. In particular, the plant has a rated core power of 2700Mwt (2754 Mwt including 2% power measurement uncertainty) and is fueled with 14x14 Guardian™ grid fuel assemblies with erbia burnable absorber fuel rods. Values for Reactor Coolant System (RCS), steam generator, safety injection system, and containment parameters that are typical of those used in LBLOCA analyses were used in the sample analysis. The plant design data used in the sample LBLOCA analysis for several important core and RCS parameters are listed in Table 6.5.1.2-1. Analyses are performed for both ZIRLO™ and Zircaloy-4 clad fuel rods.

6.5.1.3   Results

Tables 6.5.1.3-1 through 6.5.1.3-3 present important results for the sample LBLOCA analysis. Tables 6.5.1.3-1 and 6.5.1.3-2 compare the results for the cases run at the maximum stored energy burnup and the maximum rod internal pressure burnup, respectively. Table 6.5.1.3-3

compares the maximum cladding temperatures below, at, and above the elevation of cladding rupture for ZIRLO™ and Zircaloy-4 for the cases run at the maximum stored energy burnup and the maximum rod internal pressure burnup. Figures 6.5.1.3-1 through 6.5.1.3-3 compare the transient response of the cladding temperature, gap conductance, and cladding surface heat transfer coefficient at the location of the PCT for the ZIRLO™ and Zircaloy-4 cases run at the maximum stored energy burnup. The cladding oxidation percentage for the elevations with the maximum percentages are compared in Figure 6.5.1.3-4.

The sample analyses demonstrate that the impact of implementing ZIRLO™ on ECCS performance is seen primarily in the hot rod heatup analysis. Implementation of ZIRLO™ has only a minor impact on the blowdown and refill/reflood hydraulic transients. As shown in Tables 6.5.1.3-1 and 6.5.1.3-2, there are no significant differences in the timing of the hydraulic transients between the ZIRLO™ and Zircaloy-4 cases. Also, there is less than a 0.1% difference in the reflood rates between the ZIRLO™ and Zircaloy-4 cases.

As shown in the tables, the hot rod heatup transient is impacted by the implementation of ZIRLO™. In particular, as shown in Table 6.5.1.3-3, the impact on the local maximum cladding temperature depends on the location relative to the elevation of cladding rupture. The following paragraphs compare the behavior of cladding temperature for ZIRLO™ and Zircaloy-4 above, at, and below the elevation of cladding rupture.

The PCT is calculated to occur above the elevation of cladding rupture for both ZIRLO™ and Zircaloy-4 for both the maximum stored energy and maximum rod internal pressure cases. The PCT for ZIRLO™ is lower than that for Zircaloy-4 because the amount of assembly flow blockage is less for ZIRLO™ than for Zircaloy-4. As shown in Table 6.5.1.3-3, the difference in the PCT between ZIRLO™ and Zircaloy-4 is greater for the maximum stored energy case (2009°F – 1951°F = 58°F) than it is for the maximum rod internal pressure case (1971°F – 1958°F = 13°F). This is because the difference in the amount of assembly blockage is greater between ZIRLO™ and Zircaloy-4 for the maximum stored energy case than for the maximum rod internal pressure case. Also, the PCT for ZIRLO™ is greater for the maximum rod internal pressure case than it is for the maximum stored energy case because of the higher assembly blockage that occurs for the maximum rod internal pressure case.

compares the maximum cladding temperatures below, at, and above the elevation of cladding rupture for ZIRLO™ and Zircaloy-4 for the cases run at the maximum stored energy burnup and the maximum rod internal pressure burnup. Figures 6.5.1.3-1 through 6.5.1.3-3 compare the transient response of the cladding temperature, gap conductance, and cladding surface heat transfer coefficient at the location of the PCT for the ZIRLO™ and Zircaloy-4 cases run at the maximum stored energy burnup. The cladding oxidation percentage for the elevations with the maximum percentages are compared in Figure 6.5.1.3-4.

The sample analyses demonstrate that the impact of implementing ZIRLO™ on ECCS performance is seen primarily in the hot rod heatup analysis. Implementation of ZIRLO™ has only a minor impact on the blowdown and refill/reflood hydraulic transients. As shown in Tables 6.5.1.3-1 and 6.5.1.3-2, there are no significant differences in the timing of the hydraulic transients between the ZIRLO™ and Zircaloy-4 cases. Also, there is less than a 0.1% difference in the reflood rates between the ZIRLO™ and Zircaloy-4 cases.

As shown in the tables, the hot rod heatup transient is impacted by the implementation of ZIRLO™. In particular, as shown in Table 6.5.1.3-3, the impact on the local maximum cladding temperature depends on the location relative to the elevation of cladding rupture. The following paragraphs compare the behavior of cladding temperature for ZIRLO™ and Zircaloy-4 above, at, and below the elevation of cladding rupture.

The PCT is calculated to occur above the elevation of cladding rupture for both ZIRLO™ and Zircaloy-4 for both the maximum stored energy and maximum rod internal pressure cases. The PCT for ZIRLO™ is lower than that for Zircaloy-4 because the amount of assembly flow blockage is less for ZIRLO™ than for Zircaloy-4. As shown in Table 6.5.1.3-3, the difference in the PCT between ZIRLO™ and Zircaloy-4 is greater for the maximum stored energy case (2009°F − 1951°F = 58°F) than it is for the maximum rod internal pressure case (1971°F − 1958°F = 13°F). This is because the difference in the amount of assembly blockage is greater between ZIRLO™ and Zircaloy-4 for the maximum stored energy case than for the maximum rod internal pressure case. Also, the PCT for ZIRLO™ is greater for the maximum rod internal pressure case than it is for the maximum stored energy case because of the higher assembly blockage that occurs for the maximum rod internal pressure case.

A higher cladding temperature is calculated at the elevation of cladding rupture for ZIRLO™ than for Zircaloy-4 for the maximum stored energy case. This is because of the higher rupture strain calculated for the Zircaloy-4 case. With the higher rupture strain and, consequently, a larger cladding surface area, there is an increase in the energy removal from the cladding for the Zircaloy-4 case versus the ZIRLO™ case. This causes less of a heatup of the cladding at the rupture elevation after rupture for the Zircaloy-4 case than for the ZIRLO™ case. This results in a lower maximum cladding temperature for the Zircaloy-4 case at the rupture elevation. In particular, the maximum cladding temperature at the rupture elevation occurs less than 10 seconds after rupture for the Zircaloy-4 case in comparison to more than 200 seconds after rupture for the ZIRLO™ case.

In contrast to the maximum stored energy case, a lower cladding temperature is calculated at the elevation of cladding rupture for ZIRLO™ than for Zircaloy-4 for the maximum rod internal pressure case. This is a result of two factors. First, because of an earlier time of cladding rupture, the rupture elevation reaches a higher temperature for the Zircaloy-4 maximum rod internal pressure case relative to the maximum stored energy case (1825°F versus 1664°F). Secondly, for ZIRLO™ , the amount of rupture strain is greater for the maximum rod internal pressure case versus the maximum stored energy case (53.0% versus 33.2%). Consequently, the rupture elevation reaches a lower temperature for the maximum rod internal pressure case versus the maximum stored energy case (1720°F versus 1845°F) as a result of the surface area effect described in the preceding paragraph. The net effect of these two factors is that the maximum cladding temperature at the rupture elevation for the ZIRLO™ case is less than that for the Zircaloy-4 case (1720°F versus 1825°F).

Below the elevation of cladding rupture, the maximum cladding temperature for ZIRLO™ is calculated to be greater than that of Zircaloy-4 for the maximum stored energy case but less than that for Zircaloy-4 for the maximum pin pressure case. This is the same trend that is seen for the rupture elevation. However, the magnitude of the differences between the maximum cladding temperatures for ZIRLO™ and Zircaloy-4 below the rupture elevation is smaller than that calculated at the rupture elevation. Below the rupture elevation, the cladding is cooled by FLECHT-based reflood heat transfer coefficients. Since the reflood rates are essentially

identical for the ZIRLO™ and Zircaloy-4 cases, the reflood heat transfer coefficients are also essentially identical. Consequently, only small differences in maximum cladding temperature between ZIRLO™ and Zircaloy-4 are expected. The small differences in the cladding temperatures that are observed below the rupture elevation are due to differences in the amount of plastic strain calculated for ZIRLO™ and Zircaloy-4.

With respect to maximum cladding oxidation, a higher value is calculated for ZIRLO™ than for Zircaloy-4 for both the maximum stored energy case and the maximum rod internal case. For ZIRLO™ , the maximum cladding oxidation is calculated to occur at the elevation of cladding rupture, whereas for Zircaloy-4, it is calculated to occur at the elevation of PCT, which is above the elevation of cladding rupture. The differences in the location and magnitude of the maximum cladding oxidation between ZIRLO™ and Zircaloy-4 is a direct consequence of the differences in the cladding temperatures at and above the elevation of cladding rupture described above.

In summary, the sample cases demonstrate that the implementation of ZIRLO™ cladding has a very small impact on the blowdown and refill/reflood hydraulic transients of a LBLOCA. However, the implementation of ZIRLO™ does have an impact on the hot rod heatup transient, primarily as a result of the differences in the cladding rupture and blockage characteristics of ZIRLO™ relative to Zircaloy-4. The differences in the cladding rupture and blockage characteristics for ZIRLO™ result in a lower cladding temperature above the elevation of cladding rupture. At and below the cladding rupture elevation, the relative behavior of the cladding temperature is a function of burnup. For the sample LBLOCA analysis, the PCT occurred above the elevation of cladding rupture and, consequently, the PCTs for the two ZIRLO™ cases are lower than for the two Zircaloy-4 cases.

The impact on PCT of implementing ZIRLO™ cladding will be determined for each plant-specific implementation of ZIRLO™ cladding in a CENP designed PWR. Depending on whether the PCT is calculated to occur above or below the elevation of cladding rupture, the impact may be determined to be positive or negative. The impact will be reported to the NRC in accordance with 10 CFR 50.46(a)(3)(ii).

6.5.2   SBLOCA ECCS Performance

6.5.2.1   Method of Analysis

The SBLOCA ECCS performance analysis of ZIRLO™ cladding described in this section uses the S2M version of the CENP SBLOCA evaluation model (Reference 6-8) in conjunction with the ZIRLO™ cladding models described in Section 6.3 of this topical report. The computer codes that comprise the S2M evaluation model are briefly described in Section 6.2. Table 6.2-1 provides a complete listing of the topical reports (excluding this topical report) that comprise the S2M evaluation model.

The hot rod heatup portion of the analysis was performed using only the PARCH computer code and not STRIKIN-II. As described in Section 6.2, STRIKIN-II is used in a SBLOCA analysis to perform the initial portion of the hot rod heatup calculation, i.e., when the Reactor Coolant Pumps (RCPs) are maintaining forced convection heat transfer conditions in the core. PARCH is then used after the RCPs have coasted down and the mode of core heat transfer has changed to pool boiling. The PCT, which occurs during the pool boiling period of the transient (when the core is partially uncovered), is not sensitive to the specific cladding conditions calculated during the forced convection period provided that the PARCH node, in which the PCT is calculated to occur, is initialized in a post-DNB heat transfer regime.

The analysis was performed for a 0.1 ft^2 break in the RCP discharge leg (0.1 ft^2/PD). The 0.1 ft^2/PD break is a typical limiting SBLOCA for the 2700 Mwt class of CENP designed PWRs equipped with 200 psi SITs. As noted in Section 6.5.1.1 for the LBLOCA analysis, analyzing a typical limiting break size is sufficient for the purpose of the analysis.

The analysis was performed at the burnup with the maximum initial fuel stored energy.

6.5.2.2   Plant Design Data

The sample SBLOCA analysis was performed for the same typical CENP designed PWR that was used in the LBLOCA analysis described in Section 6.5.1. The plant has a rated core power

of 2700 Mwt (2754 Mwt including 2% power measurement uncertainty) and is fueled with 14x14 Guardian™ grid fuel assemblies with erbia burnable absorber fuel rods. Values for RCS, steam generator, and safety injection system parameters that are typical of those used in SBLOCA analyses were used in the sample analysis. The plant design data used in the sample SBLOCA analysis for important core and RCS parameters are listed in Table 6.5.2.2-1. Analyses are performed for both ZIRLO™ and Zircaloy-4 clad fuel rods.

6.5.2.3 Results

Table 6.5.2.3-1 lists the important results of the sample SBLOCA analysis of ZIRLO™ clad fuel assemblies. The results are compared to the results for Zircaloy-4 clad fuel assemblies in the same table. Figures 6.5.2.3-1 through 6.5.2.3-3 compare the transient response of the cladding temperature, coolant temperature and cladding surface heat transfer coefficient at the location of the PCT for ZIRLO™ and Zircaloy-4 cladding.

The implementation of ZIRLO™ has an insignificant impact on the RCS hydraulic transient response of a SBLOCA. In particular, the transient response of parameters such as core power, RCS pressure, break flow rate, and inner vessel inlet flow and two-phase level (which are the parameters typically presented in SBLOCA ECCS performance analysis licensing submittals of CENP designed PWRs) showed no significant differences for ZIRLO™ in comparison to Zircaloy-4. As shown in Figures 6.5.2.3-1 through 6.5.2.3-3, there is also very little difference in the transient behavior of the hot rod at the elevation of PCT. In particular, there is only a 4°F difference in the PCT between ZIRLO™ cladding and Zircaloy-4 cladding in the sample SBLOCA analysis. Because of the difference in the cladding rupture models, there is a difference in the time of cladding rupture and the maximum cladding temperature of the rupture elevation. As shown in Table 6.5.2.3-1, cladding rupture occurred 25 seconds earlier for the ZIRLO™ cladding (1038 seconds versus 1063 seconds). The maximum cladding temperature at the rupture elevation is 26°F higher for the ZIRLO™ cladding (1678°F versus 1652°F).

In summary, the sample SBLOCA analysis shows that the implementation of ZIRLO™ cladding has a very small impact on the hydraulic transient of a SBLOCA and on the hot rod heatup transient for elevations other than the elevation of cladding rupture. At the elevation of cladding

rupture, differences are seen in the cladding temperature due to the differences between the ZIRLO™ and Zircaloy-4 cladding rupture temperature and rupture strain models. In the sample SBLOCA analysis, the ZIRLO™ case has a higher maximum cladding temperature at the elevation of cladding rupture than the Zircaloy-4 case. In general, however, depending on the time of rupture and the rupture strain, either ZIRLO™ cladding or Zircaloy-4 cladding may have the higher maximum cladding temperature at the rupture elevation. Also, for a given hydraulic transient, the PCT may occur at the rupture elevation.

6.6   Conclusions

Section 6 describes the implementation of ZIRLO™ cladding in the 1999 EM and S2M versions of the CENP LBLOCA and SBLOCA ECCS performance evaluation models. ZIRLO™-specific models for specific heat, cladding rupture temperature, rupture strain and assembly blockage are incorporated in the evaluation models. The Zircaloy-4 models for all other cladding parameters are used without any changes for ZIRLO™ cladding. With the implementation of the ZIRLO™ models as described in Section 6.3, the 1999 EM version of the LBLOCA evaluation model and the S2M version of the SBLOCA evaluation model are applicable to ECCS performance analyses of CENP designed PWRs fueled with ZIRLO™ clad fuel assemblies.

Sample LBLOCA and SBLOCA analyses for a typical CENP designed PWR show that the transient behavior of ZIRLO™ cladding is similar to that of Zircaloy-4 cladding. The major difference in behavior occurs in the hot rod heatup transient as a result of differences between the ZIRLO™ and Zircaloy-4 cladding rupture models.

The implementation of ZIRLO™ impacts the PCT. Consequently, the effect on PCT will be reported to the NRC in accordance with 10 CFR 50.46(a)(3)(ii) for each plant-specific implementation of ZIRLO™ cladding in a CENP designed PWR.

6.7   References

6-1   CENPD-132P, "Calculative Methods for the C-E Large Break LOCA Evaluation Model," August 1974.

6-2   CENPD-132P, Supplement 1, "Calculational Methods for the C-E Large Break LOCA Evaluation Model," February 1975.

6-3   CENPD-132-P, Supplement 2-P, "Calculational Methods for the C-E Large Break LOCA Evaluation Model," July 1975.

6-4   CENPD-132, Supplement 3-P-A, "Calculative Methods for the C-E Large Break LOCA Evaluation Model for the Analysis of C-E and W Designed NSSS," June 1985.

6-5   CENPD-132, Supplement 4-P, Revision 1, "Calculative Methods for the CE Nuclear Power Large Break LOCA Evaluation Model," August 2000.

6-6   CENPD-137P, "Calculative Methods for the C-E Small Break LOCA Evaluation Model," August 1974.

6-7   CENPD-137, Supplement 1-P, "Calculative Methods for the C-E Small Break LOCA Evaluation Model," January 1977.

6-8   CENPD-137, Supplement 2-P-A, "Calculative Methods for the ABB CE Small Break LOCA Evaluation Model," April 1998.

6-9   CENPD-133P, "CEFLASH-4A, A FORTRAN-IV Digital Computer Program for Reactor Blowdown Analysis," August 1974.

6-10   CENPD-133P, Supplement 2, "CEFLASH-4A, A FORTRAN-IV Digital Computer Program for Reactor Blowdown Analysis (Modifications)," February 1975.

6-11   CENPD-133, Supplement 4-P, "CEFLASH-4A, A FORTRAN-IV Digital Computer Program for Reactor Blowdown Analysis," April 1977.

6-12   CENPD-133, Supplement 5-A, "CEFLASH-4A, A FORTRAN77 Digital Computer Program for Reactor Blowdown Analysis," June 1985.

6-13   CENPD-133P, Supplement 1, "CEFLASH-4AS, A Computer Program for the Reactor Blowdown Analysis of the Small Break Loss of Coolant Accident," August 1974.

6-14   CENPD-133, Supplement 3-P, "CEFLASH-4AS, A Computer Program for the Reactor Blowdown Analysis of the Small Break Loss of Coolant Accident," January 1977.

6-15   CENPD-134P, "COMPERC-II, A Program for Emergency Refill-Reflood of the Core," August 1974.

6-16   CENPD-134P, Supplement 1, "COMPERC-II, A Program for Emergency Refill-Reflood of the Core (Modifications)," February 1975.

6-17   CENPD-134, Supplement 2-A, "COMPERC-II, Program for Emergency Refill-Reflood of the Core," June 1985.

6-18   CENPD-135P, "STRIKIN-II, A Cylindrical Geometry Fuel Rod Heat Transfer Program," August 1974.

6-19 CENPD-135P Supplement 2, "STRIKIN-II, A Cylindrical Geometry Fuel Rod Heat Transfer Program (Modifications)," February 1975.

6-20 CENPD-135, Supplement 4-P, "STRIKIN-II, A Cylindrical Geometry Fuel Rod Heat Transfer Program," August 1976.

6-21 CENPD-135-P, Supplement 5, "STRIKIN-II, A Cylindrical Geometry Fuel Rod Heat Transfer Program," April 1977.

6-22 CENPD-138P, "PARCH, A FORTRAN-IV Digital Program to Evaluate Pool Boiling, Axial Rod and Coolant Heatup," August 1974.

6-23 CENPD-138P, Supplement 1, "PARCH, A FORTRAN-IV Digital Program to Evaluate Pool Boiling, Axial Rod and Coolant Heatup (Modifications)," February 1975.

6-24 CENPD-138, Supplement 2-P, "PARCH, A FORTRAN-IV Digital Program to Evaluate Pool Boiling, Axial Rod and Coolant Heatup," January 1977.

6-25 LD-81-095, Enclosure 1-P-A, "C-E ECCS Evaluation Model, Flow Blockage Analysis," December 1981.

6-26 CENPD-213-P, "Reflood Heat Transfer, Application of FLECHT Reflood Heat Transfer Coefficients to C-E's 16x16 Fuel Bundles," January 1976.

6-27 O. D. Parr (NRC) to F. M. Stern (C-E), June 13, 1975.

6-28 O. D. Parr (NRC) to A. E. Scherer (C-E), December 9, 1975.

6-29 D. M. Crutchfield (NRC) to A. E. Scherer (C-E), "Safety Evaluation of Combustion Engineering ECCS Large Break Evaluation Model and Acceptance for Referencing of Related Licensing Topical Reports," July 31, 1986.

6-30 S. A. Richards (NRC) to P. W. Richardson (Westinghouse CENP), "Safety Evaluation of Topical Report CENPD-132, Supplement 4, Revision 1, 'Calculative Methods for the CE Nuclear Power Large Break LOCA Evaluation Model' (TAC No. MA5660)," December 15, 2000.

6-31 K. Kniel (NRC) to A. E. Scherer (C-E), "Evaluation of Topical Reports CENPD-133, Supplement 3-P and CENPD-137, Supplement 1-P," September 27, 1977.

6-32 T. H. Essig (NRC) to I. C. Rickard (ABB CENP), "Acceptance for Referencing of the Topical Report CENPD-137(P), Supplement 2, 'Calculative Methods for the C-E Small Break LOCA Evaluation Model' (TAC No. M95687)," December 16, 1997.

6-33 K. Kniel (NRC) to A. E. Scherer (C-E), "Combustion Engineering Emergency Core Cooling System Evaluation Model," November 12, 1976.

6-34 R. L. Baer (NRC) to A. E. Scherer (C-E), "Evaluation of Topical Report CENPD-135, Supplement No. 5," September 6, 1978.

6-35 K. Kniel (NRC) to A. E. Scherer (C-E), "Evaluation of Topical Report CENPD-138, Supplement 2-P," April 10, 1978.

6-36 K. Kniel (NRC) to A. E. Scherer (C-E), August 2, 1976.

6-37 BMI-1803, "Specific Heats and Heats of Transformation of Zircaloy-2 and Low Nickel Zircaloy-2," E. A. Eldridge and H. W. Deem, May 31, 1967.

6-38   CENPD-136, "High Temperature Properties of Zircaloy and UO_2 for Use in LOCA Evaluation Models," July 1974.

6-39   NUREG-0630, "Cladding Swelling and Rupture Models for LOCA Analysis," D. A. Powers and R. O. Meyer, April 1980.

6-40   "WREM: Water Reactor Evaluation Model," Regulatory Staff, Technical Review, United States Atomic Energy Commission, October 1974.

6-41   ANL-6548, "Studies of Metal-Water Reactions at High Temperatures, III. Experimental and Theoretical Studies of the Zirconium-Water Reaction," L. Baker and L. C. Just, May 1962.

6-42   CENPD-279, Supplement 6, "Annual Report on ABB CE ECCS Performance Evaluation Models," February 1995.

6-43   CENPD-185-P-A, "Clad Rupture Behavior, LOCA Rupture Behavior of 16x16 Zircaloy Cladding," May 1975.

6-44   O. D. Parr (NRC) to A. E. Scherer (C-E), October 30, 1975.

6-45   WCAP-12610-P-A, "VANTAGE+ Fuel Assembly Reference Core Report," April 1995.

6-46   NSD-NRC-98-5575, H. A. Sepp (Westinghouse) to Document Control Desk (NRC), "1997 Annual Notification of Changes to the Westinghouse Small Break LOCA and Large Break LOCA ECCS Evaluation Models, Pursuant to 10 CFR 50.46 (a)(3)(ii)," April 8, 1998.

6-47   A. C. Thadani (NRC) to W. J. Johnson (Westinghouse), "Acceptance for Referencing of Licensing Topical Report WCAP-10924, Volume 1, Addendum 4," February 8, 1991.

Table 6.2-1

Topical Reports and Safety Evaluation Reports for the 1999 EM and the S2M

Subject	Topical Report Reference	Safety Evaluation Report Reference
LBLOCA Evaluation Model (CENPD-132)	6-1	6-27
Supplement 1	6-2	6-27
Supplement 2	6-3	6-28
Supplement 3	6-4	6-29
Supplement 4	6-5	6-30
SBLOCA Evaluation Model (CENPD-137)	6-6	6-27
Supplement 1	6-7	6-31
Supplement 2	6-8	6-32
CEFLASH-4A (CENPD-133)	6-9	6-27
Supplement 2	6-10	6-27
Supplement 4	6-11	6-30
Supplement 5	6-12	6-29
CEFLASH-4AS		
Supplement 1 to CENPD-133	6-13	6-27
Supplement 3 to CENPD-133	6-14	6-31
COMPERC-II (CENPD-134)	6-15	6-27
Supplement 1	6-16	6-27
Supplement 2	6-17	6-29
STRIKIN-II (CENPD-135)	6-18	6-27
Supplement 2	6-19	6-27
Supplement 4	6-20	6-33
Supplement 5	6-21	6-34
PARCH (CENPD-138)	6-22	6-27
Supplement 1	6-23	6-27
Supplement 2	6-24	6-35
HCROSS		
Appendix A to Enclosure 1 to LD-81-095	6-25	6-29
COMZIRC		
Appendix C to Supplement 1 to CENPD-134	6-16	6-27
Application of FLECHT Correlation to 16x16 Fuel Assemblies (CENPD-213)	6-26	6-36
Application of NUREG-0630 Cladding Rupture and Swelling Models (Enclosure 1 to LD-81-095)	6-25	6-29

Table 6.2-2

Cladding Models Used in the 1999 EM and S2M Evaluation Models

Cladding Model	Source Document Reference
Specific Heat	6-37
Density	6-37
Thermal Conductivity	6-38
Thermal Emissivity	6-38
Thermal Expansion	6-38
Modulus of Elasticity	6-38
Poisson's Ratio	6-38
Diamond Pyramid Hardness	6-38
Rupture Temperature	6-39 (LBLOCA) 6-38 (SBLOCA)
Rupture Strain	6-39 (LBLOCA) 6-38 (SBLOCA)
Assembly Blockage following Rupture	6-39 (LBLOCA)
Pre-Rupture Plastic Strain	6-40 (LBLOCA)
Metal-Water Reaction Rate	6-41

Table 6.3.1-1

ZIRLO™ Specific Heat
Used in Westinghouse Appendix K Evaluation Models

[

]

Table 6.3.1-2

ZIRLO™ Specific Heat
Used in Westinghouse Best Estimate Evaluation Model

[

]

Table 6.3.1-3

Zircaloy-4 Specific Heat
Used in CENP ECCS Performance Evaluation Models

Temperature, °F	Specific Heat, BTU/lbm-°F
68	0.070098
1067	0.082103
1112	0.086112
1468	0.086112
1535	0.136186
1580	0.148191
1661	0.197262
1679	0.197262
1787	0.085110
10000	0.085232

Table 6.3.9.1-1

ZIRLO™ Cladding Rupture Temperature Model

[

]

Table 6.3.10.1-1

ZIRLO™ Cladding Rupture Strain Model

[

]

Table 6.3.11-1

ZIRLO™ Cladding Assembly Blockage Model

[

]

Table 6.5.1.2-1

**Important Plant Design Data Used in the
LBLOCA ECCS Performance Analysis of ZIRLO™ Cladding**

Parameter	ZIRLO™ Cladding	Zr-4 Cladding
Core power (102% of rated), Mwt	2754	2754
Peak linear heat generation rate (PLHGR) of the hot rod, kw/ft	14.3	14.3
PLHGR of the average rod in assembly with hot rod, kw/ft	13.48	13.48
RCS flow rate, lbm/hr	128.4×10^6	128.4×10^6
Core flow rate, lbm/hr	123.6×10^6	123.6×10^6
RCS pressure, psia	2250	2250
Cold leg temperature, °F	546	546
Gap conductance at the PLHGR, BTU/hr-ft²-°F[1]	2389 / 2940	2156 / 2946
Fuel centerline temperature at the PLHGR, °F[1]	3381 / 3316	3417 / 3315
Fuel average temperature at the PLHGR, °F[1]	2065 / 1999	2095 / 1996
Hot rod gas pressure, psia[1]	1092 / 2351	1093 / 2304
Burnable absorber	Erbia	Erbia

Note:
(1)   Values are for the maximum initial fuel stored energy and maximum initial rod internal pressure cases, respectively.

Table 6.5.1.3-1

Important Results of the LBLOCA ECCS Performance Analysis of ZIRLO™ Cladding for the Maximum Initial Fuel Stored Energy Cases

Parameter	ZIRLO™ Cladding	Zr-4 Cladding
Peak cladding temperature (PCT), °F	1951	2009
Time of PCT, sec	264	264
Elevation of PCT, ft	7.97	7.97
Maximum cladding oxidation, %	6.80	5.04
Elevation of maximum cladding oxidation, ft	7.40	7.97
Core-wide cladding oxidation, %	0.34	0.25
Time of cladding rupture, sec	35.82	36.56
Elevation of cladding rupture, ft	7.40	7.40
Cladding rupture temperature, °F	1569	1589
Cladding differential pressure at rupture, psi	702	575
Cladding rupture strain, %	33.2	73.2
Assembly blockage, %	24.1	58.0
Time SIT flow begins, sec	17.5	17.4
Time of annulus downflow, sec	21.2	21.2
Time of beginning of reflood, sec	36.1	36.1
Time safety injection pump flow begins, sec	35.8	35.8
Time SIT flow ends, sec	68.7	68.7

Reflood rates, in./sec
  First
  Second
  Third
	
	1.714
	1.129
	0.6818
		
		1.713
		1.129
		0.6817

Table 6.5.1.3-2

Important Results of the LBLOCA ECCS Performance Analysis of ZIRLO™ Cladding for the Maximum Initial Rod Internal Pressure Cases

Parameter	ZIRLO™ Cladding	Zr-4 Cladding
Peak cladding temperature (PCT), °F	1958	1971
Time of PCT, sec	264	264
Elevation of PCT, ft	7.97	7.97
Maximum cladding oxidation, %	5.11	4.56
Elevation of maximum cladding oxidation, ft	7.40	7.97
Core-wide cladding oxidation, %	0.26	0.22
Time of cladding rupture, sec	28.46	29.04
Elevation of cladding rupture, ft	7.40	7.40
Cladding rupture temperature, °F	1454	1515
Cladding differential pressure at rupture, psi	1237	1183
Cladding rupture strain, %	53.0	65.1
Assembly blockage, %	40.2	50.4
Time SIT flow begins, sec	17.4	17.4
Time of annulus downflow, sec	21.2	21.2
Time of beginning of reflood, sec	36.1	36.1
Time safety injection pump flow begins, sec	35.8	35.8
Time SIT flow ends, sec	68.7	68.7

Reflood rates, in./sec
  First
  Second
  Third
	
	1.713
	1.128
	0.6816
		
		1.714
		1.130
		0.6818

Table 6.5.1.3-3

**Comparison of ZIRLO™ and Zircaloy-4 Maximum Cladding Temperatures
for the LBLOCA ECCS Performance Analysis**

Location on Hot Rod	Maximum Cladding Temperature, °F / Time of Max. Cladding Temp., sec	
	ZIRLO™	Zircaloy-4
Burnup with Maximum Initial Fuel Stored Energy		
Below Rupture Elevation	1881 / 188	1869 / 189
At Rupture Elevation	1845 / 265	1664 / 43
Above Rupture Elevation	1951 / 264	2009 / 264
Burnup with Maximum Initial Rod Internal Pressure		
Below Rupture Elevation	1882 / 187	1889 / 186
At Rupture Elevation	1720 / 306	1825 / 44
Above Rupture Elevation	1958 / 264	1971 / 264

Note: In each case, the cladding ruptured at the elevation of the PLHGR and the maximum cladding temperatures above and below rupture occurred in the STRIKIN-II nodes immediately above and below the rupture node.

Table 6.5.2.2-1

**Important Plant Design Data Used in the
SBLOCA ECCS Performance Analysis of ZIRLO™ Cladding**

Parameter	ZIRLO™ Cladding	Zr-4 Cladding
Core power (102% of rated), Mwt	2754	2754
Peak linear heat generation rate of the hot rod, kw/ft	14.5	14.5
RCS flow rate, lbm/hr	128.4×10^6	128.4×10^6
RCS pressure, psia	2250	2250
Cold leg temperature, °F	546	546
Burnable absorber	Erbia	Erbia

Table 6.5.2.3-1

Important Results of the SBLOCA ECCS Performance Analysis of ZIRLO™ Cladding

Parameter	ZIRLO™ Cladding	Zr-4 Cladding
Peak cladding temperature (PCT), °F	1712	1716
Time of PCT, sec	1225	1235
Elevation of PCT, ft	11.39	11.39
Maximum cladding oxidation, %	3.36	3.51
Elevation of maximum cladding oxidation, ft	10.82	10.82
Core-wide cladding oxidation, %	0.35	0.36
Time of cladding rupture, sec	1038	1063
Elevation of cladding rupture, ft	10.82	10.82
Maximum cladding temperature at elevation of cladding rupture, °F	1678	1652

Figure 6.3.1-1

Comparison of the Westinghouse EM Specific Heat Models for ZIRLO™ to the CENP EM Specific Heat Model for Zircaloy-4

[

]

Figure 6.3.3-1

Comparison of the Westinghouse EM Thermal Conductivity Model for ZIRLO™ to the CENP EM Thermal Conductivity Models for Zircaloy-4

[

]

Figure 6.3.4-1

CENP EM Thermal Emissivity Model for Zircaloy-4
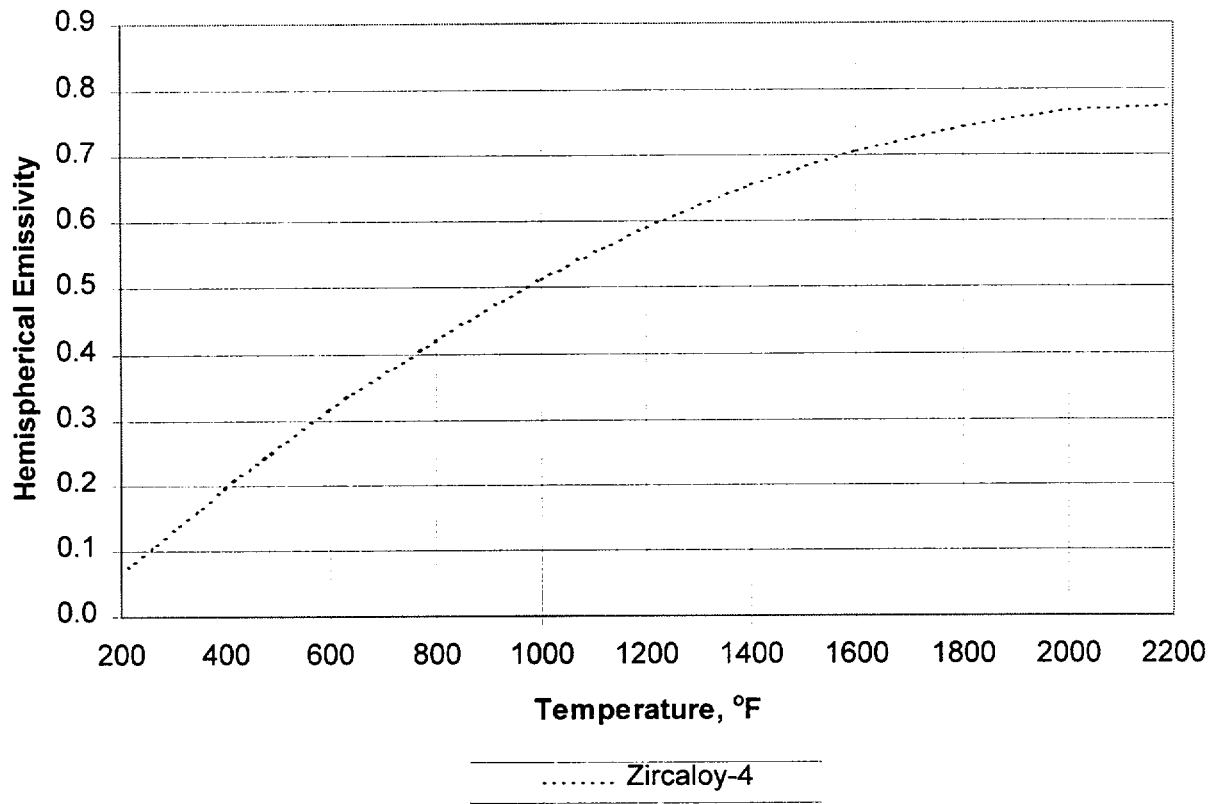
Figure 6.3.5-1

Comparison of the Westinghouse EM Thermal Expansion Model for ZIRLO™
to the CENP EM Thermal Expansion Models for Zircaloy-4

[

]

Figure 6.3.6-1

CENP EM Modulus of Elasticity Model for Zircaloy-4

[

]

Figure 6.3.7-1

CENP EM Poisson's Ratio Model for Zircaloy-4

[

]

Figure 6.3.8-1

CENP EM Diamond Pyramid Hardness Model for Zircaloy-4

[

]

Figure 6.3.9.1-1

**Comparison of the ZIRLO™ and NUREG-0630
Cladding Rupture Temperature Models**

[

]

6-54

Figure 6.3.9.2-1

**Comparison of the ZIRLO™ and CENP SBLOCA EM
Cladding Rupture Temperature Models**

[

]

Figure 6.3.10.1-1

**Comparison of the ZIRLO™ and NUREG-0630
Cladding Rupture Strain Models**

[

]

Figure 6.3.10.2-1

**Comparison of the ZIRLO™ and CENP SBLOCA EM
Cladding Rupture Strain Models**

[

]

Figure 6.3.11-1

**Comparison of the ZIRLO™ and NUREG-0630
Assembly Blockage Models**

[

]

Figure 6.3.13-1

Comparison of the ZIRLO™ and Baker-Just Model Parabolic Rate Correlations

[

]

Figure 6.5.1.3-1

Peak Cladding Temperature
for the LBLOCA ECCS Performance Analysis of ZIRLO™ Cladding
(0.6 DEG/PD Break, Maximum Stored Energy Case)

———————— ZIRLO
·················· Zircaloy-4

Figure 6.5.1.3-2

Hot Spot Gap Conductance
for the LBLOCA ECCS Performance Analysis of ZIRLO™ Cladding
(0.6 DEG/PD Break, Maximum Stored Energy Case)
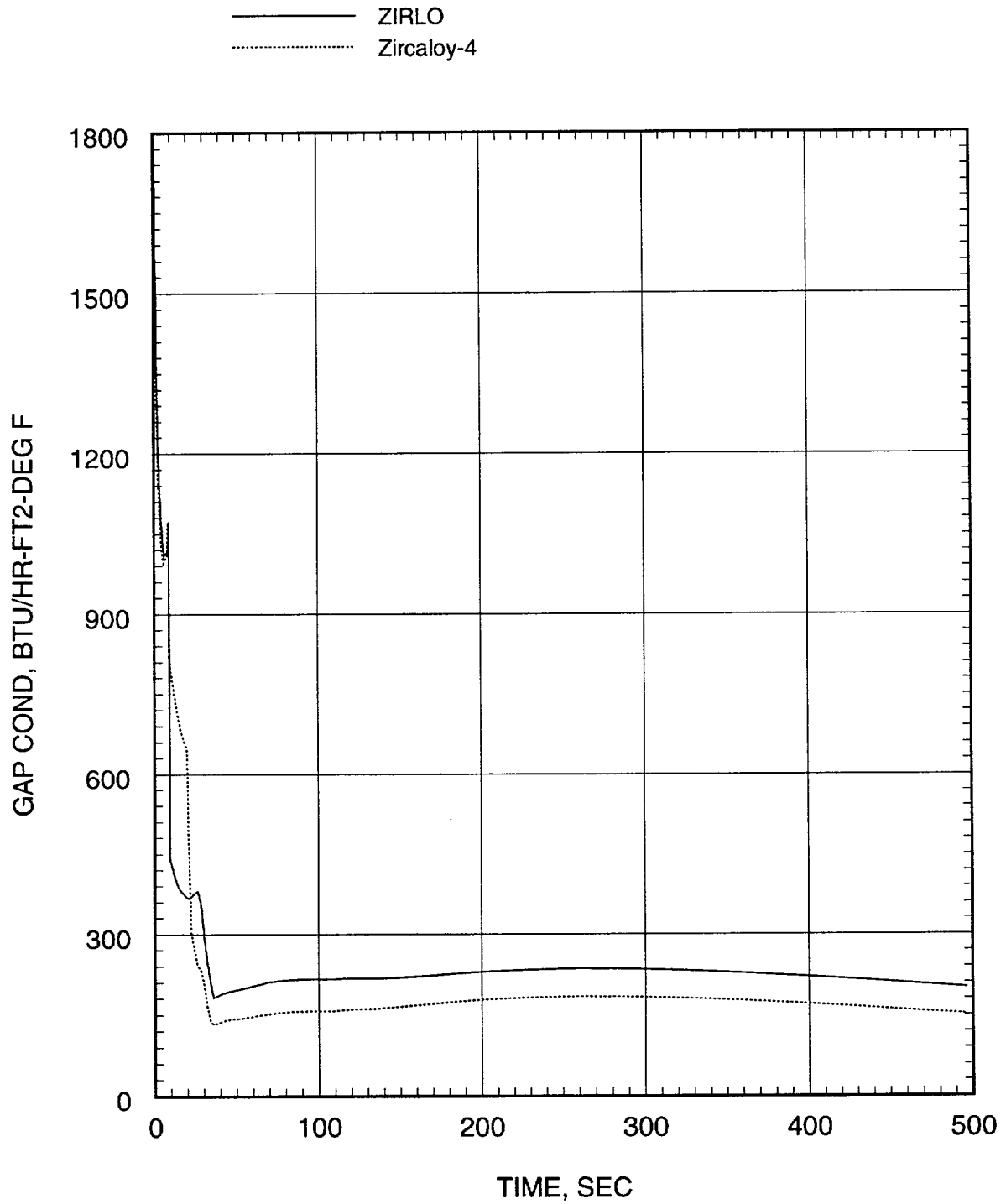
Figure 6.5.1.3-3

**Hot Spot Heat Transfer Coefficient
for the LBLOCA ECCS Performance Analysis of ZIRLO™ Cladding
(0.6 DEG/PD Break, Maximum Stored Energy Case)**

ZIRLO

Zircaloy-4
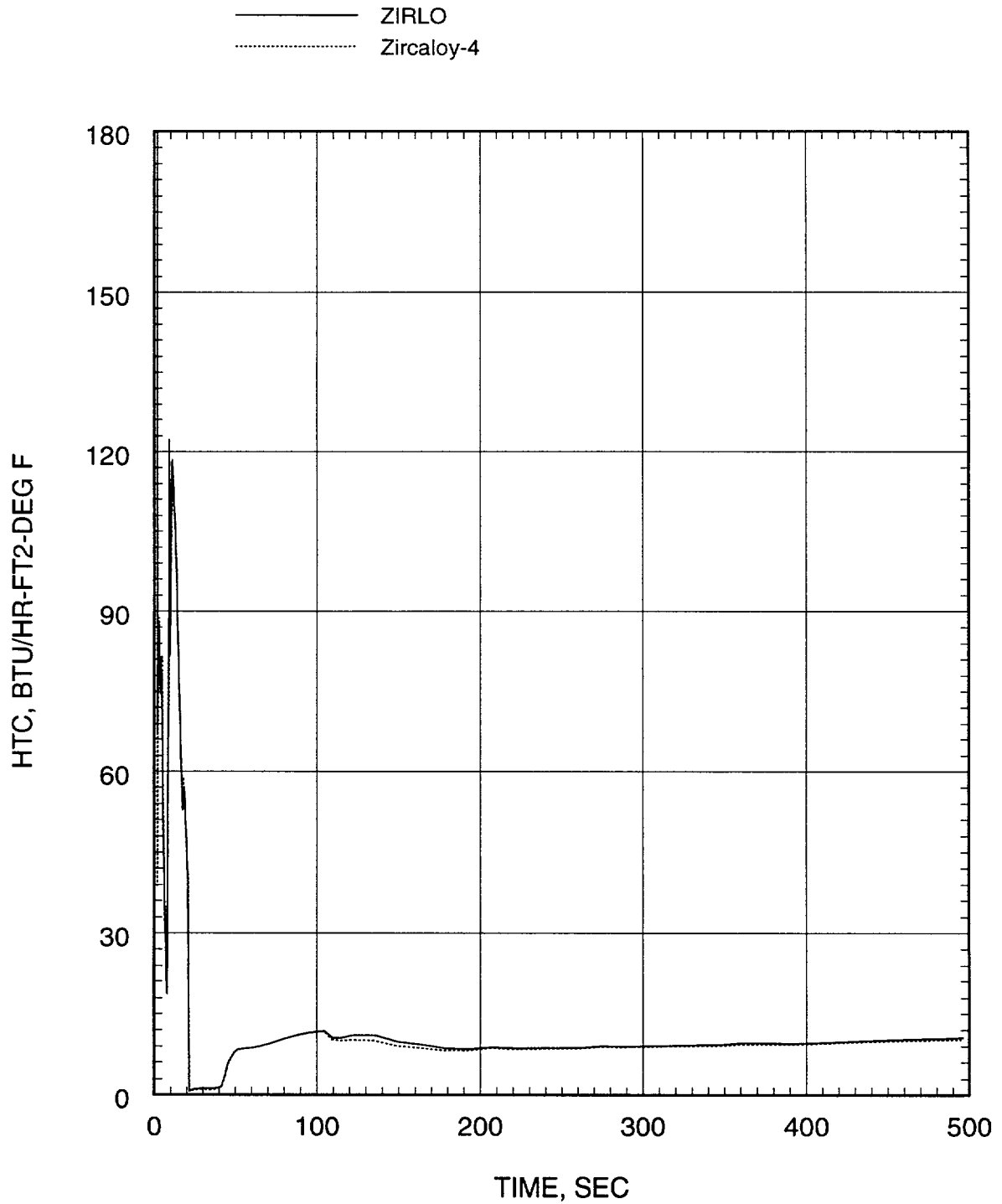
Figure 6.5.1.3-4

**Maximum Cladding Oxidation Percentage
for the LBLOCA ECCS Performance Analysis of ZIRLO™ Cladding
(0.6 DEG/PD Break, Maximum Stored Energy Case)**
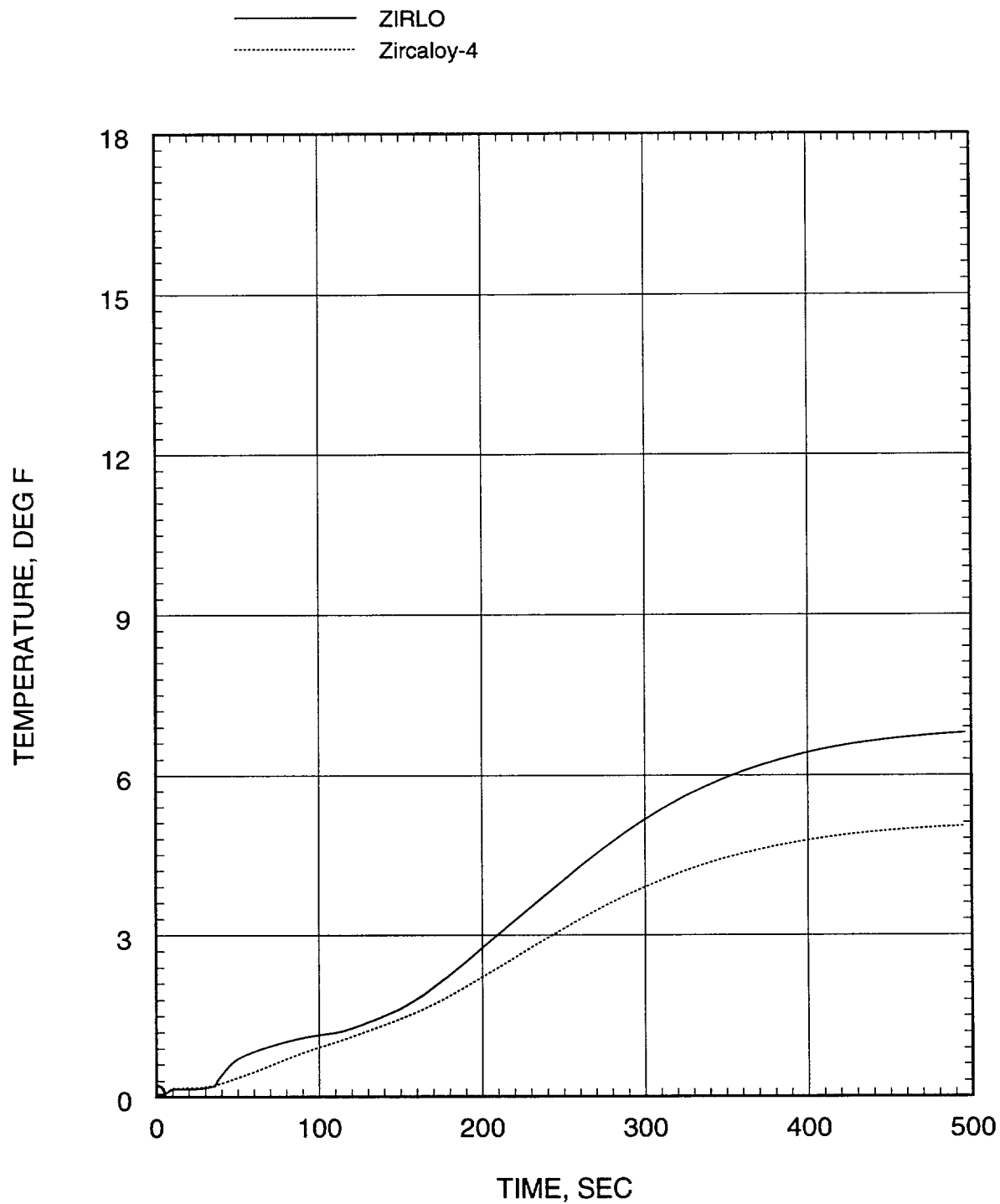
————————— ZIRLO
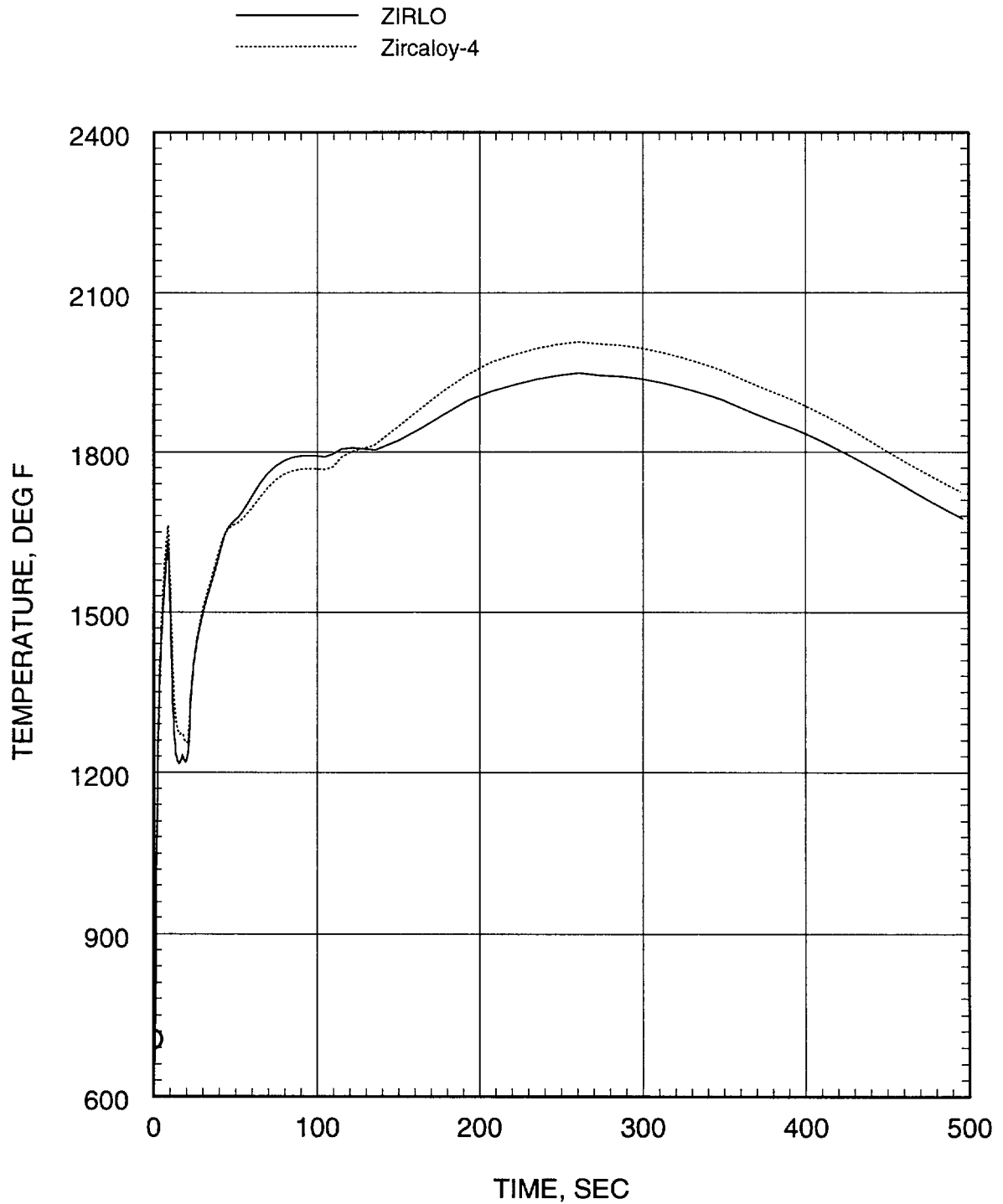························ Zircaloy-4

Figure 6.5.2.3-1

**Peak Cladding Temperature
for the SBLOCA ECCS Performance Analysis of ZIRLO™ Cladding
(0.1 ft²/PD Break)**

──────────── ZIRLO
············ Zircaloy-4

Figure 6.5.2.3-2

**Coolant Temperature at the Elevation of the PCT
for the SBLOCA ECCS Performance Analysis of ZIRLO™ Cladding
(0.1 ft²/PD Break)**

———————— ZIRLO

······················· Zircaloy-4

Figure 6.5.2.3-3

**Heat Transfer Coefficient at the Elevation of the PCT
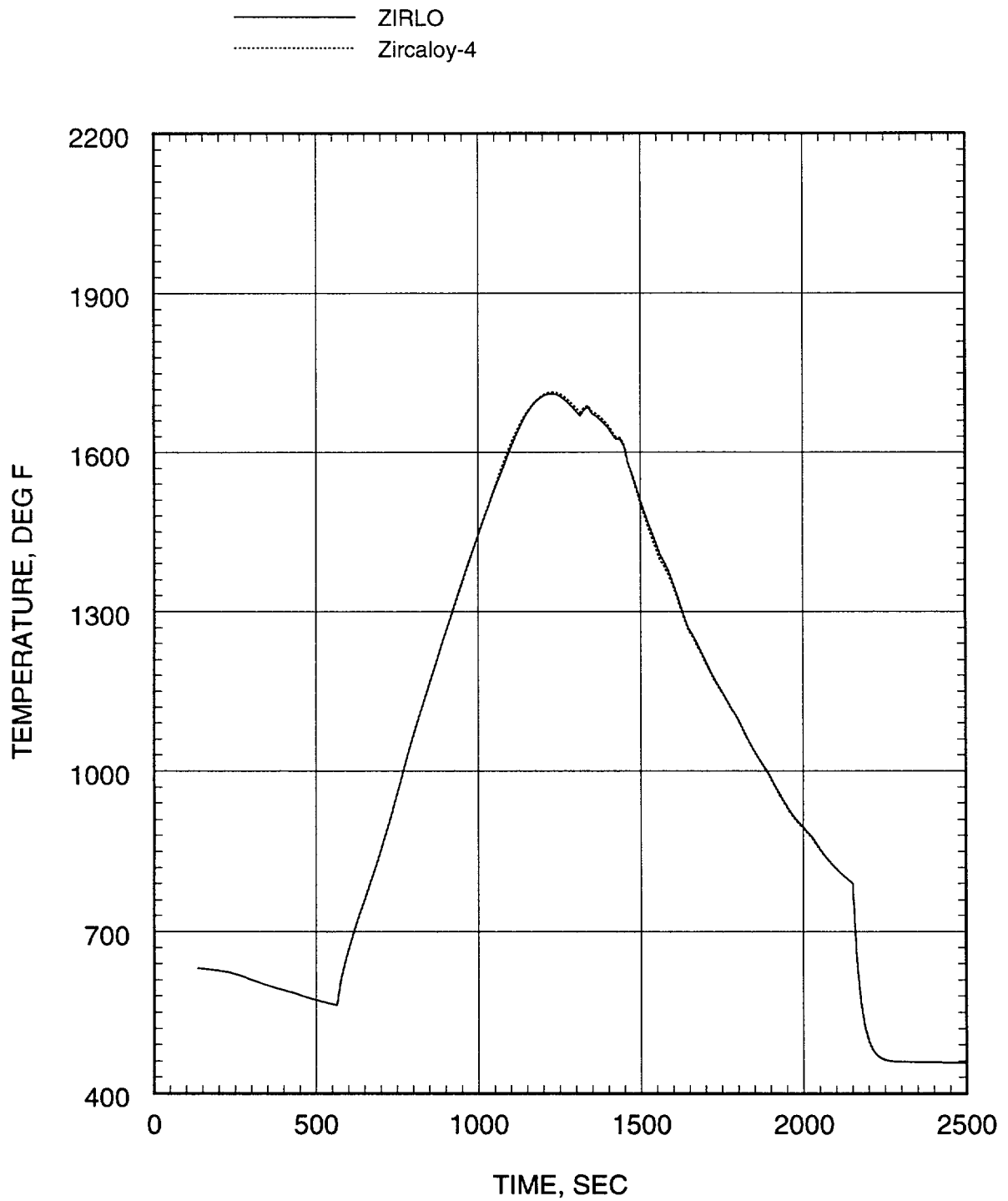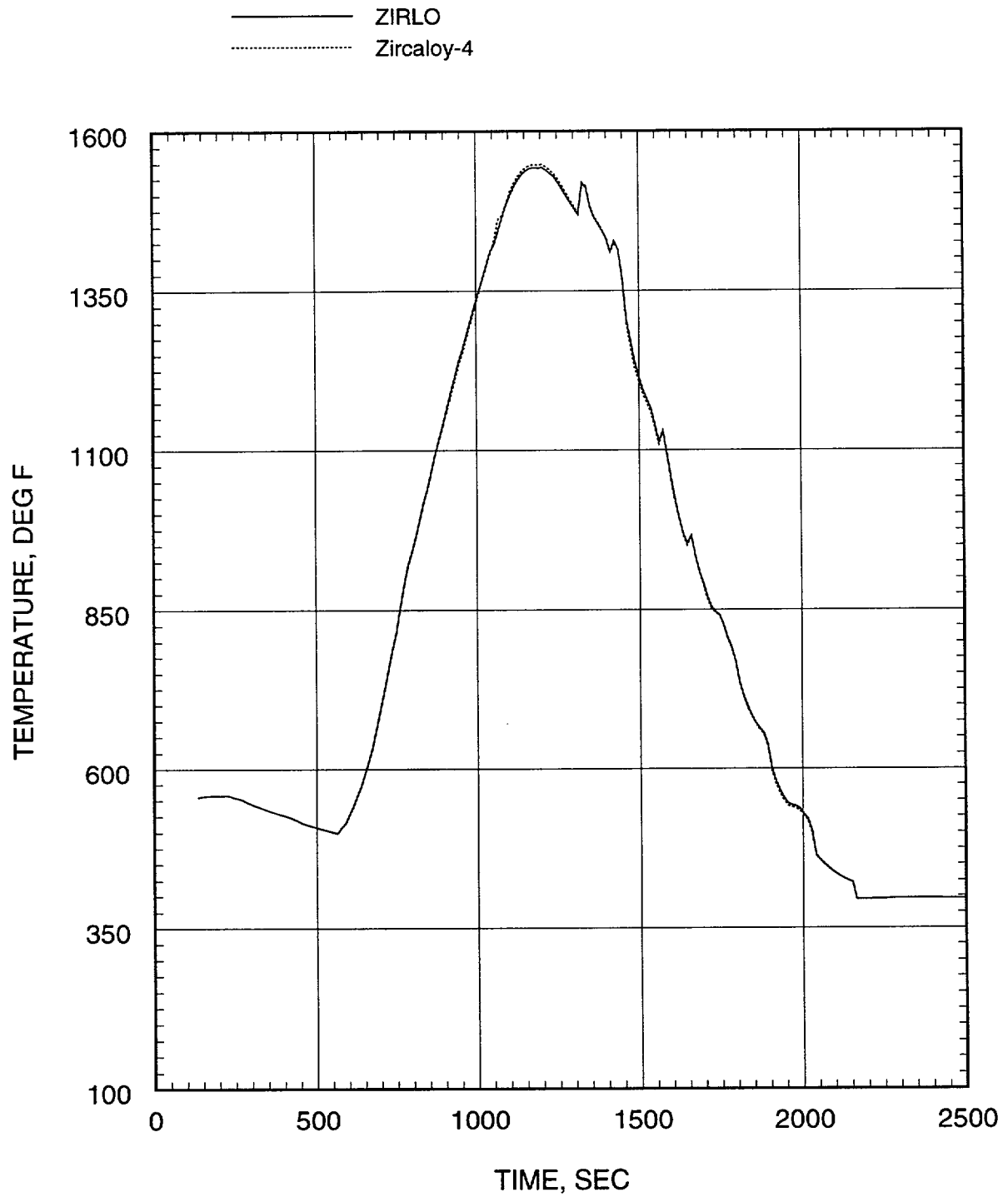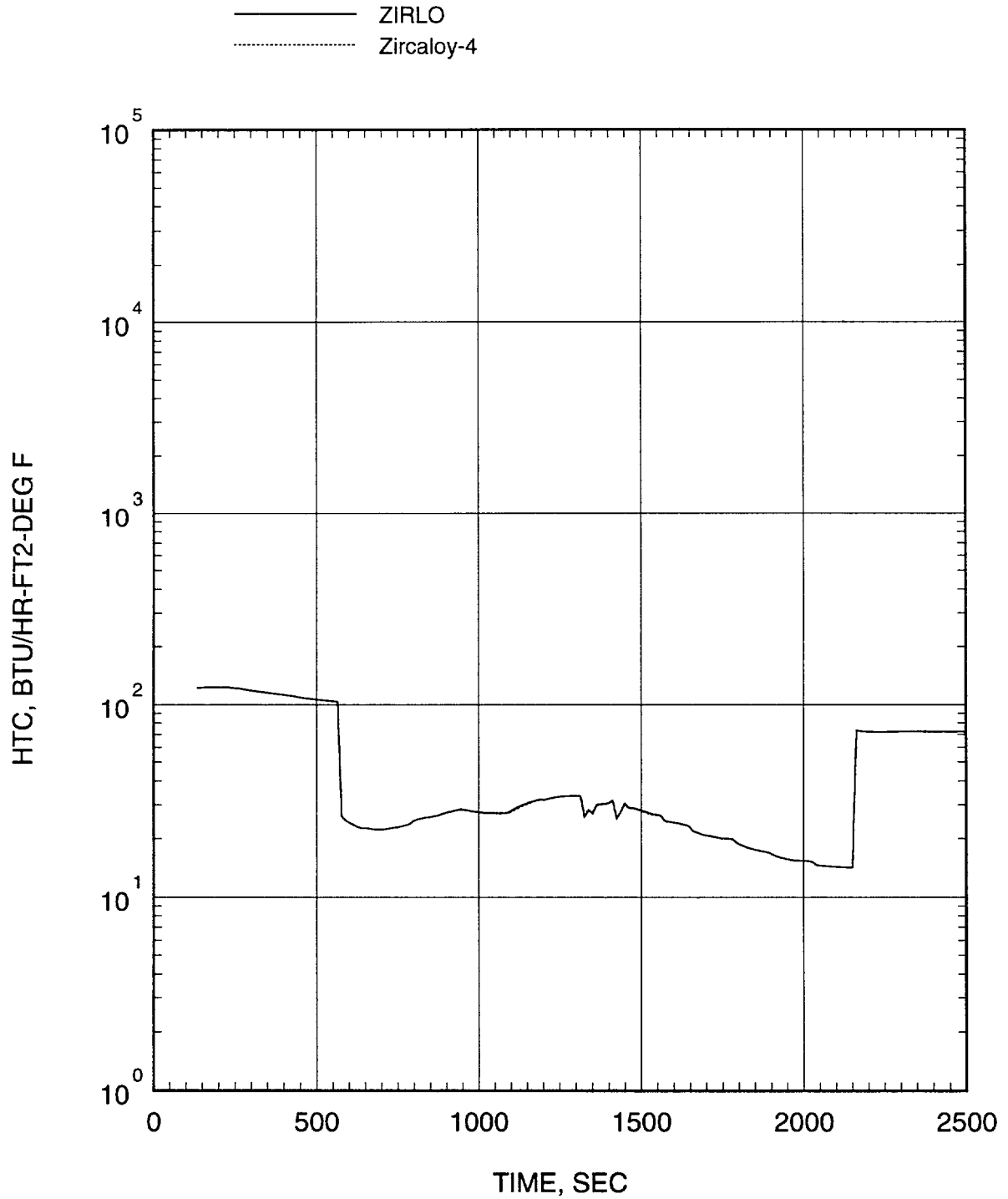for the SBLOCA ECCS Performance Analysis of ZIRLO™ Cladding
(0.1 ft²/PD Break)**

ZIRLO
Zircaloy-4

7.0 Non-LOCA Accidents

7.1 Introduction

This section discusses the effect of using CENP fuel designs clad with ZIRLO™ on non-LOCA safety analyses (typically FSAR Chapter 15). The methods and computer codes currently used in the analysis of the non-LOCA licensing basis events remain valid for fuel rods clad with ZIRLO™ . It has been shown that licensing basis criteria continue to be met and the margin to safety is not reduced.

7.2 Summary of Cladding-Related Models in the Non-LOCA Transient Evaluation Models

An investigation has determined the ZIRLO™ material properties important to non-LOCA transient analyses, with the objective of providing experimental data for comparison with Zircaloy-4 material properties. Experimental data and subsequent evaluations demonstrate that the properties of Zircaloy-4 and ZIRLO™ are essentially the same with the exception of the differences in the phase change temperature and its related effect on the thermophysical properties.

The phase change temperature shift affects the relationship of specific heat as a function of temperature. Zircaloy-4 and ZIRLO™ specific heats are essentially identical up to a temperature of approximately 1380°F, (750°C) at which temperature ZIRLO™ begins to undergo an alpha-beta phase change and its specific heat (which is defined to include the phase change heat of transformation) rises to a plateau value. Then, as the temperature continues to increase, the specific heat is reduced to near its original value. Zircaloy-4 exhibits a behavior similar to that of ZIRLO™, except that the phase change occurs at a higher temperature range (1504 - 1717°F). The difference in the specific heat versus temperature relationship between ZIRLO™ and Zircaloy-4 potentially affects the clad temperature response, as the clad temperature reaches the ZIRLO™ phase change temperature.

7.2.1 STRIKIN-II Code

The STRIKIN-II computer code (Reference 7-1) is used for the hot channel heatup calculations in licensing safety analyses. STRIKIN-II is used to calculate the transient heat flux, transient DNBR, coolant enthalpy and hot rod fuel temperatures in the hot assembly, using nuclear power and local coolant conditions (i.e., pressure, flow, temperature) as input. STRIKIN-II is used to predict transient heat fluxes, average and peak fuel pellet and clad temperatures for non-LOCA transients. These analyses are used to demonstrate compliance with DNBR, fuel melt, and fuel pellet enthalpy licensing basis criteria.

STRIKIN-II code accounts for the effect of thermal and mechanical properties of both the fuel pellet and clad. In order to model the ZIRLO™ cladding properties, changes were made to the clad specific heat versus temperature property data block used by STRIKIN-II. These changes are implemented in STRIKIN-II as user inputs. The cladding thermal conductivity model was not changed for the reasons discussed in Section 6.3.3. As discussed earlier, all other ZIRLO™ properties used in Non-LOCA analysis are essentially identical to Zircaloy-4, and thus, no other changes are necessary to effectively model the influence of ZIRLO™ in non-LOCA licensing basis analyses.

7.2.2 CENTS Code

The CENTS computer code (Reference 7-2) is an interactive, faster than real time computer code for the simulation of the NSSS and related systems. It is capable of calculating the behavior of a PWR for both normal and abnormal conditions, including accidents.

A review of CENTS indicated that the cladding material properties employed are cladding thermal conductivity and specific heat. The correlation used by CENTS to model Zircaloy-4 thermal conductivity was compared to the ZIRLO™ thermal conductivity correlation. The result of this comparison is that there is a negligible difference in thermal conductivity over the expected range of fuel operating temperature. The CENTS code's modeling of Zircaloy-4 specific heat is essentially identical to that of ZIRLO™ up to a temperature of approximately 1380°F. As this temperature, 1380°F, is beyond the expected operating temperature range of the cladding (for Non-LOCA transients modeled by CENTS), the difference between the

Zircaloy-4 specific heat used by CENTS and the ZIRLO™ specific heat correlation is negligible. Consequently, no change to accommodate a ZIRLO™ specific heat material property is needed.

As discussed earlier, all other ZIRLO™ properties used in Non-LOCA analysis are essentially identical to Zircaloy-4, and thus, no changes are necessary to model the effect of ZIRLO™ in non-LOCA licensing basis analyses.

7.2.3 CESEC Code

Like CENTS, the CESEC computer code (References 7-3) is used for the simulation of the NSSS and related systems. CESEC is capable of calculating the behavior of a PWR for both normal and abnormal conditions, including accidents.

A review of CESEC indicated that the cladding material properties employed are thermal conductivity and specific heat. The correlation CESEC uses for Zircaloy-4 thermal conductivity was compared to the ZIRLO™ thermal conductivity correlation. This comparison showed that there is negligible difference in thermal conductivity over the expected range of fuel operating temperature. CESEC's modeling of Zircaloy-4 cladding specific heat is essentially identical to that of ZIRLO™ up to a temperature of approximately 1380°F. As this temperature, 1380°F, is beyond the expected range of cladding operating temperature (for transients modeled by CESEC), the difference between the Zircaloy-4 specific heat used by CESEC and the ZIRLO™ specific heat correlation is negligible. Consequently, no change to accommodate a ZIRLO™ specific heat material property is needed.

As discussed earlier, all other ZIRLO™ properties used in Non-LOCA analysis are essentially identical to Zircaloy-4, and thus, no changes are necessary to model the effects of ZIRLO™ in non-LOCA licensing basis analyses.

7.2.4 HERMITE Code

HERMITE (Reference 7-4) is a space-time kinetics computer code. HERMITE was developed for the analysis of design and off-design transients in PWRs by means of a numerical solution to the multi-dimensional, few-group, time-dependent neutron diffusion equation including feedback

effects of fuel temperature, coolant temperature, coolant density and control rod motion. The heat conduction equation in the fuel pellet, gap and clad is solved by a finite difference method. Continuity and energy conservation equations are solved for the coolant enthalpy and density.

A review of HERMITE indicated that the cladding material properties employed are thermal conductivity and specific heat. The correlation HERMITE uses to model Zircaloy-4 thermal conductivity was compared to that of ZIRLO™. The result of this comparison is that there is a negligible difference in thermal conductivity over the expected range of fuel operating temperature. The HERMITE code's modeling of the Zircaloy-4 specific heat is essentially identical to that of ZIRLO™ up to a temperature of approximately 1380°F. As this temperature, 1380°F, is beyond the expected range of cladding operating (as modeled for non-LOCA transients), the difference between the Zircaloy-4 specific heat used in HERMITE and the ZIRLO™ specific heat correlation is negligible. Consequently, no change to accommodate a ZIRLO™ specific heat material property is needed.

As discussed earlier, all other ZIRLO™ properties used in Non-LOCA analysis are essentially identical to Zircaloy-4, and thus, no changes are necessary to model the effects of ZIRLO™ in the non-LOCA licensing basis analyses.

7.3   ZIRLO™ Impact on Accident Parameters

This section discusses the effect of ZIRLO™ on non-LOCA licensing basis analyses. As previously discussed, the thermophysical properties of ZIRLO™ and Zircaloy-4 are essentially identical except for the effect of the phase change temperature shift on the specific heat versus temperature relationship. The ZIRLO™ phase change begins at a temperature of approximately 1380°F. Below this temperature, the specific heat of Zircaloy-4 and ZIRLO™ are essentially identical. Therefore, for those non-LOCA accident analyses in which the clad temperature does not reach or exceed a value of 1380°F, the use of ZIRLO™ cladding will have no effect on analysis results relative to results obtained for Zircaloy-4 clad fuel rods.

A review was conducted of non-LOCA licensing basis analyses typically performed for CENP designed nuclear power plants (see Table 7.3-1). This review included fuel assembly array sizes of 14x14 and 16x16. Based on this review, it was concluded that only two non-LOCA

licensing basis analyses resulted in clad temperatures which were predicted to reach 1380°F or greater. These analyses are 1) Control Element Assembly (CEA) ejection, and 2) Locked Rotor/Shaft Break analysis. For other non-LOCA analyses, clad temperatures remain below approximately 1000°F. Therefore, the use of ZIRLO™ cladding has no effect on the results of these licensing basis analyses.

Each of the two potentially affected non-LOCA licensing basis analyses were evaluated to determine what effect the use of ZIRLO™ may have on analysis results and the margin to acceptance criteria.

7.3.1 CEA Ejection

The CEA ejection accident is defined as the mechanical failure of a control element drive mechanism (CEDM) pressure housing or CEDM nozzle, resulting in the ejection of a CEA and drive shaft. The consequences of such a mechanical failure are a rapid positive reactivity insertion and system depressurization together with an adverse core power distribution, possibly leading to localized fuel rod damage.

Licensing Criteria

The CEA ejection event is analyzed at hot full power (HFP) and hot zero power (HZP) conditions. The analyses demonstrate that any consequential damage to the core or the reactor coolant system does not prevent long-term core cooling and that off-site doses remain within the guidelines of 10CFR100. More specific and restrictive criteria are applied to ensure that fuel dispersal into the coolant, gross lattice distortion, or severe shock waves do not occur. These criteria are:

1. The average fuel pellet energy at the hot spot remains below 200 cal/gm.
2. Fuel centerline temperature is limited to less than the incipient melting temperature of the fuel.
3. Peak RCS pressure is less than that which would cause clad stresses to exceed the faulted condition stress limits.

The FATES3B computer code (discussed in Section 4.0) is used to analyze the fuel performance properties. The fuel performance properties are used as input to the STRIKIN-II code, which in turn calculates fuel and clad temperatures versus time, as well as the fuel stored energy. A detailed discussion of the analysis methodology may be found in Reference 7-5.

Evaluation

Sensitivity analyses of the HFP and HZP CEA ejection events were performed, accounting for the specific heat versus temperature relationship of ZIRLO™. These analyses demonstrate that the use of ZIRLO™ cladding results in a [   ] in both the fraction of fuel melted at the hot spot as well as the peak fuel stored energy when compared to the results for Zircaloy-4.

7.3.2 Locked Rotor/Shaft Break

The Locked Rotor/Shaft Break accident is an instantaneous seizure of the reactor coolant pump (RCP) rotor or a break of the RCP shaft. Flow through the affected reactor coolant loop is rapidly reduced, leading to the initiation of a reactor trip on low loop flow. Following reactor trip, heat stored in the fuel rods continues to be transferred to the coolant causing the coolant to expand, resulting in an insurge into the pressurizer and an increase in the RCS pressure. The rapid flow reduction also results in a reduction in the minimum DNBR and potentially results in some fuel rods experiencing DNB.

Licensing Criteria

The Locked Rotor/Shaft Break event is analyzed using the following computer codes. The CENTS or CESEC computer code is used to calculate nuclear power, RCS flow and pressure during the transient. The TORC computer code (Reference 7-6) is then used to calculate the DNB vs. Integrated Radial Peaking Factor (Fr) for the limiting conditions. The ABBFFEC utility code is then used to calculate the number of fuel pins experiencing DNB and the number that subsequently fail based on both statistical convolution and deterministic methods. Two separate analyses are performed. The first analysis is performed to determine the limiting coolant conditions (i.e., pressure, flow, temperature), and the associated DNB vs. Fr pairs. A second

analysis is performed to predict the number of fuel rods experiencing DNB. The second analysis is not affected by the use of ZIRLO™ because the ABBFFEC code results are not dependent on the type of cladding.

Evaluation

Sensitivity analyses have been performed to determine the effect of ZIRLO™ on the limiting coolant conditions (i.e., pressure, flow, and temperature), and the associated DNB vs. Fr pairs. Conservative analyses have determined that use of ZIRLO™ results in a [   ] when compared to Zircaloy-4.

7.4   Conclusions

Based on a review of typical non-LOCA licensing basis analyses performed for CENP designed nuclear power plants, it has been determined that only two non-LOCA events resulted in clad temperatures which were predicted to reach a clad temperature of 1380°F or greater. These analyses are 1) CEA ejection, and 2) Locked Rotor/Shaft Break accident. For other non-LOCA analyses, the clad temperatures remain below approximately 1000°F. Therefore, the introduction of ZIRLO™ cladding has no effect on these analyses.

Each of the two potentially affected non-LOCA licensing basis analyses were evaluated to determine what effect the use of ZIRLO™ may have on analysis results. This evaluation showed that use of ZIRLO™ clad material in CENP designed fuel produces acceptable results.

7.5   References

7-1   CENPD-135-P, "STRIKIN-II, A Cylindrical Geometry Fuel Rod Heat Transfer Program," August 1974

7-2   CENPD-282-P-A, "Technical Manual for the CENTS Code," February 1991.

7-3   LD-82-001 (dated 1/6/82) "CESEC Digital Simulation of a Combustion Engineering Nuclear Steam Supply System," Enclosure 1-P to letter from A. E. Scherer to D. G. Eisenhut, December 1981

7-4   CENPD-188-A, "A Multi-Dimensional Space-Time Kinetics Code for PWR Transients," July 1976.

7-5   CENPD-190-A, "C-E METHOD FOR CONTROL ELEMENT ASSEMBLY EJECTION ANALYSIS," January 1976.

7-6   CENPD-161-P-A, "TORC Code, A Computer Code for Determining the Thermal Margin of a Reactor Core," April 1986.

Table 7.3-1

Non-LOCA Events Typically Analyzed for CENP Designed Nuclear Power Plants

Event name / description	Type of event	Primary code used in modeling the event	Secondary code used in modeling the event
Decrease Feedwater Temperature	Cool down	CESEC/CENTS	none
increasing Feedwater Flow	Cool down	CESEC/CENTS	none
Increase Steam Flow	Cool down	CESEC/CENTS	none
Inadvertent Atmospheric Dump Valve opening	Cool down	CESEC/CENTS	none
Post –Trip Main Steam Line Break	Cool down	CESEC/CENTS	HRISE
Pre-Trip Steam Line Break	Cool down	CESEC/CENTS	TORC/CETOP
Emergency Feedwater Extraction Line Break	Cool down	CESEC/CENTS	none
Chemical Volume Control System mis-operation	Cool down	CESEC/CENTS	none
Letdown Line Break	Cool down	CESEC/CENTS	none
Steam generator Tube Rupture	Cool down	CESEC/CENTS	none
Loss of Load / Turbine Trip	Heat up	CESEC/CENTS	none
Loss of Condenser Vacuum	Heat up	CESEC/CENTS	none
Loss of Flow / Loss of AC Power	Heat up	HERMITE	none
Loss of Feedwater	Heat up	CESEC/CENTS	none
Feedwater Line Break	Heat up	CESEC/CENTS	none
CEA Withdrawal (Bank, Group, subgroup, & Single)	Heat up	CESEC/CENTS	TORC/CETOP
Seized Rotor / Sheared Shaft	Heat up	CESEC/CENTS	TORC/CETOP
Asymmetric steam Generator Transient	Heat up	CESEC/CENTS	TORC/CETOP
CEA Ejection	Heat up	STRIKIN-II	none
CEA Drop		Hand calculation	none
CEA mis-operation		CESEC/CENTS	TORC/CETOP
Boron Dilution		Hand calculation	none

7-9

8.0 Nuclear Design

8.1 Impact of ZIRLO™ Implementation on Nuclear Design

The implementation of ZIRLO™ has negligible effect on the nuclear performance (i.e., physics) of the reactor core. The primary change, with regard to nuclear performance relative to OPTIN™ is the increased concentration of niobium. This increased niobium concentration results in a small increase in neutron absorption (approximately 20 pcm for a fully loaded core) relative to OPTIN. An increase of this magnitude in neutron absorption has no significant effect on nuclear performance relative to cores containing OPTIN clad fuel. Thus, nuclear engineering parameters used in licensing design and safety analyses, including neutron flux and power distributions, reactivity coefficients, and control rod worths are not significantly effected.

The density of ZIRLO™ is essentially the same as the density of OPTIN. Thus the fraction of fission energy deposited directly in the fuel rod (Energy Redistribution Factor) for ZIRLO™ will be essentially the same as those calculated for OPTIN clad fuels. Thus, the OPTIN Energy Redistribution Factors are directly applicable for ZIRLO™ analyses.

Overall, the implementation of ZIRLO™ in CENP fuel designs has an insignificant effect on nuclear engineering aspects of core design. Furthermore, implementation of ZIRLO™ does not require modification of any nuclear engineering methodologies or computer codes. The negligible differences between ZIRLO™ and OPTIN make its implementation essentially transparent for nuclear engineering purposes.

9.0 Summary and Conclusions on ZIRLO ™ Cladding Implementation

The purpose of this report is to provide the justification and description of the implementation of ZIRLO™ cladding in CENP designed fuel. ZIRLO™ cladding properties and irradiation behavior characteristics have been measured by Westinghouse, compared with Zircaloy-4, and submitted to, reviewed by, and accepted by the NRC. These NRC approved ZIRLO™ material properties were incorporated into NRC approved Westinghouse design and licensing safety analysis methodologies. CENP has pursued a similar course. That is, using the Westinghouse developed and NRC accepted ZIRLO™ material properties, CENP has incorporated those ZIRLO™ material properties in its design and licensing safety analysis methodologies. CENP has reached the following conclusions regarding its implementation of ZIRLO™:

1. Implementation of ZIRLO™ is very beneficial to the reduction of waterside corrosion and elimination of the potential for spallation which has been observed in OPTIN™ cladding when operating under high duty cycles currently being imposed on CENP fuel designs.

2. Considerable successful operating experience has been accumulated in Westinghouse designed PWRs with ZIRLO™ cladding and Zircaloy-4 structural components. This experience includes duty cycles that are similar to and bound the duty cycles experienced in CENP designed PWRs. Thus, Westinghouse's experience is directly applicable to CENP designed PWRs. CENP also has its own LTA experience with ZIRLO™-like alloys and Zircaloy-4 structural components that have operated in both CENP's 14x14 and 16x16 fuel designs for several operating cycles. Consequently, Westinghouse's operational experience with ZIRLO™ in conjunction with CENP's ZIRLO™-like alloys LTA experience supports CENP implementation of ZIRLO™ in full batch reloads without the need for a standalone CENP ZIRLO™ specific LTA program.

3. Incorporation of the analytical capability to model ZIRLO™ cladding in the NRC approved CENP design and safety analyses is straightforward. ZIRLO™ properties and correlations are consistent with CENP's application, existing

models, methodology, design criteria and regulatory acceptance criteria (e.g., the NRC has already incorporated ZIRLO™ in the applicable sections of Title 10 of the Code of Federal Regulations).

4.   The impact of ZIRLO™ on fuel thermal performance, mechanical performance, LOCA analyses, and non-LOCA accident analyses has been thoroughly evaluated. Results of design and safety analyses with ZIRLO™ clad fuel rods are, as expected, well behaved and are generally benign and/or insignificant.

5.   Therefore, CENP concludes that implementation of ZIRLO™ cladding will provide an improvement to its fuel designs when incorporated into reloads for CENP designed nuclear power plants.